Eukaryotic chromosome segregation: New aspects of separase regulation by securin, Cdk1, PP2A and auto-cleavage

DISSERTATION

zur Erlangung des Grades
- Doktor der Naturwissenschaften -
der Fakultät für Biologie, Chemie und Geowissenschaften
der Universität Bayreuth

vorgelegt von
Franziska Böttger
aus Berlin

Bayreuth 2011

Die vorliegende Arbeit wurde zwischen Dezember 2006 und Juli 2011 unter Anleitung von Prof. Dr. Olaf Stemmann in der Abteilung für Molekulare Zellbiologie am Max-Planck-Institut für Biochemie in Martinsried sowie am Lehrstuhl für Genetik der Universität Bayreuth durchgeführt.

Vollständiger Abdruck der von der Fakultät für Biologie, Chemie und Geowissenschaften der Universität Bayreuth genehmigten Dissertation zur Erlangung des akademischen Grades eines Doktors der Naturwissenschaften (Dr. rer. nat.)

Promotionsgesuch eingereicht am 13.07.2011
Tag der mündlichen Prüfung: 12.10.2011

Erstgutachter: Prof. Dr. Olaf Stemmann
Zweitgutachter: PD Dr. Stefan Geimer

SUMMARY

The universal triggering event of eukaryotic chromosome segregation is the proteolytic cleavage of chromosomal cohesin by separase. The activity of this essential but potentially also very dangerous protease must be tightly controlled. Prior to the onset of anaphase separase is kept inactive by association with either securin or cyclin-dependent kinase 1 (Cdk1) in conjunction with cyclin B1. Only when all chromosomes interact properly with the mitotic spindle apparatus does the anaphase promoting complex or cyclosome (APC/C), a multisubunit E3 ligase, mediate the ubiquitylation of securin and cyclin B1. Their subsequent proteasomal degradation then releases active separase. Murine embryonic stem cells, which lack securin and express a Cdk1-resistant phosphorylation site mutant separase are viable. Thus, additional regulations of sister chromatid separation by separase must exist.

It was reported that human separase cleaves not only cohesin but also itself and, furthermore, that it interacts with protein phosphatase 2A (PP2A). However, the functions of separase's auto-cleavage and PP2A-interaction remain enigmatic. Moreover, securin was reported to also interact with PP2A but, strangely, with a different isoform of the phosphatase. Thus, the question needs clarification of whether separase or securin or both interact with which isoform of PP2A.

In this study, further insights into the relationship between separase auto-cleavage and PP2A binding are presented. Phosphorylation of a serine residue in close proximity to the major cleavage site of separase was found to stimulate auto-cleavage of separase. Interestingly, a quantitative mass-spectrometric approach (SILAC) identified this serine residue as a substrate of separase-bound PP2A. Furthermore, a point mutation within separase was identified, which totally abolishes PP2A binding and which maps to the immediate vicinity of the auto-cleavage sites. Thus, PP2A prevents the auto-cleavage of separase both catalytically and sterically. It could further be shown that non-cleavable separase exhibits increased association with PP2A and that forced cleavage of separase displaces PP2A. Taken together, these results demonstrate that auto-cleavage and PP2A binding constitute two antagonistic mechanisms of separase regulation.

Evidence is provided that the interaction of PP2A with securin is indirect and bridged by separase, and that it is the B56- and not the B55-isoform of PP2A which associates with the separase-securin complex. Moreover, free securin is shown to be degraded in early mitosis in a phosphorylation- and APC/C-dependent manner, while separase-associated securin is kept dephosphorylated and, thus, protected by PP2A.

Securin levels are frequently increased in tumors. In normal cells, the early removal of excessive securin might later ensure swift separase activation and anaphase onset, thereby contributing to faithful chromosome segregation.

ZUSAMMENFASSUNG

Das auslösende Ereignis eukaryotischer Chromosomensegregation ist die proteolytische Spaltung des chromosomalen Cohesins durch Separase. Die Aktivität dieser wichtigen, aber potentiell auch sehr gefährlichen Protease muss streng reguliert werden. Vor Beginn der Anaphase wird Separase durch Assoziation mit Securin oder Cyclin-abhängiger Kinase 1 (Cdk1) in Verbindung mit Cyclin B1 inaktiv gehalten. Erst wenn alle Chromosomen korrekt mit dem mitotischen Spindelapparat assoziiert sind, wird der *Anaphase Promoting Complex* oder *Cyclosome* (APC/C), eine E3-Ligase, aktiviert und vermittelt die Ubiquitinierung von Securin und Cyclin B1. Der anschließende proteasomale Abbau dieser Inhibitoren entlässt Separase in aktivierter Form. Murine embryonale Stammzellen, denen Securin fehlt und die eine Cdk1-resistente Separase-Mutante überexprimieren, sind lebensfähig. Daher muss es zusätzliche Regulationsmechanismen für Separase geben, welche die Schwesterchromatid-Trennung regulieren.

Es wurde berichtet, dass menschliche Separase nicht nur Cohesin sondern auch sich selbst spalten kann. Außerdem interagiert Separase mit Protein Phosphatase 2A (PP2A). Allerdings sind die Funktionen dieser Selbstspaltung und PP2A-Interaktion noch immer ungeklärt. Darüber hinaus wurde berichtet, dass Securin auch mit PP2A interagieren kann, allerdings mit einer anderen Isoform. Daher muss die Frage geklärt werden, ob Separase oder Securin oder beide mit welcher Isoform von PP2A interagieren.

In dieser Studie werden neue Einblicke in die Beziehung zwischen Separase-Selbstspaltung und PP2A-Bindung geliefert. Es konnte die Phosphorylierung eines Serinrestes in unmittelbarer Nähe zu der wichtigsten Selbstspaltstelle von Separase festgestellt werden. Außerdem konnte gezeigt werden, dass diese die Selbstspaltung der Separase stimuliert. Interessanterweise konnte in einem quantitativen massenspektrometrischen Ansatz (SILAC) dieser Serinrest als Substrat der Separase-gebundenen PP2A identifiziert werden. Darüber hinaus konnte eine Punktmutation in Separase identifiziert werden, welche die Interaktion mit PP2A verhindert und in umittelbarer Nähe zu den Selbstspaltstellen liegt. PP2A verhindert also die Selbstspaltung der Separase sowohl auf eine katalytische als auch auf eine sterische

Art. Es konnte weiterhin gezeigt werden, dass nicht-spaltbare Separase stärker mit PP2A interagiert und erzwungene Spaltung PP2A von Separase verdrängt. Zusammengenommen zeigen diese Ergebnisse, dass Selbstspaltung und PP2A-Bindung zwei antagonistische Mechanismen der Separaseregulation darstellen.

Es konnte nachgewiesen werden, dass die Interaktion von PP2A mit Securin indirekt ist und durch Separase überbrückt wird. Außerdem wurde gezeigt, dass es sich hierbei um die B56- und nicht um die B55-Isoform der PP2A handelt. Weiterhin konnte ein phosphorylierungs- und APC/C-abhängiger Abbau von Separase-freiem Securin in früher Mitose gezeigt werden, während Separase-assoziiertes Securin durch PP2A dephosphoryliert und geschützt wird.

In Tumoren sind die Securinmengen oft erhöht. In normalen Zellen könnte die frühzeitige Entfernung des überflüssigen Securins später eine rasche Separase-Aktivierung sowie einen zeitgerechten Anaphase-Beginn gewährleisten und damit eine akkurate Chromosomensegregation ermöglichen.

1. INTRODUCTION

1.1. The eukaryotic cell cycle - principles of regulation and control

The ability of cells to duplicate and divide is of fundamental importance for all living organisms, not only in embryonic development but also in the regeneration of adult tissues. In the course of a cell cycle, the genetic material must first be duplicated completely and accurately before being equally distributed between the two arising daughter cells. In eukaryotes, this is achieved in two timely distinct phases, S phase (synthesis) and M phase (mitosis), which are separated by gap phases G1 (between M and S) and G2 (between S and M) (Fig. 1). G1 phase is characterized by cell growth and extensive protein biosynthesis, especially of proteins required for subsequent DNA replication in S phase, while G2 phase prepares cells for upcoming mitosis by the production of critical mitotic proteins such as the microtubules needed to form the mitotic spindle. G1, S and G2 phases, which together take up to 95% of the time of a typical human somatic cell cycle, constitute the time between two consecutive M phases and are therefore collectively referred to as interphase. Cells may become quiescent or senescent and leave the cell cycle in G1 to enter G0 phase, a phase where cells temporarily or terminally stop proliferating. While many cell types in mature organisms, such as neurons, are thought to be in a 'post-mitotic', terminally differentiated state, other types of cells, such as epithelial cells, will continue to divide throughout an organism's life and enter G0 only in response to a lack of growth factors or nutrients.

To minimize cell cycle errors, which can cause birth defects and contribute to cancer, and to ensure faithful DNA replication in S phase and DNA segregation in mitosis, so-called checkpoints supervise critical cell cycle transitions. These control systems are highly regulated and constitute all-or-nothing switches. In G1 phase, a 'restriction' checkpoint controls if cells are ready to enter S phase and start duplicating their genetic material or whether cells are destined to leave the cell cycle at this stage and enter the resting G0 phase. Once this checkpoint is passed, cells are liscensed to enter a full cell cycle. In G2, the DNA damage checkpoint is responsible for preventing mitotic entry until replication defects or DNA damage of other sorts have

been repaired. Finally, at the metaphase-to-anaphase transition of mitosis, the 'spindle assembly checkpoint' (SAC) closely monitors correct spindle attachment before the DNA is allowed to segregate. After the cell has split into its two daughter cells, these re-enter G1 phase (Morgan, 2007) (Fig. 1).

The course of cell cycle events is controlled primarily by reversible, post-translational modifications of proteins, such as phosphorylation, and by irreversible, switch-like degradation of proteins (Murray and Kirschner, 1989). The family of cyclin-dependent kinases (Cdks) are the key enzymes that drive cell cycle progression. The regulated cyclic synthesis of cyclins, Cdk associating and activating proteins, promotes oscillating Cdk activities throughout the cell cycle and therefore cyclical changes in the phosphorylation of components of the cell cycle machinery. Irreversible destruction of cyclins leads to inactivation of Cdks, which in turn allows phosphatases to dephosphorylate Cdk substrates. Specific pairs of Cdk-cyclin complexes are formed and activated throughout the cell cycle. In mammalian cells, the main Cdk-cyclin complexes are formed by cyclin A, cyclin B and cyclin E. Cdk1 together with cyclin B1 triggers entry into mitosis and is hence also referred to as MPF (mitosis promoting factor). Cyclin A in complex with Cdk1 or 2 drives S and G2 phase progression, while Cdk2-cyclin E regulates G1/S transit and DNA synthesis (Fig. 1).

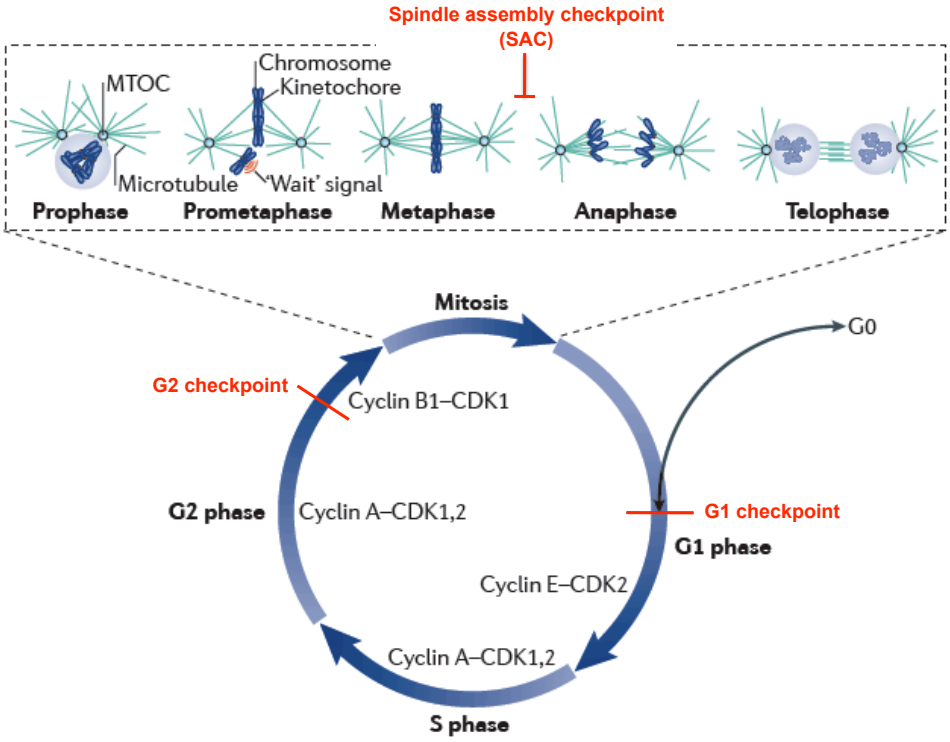

FIGURE 1. Schematic overview of the cell cycle.

Depicted are the main cell cycle phases of a typical mammalian somatic cell. The corresponding Cdk-cyclin complexes that govern these phases are indicated. Highlighted in red are critical control points that monitor the correct course of important cell cycle transitions. See text for details. Figure taken and modified from (Pines, 2011).

1.2. The establishment of sister chromatid cohesion in S phase

In the course of a cell cycle, the cell always has to know which pairs of double-stranded DNA molecules (sister chromatids) belong together. This is essential, both to allow for equal distribution of the genetic information to each daughter cell in mitosis, but also to enable postreplicative repair of DNA double-strand breaks by homologous recombination in G2 phase. Therefore, mechanisms are in place that hold sister chromatids together from the time of DNA replication in S phase until the metaphase-to-anaphase transition of mitosis. This sister chromatid cohesion is mediated on the one hand by topological inter-sister DNA links (DNA catenation), which naturally occur when replication forks meet during DNA synthesis, and by the cohesin complex.

This ring-shaped multi-protein complex contains four main subunits - Smc1 and Smc3, which belong to the familiy of 'structural maintenance of chromosomes' (SMC) proteins, the kleisin subunit Scc1/Rad21 and Scc3/SA (SA1 and SA2 in vertebrates) (Fig. 2). SMC proteins are widely conserved in the three domains of life and contribute to a variety of processes involving chromosome dynamics, not only chromosome segregation but also DNA recombination and repair. Structurally, SMC proteins are characterized by a large, elongated coiled coil region that forms an ATPase 'head' at one end, where N- and C-terminus of the back-folded proteins meet, and a so-called 'hinge' domain at the other end. Within the cohesin ring, the two SMC subunits dimerize over their hinge regions, forming a V-shape that can be visualized by electron miscroscopy. Over the ATPase head domains situated at the top of the V-shape, Smc1 and Smc3 interact with the C- and N-terminus of the Scc1 subunit, respectively, thereby completing the ring. Scc1 is further associated with a fourth, peripheric subunit, Scc3/SA, which exists in two different versions in somatic vertebrate cells, SA1 and SA2 (Losada et al., 1998; Losada et al., 2000; Melby et al., 1998; Michaelis et al., 1997). Beside these core subunits, a variety of accessory proteins have been identified that can modulate cohesin behavior and stability. Among these are Wapl (wings apart-like) and Pds5 (precocious dissociation of sisters 5), which interact not only with Scc1 and Scc3/SA but also with each other, and have been characterized as possessing an anti-establishment activity, being involved in destabilizing cohesin-chromatin interactions in G2 and prophase of mitosis (Gandhi et al., 2006; Kueng et al., 2006; Shintomi and Hirano, 2009). Antagonistically, cohesin-associating protein soronin has been implicated in cohesion establishment and/or maintenance in G2 phase (Schmitz et al., 2007). Soronin, which can only bind to replicated chromatin associated with cohesin, is potentially involved in stabilizing 'established' cohesion (Lafont et al., 2010).

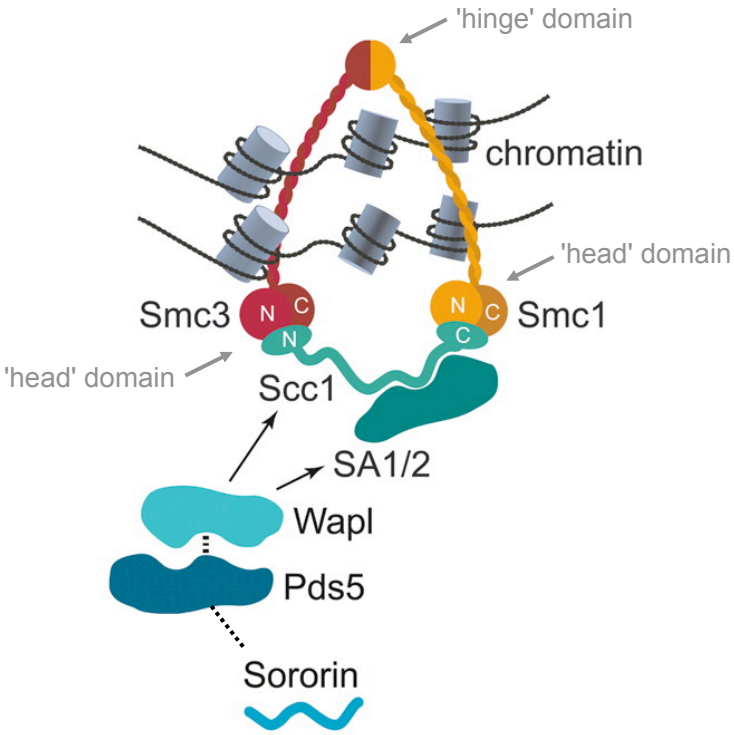

FIGURE 2. Schematic depiction of the cohesin ring complex.

According to the ring model, the subunits of the cohesin complex form a large ring that encircles both sister chromatids, therey providing a topological linkage between sister chromatids from the time of their synthesis in S phase until the metaphase-to-anaphase transition of mitosis. See text for details. Figure taken and modified from (Peters et al., 2008).

Cohesin is loosely loaded onto chromatin before DNA replication (in late G1 phase in budding yeast or already in telophase of mitosis in higher eukaryotes), by a process involving the proteins Scc2 and Scc4 in yeast (Ciosk et al., 2000), as well as orthologs of Scc2 and Scc4 in addition to pre-replication factors in higher eukaryotes (Takahashi et al., 2004; Watrin et al., 2006) (Fig. 3). In S phase, concomitant with DNA replication, previously loaded cohesin now forms a tight link between the newly synthesized sister chromatids (Toth et al., 1999). This establishment requires the activity of the Eco1/Ctf7 (Esco1 and Esco2 in humans) acetyltransferase (Ivanov et al., 2002; Toth et al., 1999), which can acetylate cohesin subunit Smc3, leading to the dissociation of anti-establishment factors Wapl1 and Pds5. Eco1 has been shown to interact with several DNA replication-fork components, including the DNA polymerase processivity clamp PCNA (Moldovan et al., 2006; Skibbens et al., 1999), arguing for replication-coupled cohesion establishment.

In an unperturbed cell, no cohesin is established *de novo* after S phase, but the already established cohesin must be maintained throughout G2 phase until mitosis. Recently, a possible mechanism by which cohesion establishment is restricted to S phase was revealed. Cdk1-dependent phosphorylation of Eco1 from late S phase until mitosis was shown to lead to its SCF-dependent degradation (Lyons and Morgan, 2011). In the event of DNA damage however, Eco1 is stabilized and can acetylate cohesin subunit Scc1, again counteracting the anti-establishment activity of Wapl1 (Heidinger-Pauli et al., 2009). Thus, new cohesion can be established to aid in DNA repair.

How cohesin exerts its cohesion mediating function on chromosomes is still subject of ongoing debate. Based on its large ring structure and strong biochemical evidence, the most appealing model (the so-called 'ring model') is that a single cohesin ring encircles the two sister chromatids, thereby acting as a topological linker rather than directly binding to the chromosomes (Anderson et al., 2002; Gruber et al., 2003; Haering et al., 2002) (Fig. 2).

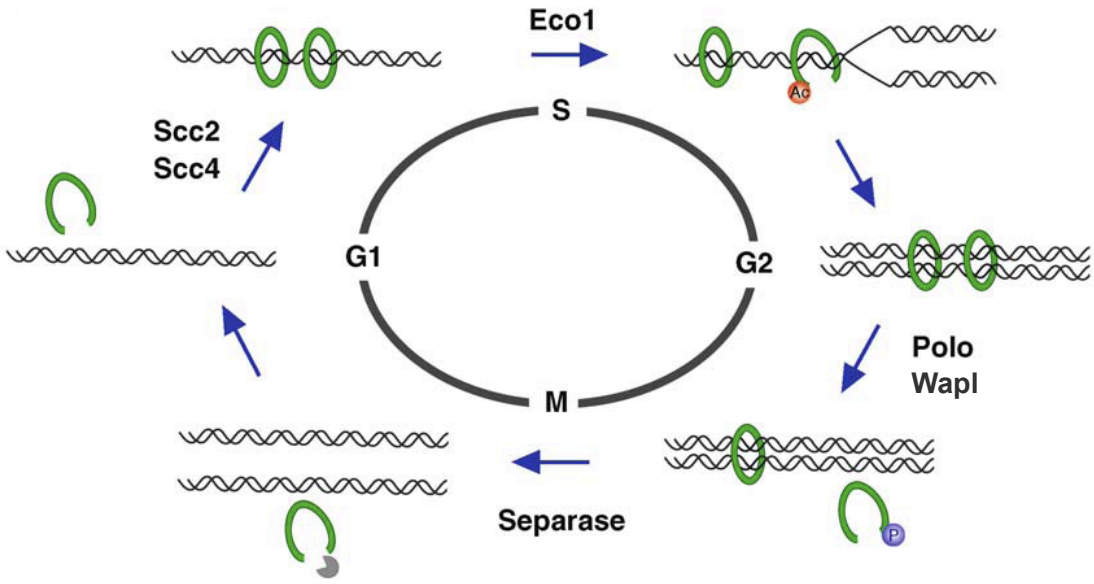

FIGURE 3. Model of cohesin and its establishment/resolution cycle.

Shown is the cohesin cycle from *S. cerevisiae*. Note that in higher eukaryotes, loading of cohesin (represented here by green rings) onto DNA commences as early as telophase of mitosis and additionally depends on pre-replicative complexes. Cohesin is then established in S phase. Resolution of cohesin begins in prophase of mitosis and is completed at the metaphase-to-anaphase transition by the action of separase. See text for details. Figure taken from (Carretero et al., 2010).

1.3. The process of sister chromatid separation in mitosis

In higher eukaryotes, mitosis begins with the condensation of DNA into densly packed chromosomes in the nucleus. At the same time, centrosomes, the microtubule organizing centers (MTOCs) localised in the cytoplasm of animal cells, separate and initiate the assembly of the mitotic spindle (prophase). In prometaphase, the nuclear envelope breaks down (nuclear envelope breakdown, NEB) and the condensed chromosomes start migrating to the center of the cell and attaching to the biopolar array of microtubules. Attachment occurs via protein complexes known as kinetochores, that assemble at the primary constriction regions of the mitotic chromosomes, the centromeres, onto chromatin containing the histone H3 variant CENP-A (centromeric protein-A). The two sister chromatids of a chromosome are each attached to microtubules emanating from opposite poles of the spindle by metaphase. At this stage, the spindle assembly checkpoint (SAC) monitors kinetochor-microtubule attachment and tension generated by correct bipolar kinetochor-microtubule attachment. Once the SAC is satisfied, the separation of sister chromatids at the metaphase-to-anaphase transition can be triggered by a protease called separase, which cleaves cohesin, the multisubunit ring structure responsible for holding the sister chromatids together. This process is mediated by a ubiquitin protein ligase called the anaphase-promoting complex or cyclosome (APC/C). Every chromatid is then moved towards its pole by shortening of the spindle microtubules (anaphase A) and by an increase in interpolar distance (anaphase B). During telophase, the spindle dissamsembles and a nuclear envelope reforms around the now decondensing chromosomes. Finally, a contractile actinmyosin ring creates a cleavage furrow and mediates cleavage and abscission of the two daughter cells (Morgan, 2007) (Fig. 1).

1.3.1. The resolution of cohesion in mitosis

To enable the synchronous separation of sister chromatids at the metaphase-to-anaphase transition of mitosis, removal of all cross-links between sister chromatids must be carefully orchestrated. Untanglement of inter-sister DNA catenation takes place throughout G2 and is catalyzed by topoisomerase II. In addition, a complex structurally related to cohesin, the condensin complex, associates with chromatin at

the onset of mitosis and is involved in DNA condensation and the resolution of sister chromatids in preparation for their segregation. By early mitosis, most catenations are resolved and DNA is highly condensed. At this stage, cohesin, which is distributed along the entire length of chromosomes as cells enter mitosis, constitutes the major topological link between sister chromatids. In higher eukaryotes, cohesin is removed from chromosomes in two waves (Sumara et al., 2000; Waizenegger et al., 2000) (Fig. 4). Already in prophase more than 90% of cohesin is removed from chromatid arms by the action of protein kinases Plk1 (polo-like kinase 1) and Aurora B (Losada et al., 2002; Peters et al., 2008; Sumara et al., 2000). Plk phosphorylates the Scc3 subunit of cohesin (Hauf et al., 2005), thereby possibly enabling Wapl1-Pds5 to promote a conformational change in the cohesin ring which leads to its dissociation (Gandhi et al., 2006). This so-called 'prophase pathway' in early mitosis gives rise to the typical X-shaped morphology of metaphase chromosomes, characterized by their centromeric constriction. Protected from the cohesin removal induced by Plk and Aurora B are the centromeric regions of chromosomes, where shugoshin (Sgo1) and its partner PP2A are localized. While Sgo1 itself may serve as a physical protector for centromeric cohesin, its recruitment of PP2A serves to counteract cohesin phosphorylation and thereby stabilizes cohesin rings in this region (Kitajima et al., 2006; Riedel et al., 2006; Tang et al., 2006).

The resolution of DNA catenation and the removal of all chromosome arm cohesion by metaphase means that sister chromatids are only held together by residual cohesin around the centromeric regions of chromosomes at this stage. At the metaphase-to-anaphase transition, the protease separase is activated via the APC/C^{Cdc20}-mediated degradation of its inhibitor proteins securin and cyclin B1 and cleaves the Scc1 subunits of the remaining cohesin complexes on all chromosomes (Hauf et al., 2001; Uhlmann et al., 1999) (Fig. 4).

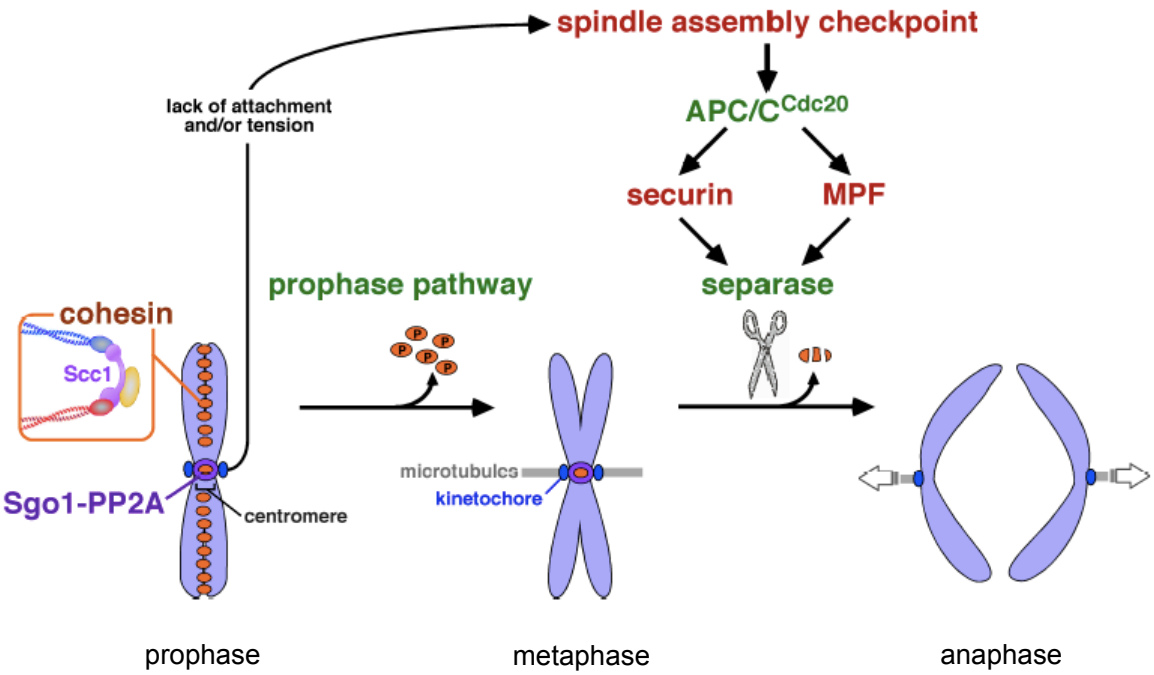

FIGURE 4. Model of sister chromatid separation in higher eukaryotic mitosis.

In higher eukaryotes, cohesin is removed from chromosomes in 2 steps. In the so-called prophase pathway, cohesin is initially removed from chromosome arms. Centromeric cohesin is protected by the Sgo1-PP2A complex, giving rise to the characteristic X-shaped metaphase chromosome structure. Once all chromosomes are correctly attached to the mitotic spindle and the spindle assembly checkpoint is satisfied, separase inhibitors securin and MPF (cyclin B1 of the Cdk1-cyclin B1 complex) are degraded in an APC/C^{Cdc20}-dependent manner, liberating active separase. Separase then proteolytically cleaves any remaining cohesin, separating the sister chromatids from each other. Figure modified from O. Stemmann.

1.3.2. The spindle assembly checkpoint

Separase is activated by the concomitant APC/C^{Cdc20}-mediated targeting of its inhibitors securin and Cdk1 regulatory subunit cyclin B1 for proteasomal degradation (Cohen-Fix et al., 1996; King et al., 1995; Zou et al., 1999). It is crucial for the fidelity of sister chromatid segregation that this irreversible all-or-nothing step is only activated once all chromosomes are bioriented at the metaphase plate, i.e. attached to microtubules emanating from opposite poles of the cell. This is controlled by a cellular surveillance machinery known as the spindle assembly checkpoint (SAC), that monitors the attachment of spindle microtubules to the kinetochores of chromosomes and delays anaphase onset in response to spindle defects (Fang et al., 1998; Schott and Hoyt, 1998). Only when the SAC is satisfied and the SAC signal

inactivated can its central target, the APC/C, be activated. It is still not clear whether the SAC, which is essential in mammalian cells and is triggered in every mitosis, even in unperturbed cell cycles, is an attachment- or a tension-sensing activity, or whether both parameters are detected to generate a 'wait anaphase' signal in the presence of unattached kinetochors. On a molecular basis, the APC/C is inhibited in such an event by a four-protein complex known as the mitotic checkpoint complex (MCC), which consists of the checkpoint proteins Mad2 (mitotic arrest deficient), Bub3 (budding uninhibited by benzimidazole), BubR1, and the APC/C activator Cdc20 (Sudakin et al., 2001) (Fig. 5). Additionally, proteins like Mad1 as well as the kinases Bub1, Mps1 and Aurora B are involved in regulating SAC activity, signal amplification and the rate of MCC formation. Within the MCC, Mad2 and BubRI can directly interact with and inhibit Cdc20. It is thought that MCC formation occurs directly at unattached kinetochores. All MCC components are found to localize here. According to the so-called 'template model', Mad1 bound to unattached kinetochores serves as a template for the conformational activation of central MCC component Mad2. Mad2 can adopt two native conformations, known as Mad2-open ($Mad2^{O}$) and Mad2-closed ($Mad2^{C}$), Mad2-closed being the form that can bind Cdc20 and thereby inhibit the APC/C (De Antoni et al., 2005; Luo et al., 2004). Briefly, soluble cytosolic Mad2-open is converted into Mad2-closed by a transient interaction with stably kinetochore-bound Mad1. Thus activated Mad2-closed bound to Mad1 now itself serves as a template for further Mad2-open forms, which are recruited to the site of unattached kinetochores, converted to Mad2-closed, and thereby activated to bind Cdc20. In this way, the checkpoint signal at a single unattached kinetochor is amplified rapidly (De Antoni et al., 2005). Inactivation of the SAC signal upon correction of all erroneous microtubule-kinetochore attachments occurs in a switch like manner. The exact mechanism of MCC disassembly, which ultimately releases Cdc20, making it available for the formation of an active APC/C, is still incompletely understood, but involves both the motor protein dynein and the Mad2-open mimicking inhibitor $p31^{comet}$ (Howell et al., 2001; Mapelli et al., 2006; Xia et al., 2004).

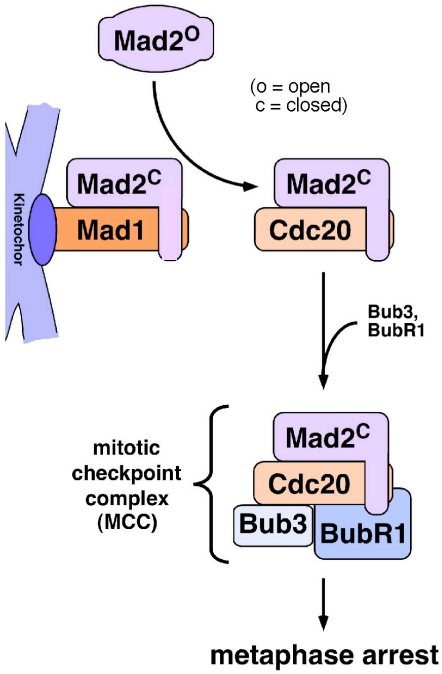

FIGURE 5. The 'template model' of spindle assembly checkpoint signaling.

The template model of SAC activation and signal amplification describes how Mad1-Mad2 complexes at unattached kinetochores may induce a conformational conversion of soluble Mad2-open ($Mad2^{O}$) into Mad2-closed ($Mad2^{C}$), thereby catalyzing Mad2 binding to its target Cdc20. Together with Bub3 and BubR1, the Cdc20-$Mad2^{C}$ complex then forms the so-called mitotic checkoint complex (MCC), which inhibits APC/C^{Cdc20} activation and therby induces a mitotic arrest until all kinetochors are correctly attached to the mitotic spindle. Figure modified from O. Stemmann.

1.3.3. The ubiquitin-proteasome system

Proteolysis via the ubiquitin-proteasome system (UPS) controls mitotic progression at multiple stages, namely at sister chromatid separation, Cdk1 inactivation and exit from mitosis. The first step of this pathway is to mark substrates that are destined for degradation with the small (79 aa) ubiquitous protein ubiquitin. The assembly of polyubiquitin chains on substrate proteins like securin and cyclin B1 (ubiquitylation) is sequentially performed by the ubiquitin activating enzyme (E1), the ubiquitin conjugating enzyme (E2) and a ubiquitin ligase (E3). ATP-dependent activation of a ubiquitin protein is achieved by the covalent attachment of the carboxyl terminus of a glycine residue of ubiquitin to the sulfhydryl group of a cysteine in the active site of

the E1 enzyme, forming a high energy thioester bond. The activated ubiquitin is then transferred to the active site cysteine of the E2 enzyme, which catalyzes the formation of an isopeptide bond between the glycine residue of the ubiquitin and the amino group of a lysine side chain of the target protein. This ubiquitylation reaction is dependent on the E3 enzyme, which either serves as a platform to bring together the E2 enzyme and specific substrates, or takes over the activated ubiquitin from the E2 enzyme to then conjugate it onto the substrates. Additional ubiquitins are subsequently added onto pre-conjugated ones to form long polyubiquitin chains that are recognized by the 26S proteasome, a large multisubunit protease complex, which degrades the ubiquitylated protein to small peptides (Peters, 2006; Pickart and Eddins, 2004) (Fig. 6).

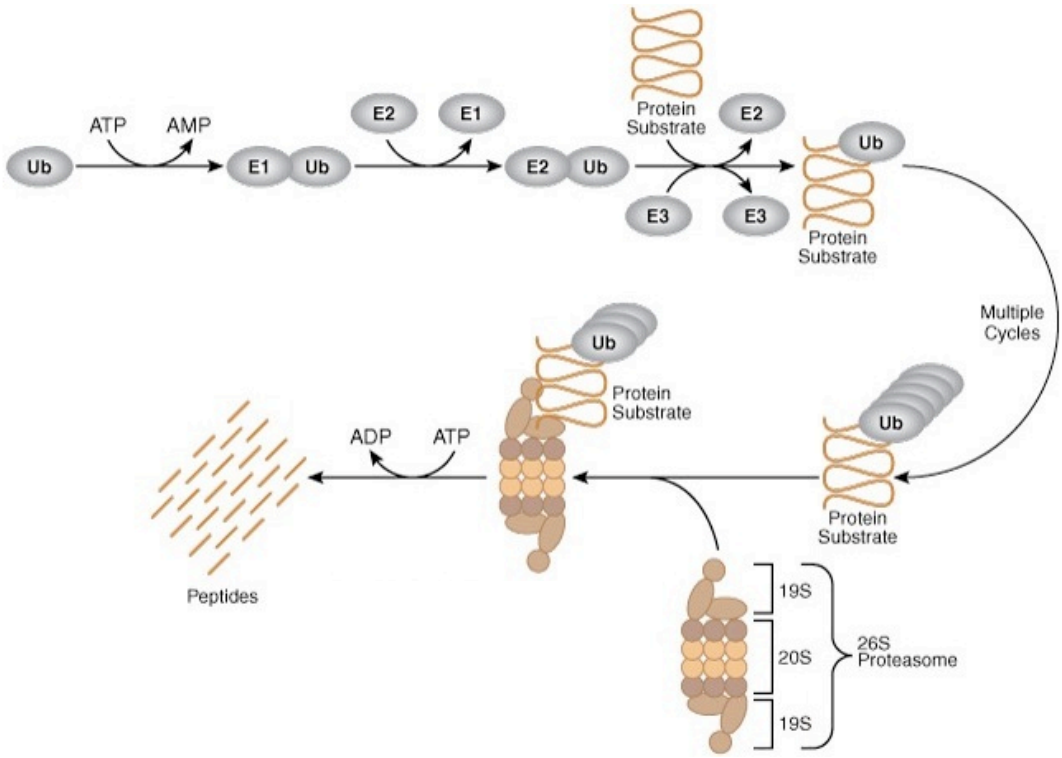

FIGURE 6. Overview of the ubiquitin/proteasome pathway.

Proteins designated for rapid proteasomal destruction are marked for recognition by the 26S proteasome by the covalent addition of a long polyubiquitin chain. This ubiquitylation is achieved by the successive action of three enzymes termed E1, E2 and E3. E3 is a ubiquitin ligase which catalyzes the final conjugation of a ubiquitin to the target protein. The key mitotic E3 ubiquitin ligase is the anaphase promoting complex/cyclosome (APC/C). Figure taken and modified from (CellSignalingTechnology, 2010).

The key mitotic E3 ubiquitin ligase is the anaphase promoting complex/cyclosome (APC/C), which targets critical mitotic reguatory proteins like securin and A- and B-type cyclins, leading to activation of separase and inactivation of the corresponding Cdk kinase. The human APC/C is a complex of 13 subunits, including the cullin subunit (Apc2), the RING finger subunit (Apc11) as part of the active, E2 ubiquitin conjugate binding site, the Apc10 subunit involved in substrate recognition and the tetratrico peptide repeat (TPR) subunit Apc3/Cdc27, over which the APC/C core complex interacts with one of two co-activator proteins. These are Cdc20 and Cdh1, both characterized by an N-terminal "C-box", which is needed for binding the APC/C core and for promoting ubiquititylation, and a C-terminal isoleucin-arginine (IR) tail, which meditiates interaction with the Apc3/Cdc27 subunit of the APC/C core. Additionally, the C-termini of these APC/C co-activators contain a so-called WD40 domain made up of tryptophan-aspartate-rich repeats that are predicted to fold into seven-bladed ß-propeller-like structures and are involved in binding to specific recognition motifs within the substrates. Substrates may contain one or several so-called KEN- and/or destruction (D)-boxes. The KEN motif comprises the amino acids lysine, glutamate and asparagine, while D-boxes are characterized by a conserved arginine-leucine (RxxL) consensus motif. Both resemble recognition sites for the APC/C and as such are part of the degrons that ultimately lead to substrate degradation.

In mitosis, the APC/C co-operates with Cdc20, which can only associate with and activate the APC/C when several APC/C subunits have been phosphorylated by different kinases like Plk1 and Cdk1 during S and G2 phase and early mitosis, and when Emi1, a strong interphase inhibitor of APC/C^{Cdc20}, has been degraded (via the SCF complex, another E3 ubiquitin ligase). Active APC/C^{Cdc20} then mediates the degradation of substrates like cyclin A and Nek2A in prometaphase and of securin and cyclin B1 at the metaphase-to-anaphase transition. The drop in Cdk1 activity associated with cyclin B1 degradation promotes the formation of an APC/C^{Cdh1} complex during anaphase and telophase, which then stays active throughout G1 phase and mediates the degradation of securin, cyclins, Plk1, Cdc20, thus inactivating the APC/C^{Cdc20}, and finally of the E2 enzyme UbcH10, thereby inactivating itself and allowing S phase entry by accumulation of S phase cyclins (Peters, 2006).

A second major E3 ubiquitin ligase involved in cell cycle progression is the SCF complex. The human SCF complex is composed of 3 core subunits (Skp1, the cullin Cul1 and the RING protein Rbx1) and one member of a large family of F-box proteins. In humans, 69 different F-box protein genes have been identified to date. F-box proteins are characterized by the presence of an F box domain, which interacts directly with the Skp1 subunit of the SCF core (Bai et al., 1996), and usually contain WD40 or leucine-rich repeats that can directly interact with the target proteins and confer substrate specificity. The SCF core complex is active throughout the cell cycle, and regulation of substrate ubiquitylation is mostly controlled on the level of subtrate phosphorylation. In addition, conjugation of the ubiquitin-like protein NEDD8 to the cullin subunit (neddylation) appears to be required for SCF function (Saha and Deshaies, 2008).

Polyubiquitylated proteins are targeted to the 26S proteasome for proteolytical destruction. This giant protease complex (approx. 2.5 MDa) is part of the ubiquitin-proteasome system (UPS), which constitutes the major cytosolic proteolytic system in eukaryotes. Structurally, the proteasome contains two functionally distinct particles, the 20S core particle and two distally positioned 19S regulatory particles (Fig. 6), which are both connected to the core by a substrate translocation channel. Generally, ubiquitylated proteins are recognized by the 19S regulatory particle in an ATP-dependent manner and are subsequently unfolded and deubiquitylated here. Importantly, ubiquitin molecules are recycled by the cell, and can be re-activated by E1 enzymes to start ubiquitylation of new proteins. Following their translocation into the 20S core particle, proteins are degraded by proteolysis (Fig. 6). This compartmentalized structure of the proteasome holoenzyme enables substrate proteins to be degraded in a very selective and processive manner, in contrast to the low specificity degradation of proteins by proteases in the lysosome, for example (Finley, 2009; Pickart and Cohen, 2004).

1.3.4. Regulation of separase activity

APC/C-mediated securin and cyclin B1 degradation initiates the activation of separase, which then performs the decisive step in sister chromatid separation by

cleaving the last persisting cohesin bonds between sister chromatids. Separase, which belongs to the family of Cys-endopeptidases, is considered the universal trigger of eukaryotic anaphase (Kumada et al., 2006; Wirth et al., 2006). Separase is essential for viability. This is underlined by the fact that deletion of both copies of separase causes embryonic lethality in mice, and mouse embryonic fibroblasts lacking separase become highly polyploid (Wirth et al., 2006). Despite low conservation of their primary structures, separases from different species might have conserved tertiary structures (Jager et al., 2004). The active site of this large protein (233 kDa in humans) is located near the C-terminus and contains a conserved histidine and cysteine residue forming the catalytic dyad (Uhlmann et al., 2000). Active separase, which cleaves proteins specifically after the arginine of an ExxR consensus sequence (Stemmann et al., 2001; Sullivan et al., 2004; Uhlmann et al., 1999), cleaves the Scc1 subunit of both chromosomal and centrosomal cohesin (Schöckel et al., 2011; Tsou and Stearns, 2006; Uhlmann et al., 1999). In addition, the meiotic Scc1-homolog Rec8 (Petronczki et al., 2003) and the kinetochore-associated protein Slk19 in budding yeast (Sullivan et al., 2001) have been identified as separase substrates. In higher eukaryotes, active separase also cleaves itself. Once cleaved, the generated separase fragments remain associated and catalytically active. Thus, cleavage is not required for separase activation, at least *in vitro* (Waizenegger et al., 2002; Zou et al., 2002). Thus, the functional relevance of this mechanism is still unclear.

Based on low resolution electron microscopy pictures of the human separase-securin complex, as well as detailed bioinformatic analysis of the human separase sequence (2120 residues), general structural characteristics of this protease complex were proposed (Viadiu et al., 2005). The N-terminal half of separase might have a superhelical structure and consist of 26 ARM or HEAT repeats, which are often implicated in protein-protein interactions, whereas the C-terminal half is predicted to consist of two caspase domains, of which only the most C-terminal one is active. N- and C-terminus are separated by a 280 residue long unstructured region (amino acids 1276-1556). Most mapped phosphorylation sites as well as separase's auto-cleavage sites fall into this unstructured stretch, suggesting that this region has a central regulatory function (Fig. 7).

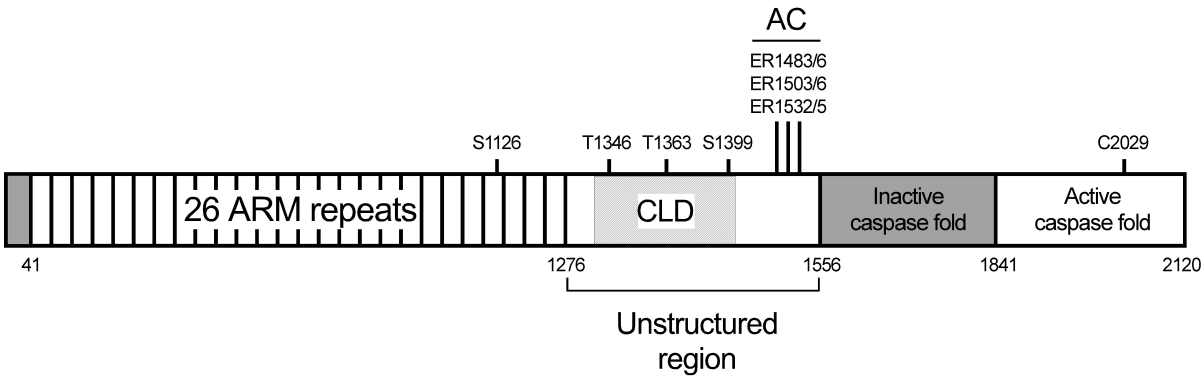

FIGURE 7. Proposed domain structure of human separase.

Overview of important regulatory residues and domains within human separase. The serine at position 1126 as well as the highlighted residues within the central Cdc6-like domain (CLD, amino acid position 1342-1400) are critical for cyclin B1-Cdk1 binding. In close proximity are separase's main auto-cleavage (AC) sites (ExxR sites at amino acid positions ER1483/6, ER1503/6 and ER1532/5). The PP2A binding site characterized by Holland and colleagues (amino acid position 1419-1474; Holland et al., 2007) maps to a region between the CLD and the AC sites. The cysteine at position 2029 is essential for separase's proteolytic activity.

To date, human separase has been shown to interact with three different partners. Prior to anaphase, separase is inhibited by (mutually exclusive) association with cyclin B1-Cdk1 complex (also known as mitosis promoting factor, MPF) or securin (Funabiki et al., 1996; Gorr et al., 2005; Stemmann et al., 2001; Stratmann and Lehner, 1996; Yamamoto et al., 1996; Zou et al., 1999). In addition, protein phosphatase 2A (PP2A) can interact with human separase, although the function of this association remains unknown (Holland et al., 2007).

1.3.4.1. Securin-mediated separase inhibition

Securins from different eukaryotic species are conserved in their function as small stoichiometric inhibitors of anaphase, but show little or no sequence homolgy. Generally, securins are considered to be natively unfolded proteins and as such contain little secondary structure elements (Csizmok et al., 2008; Sanchez-Puig et al., 2005). Common features of all securins however include their basic amino-terminal halves, which contain at least one APC/C recognition motif (KEN- and/or D-box), their acidic carboxy-terminal halves, which have been implicated in binding

separase, as well as their relatively small size (< 30 kDa). How exactly securin binds and inhibits separase is still not fully understood. Both separase termini have been reported to be involved in binding securin, suggesting that separase that is bound to securin may adopt a conformation, in which the amino terminus is in close proximity to the carboxy terminus (Hornig et al., 2002; Jager et al., 2001; Jensen et al., 2001; Kumada et al., 1998). Indeed, there is evidence that separase can undergo large conformational changes, both upon dissociation from its inhibitors securin (Hornig et al., 2002) and as a result of phosphorylation by MPF (Boos et al., 2008).

In fission yeast and *Drosophila*, securin is essential for chromosome segregation (Funabiki et al., 1996; Stratmann and Lehner, 1996; Yamamoto et al., 1996). It might also serve as a recruitment factor for correct intracellular localization of separase in fission and budding yeast (Hornig et al., 2002; Jensen et al., 2001; Kumada et al., 1998). In higher eukaryotes, securin is dispensible for viability. Both mice and cultured human cells are viable and show only a mild phenotype upon knock-out of securin (Mei et al., 2001; Pfleghaar et al., 2005; Wang et al., 2003). This can be explained by the existance of MPF, which can phosphorylate and then bind to inhibit separase in mitosis (Stemmann et al., 2001).

Surprisingly, securin not only functions as an inhibitor but also as an activator of separase, since knockout of securin in vertebrates leads to a reduced level and activity of separase (Pfleghaar et al., 2005). How securin exerts its positive effect on separase has not yet been elucidated. It might be involved in proper localization of separase (Jensen et al., 2001) or act as a chaperone assisting in correct folding (Nagao et al., 2004).

1.3.4.2. MPF-mediated separase inhibition

MPF (Cdk1-cyclin B1) mediated phosphorylation of Ser1126 on human separase indirectly promotes the stepwise formation of a separase-MPF complex that, ultimately, inhibits not only separase but also leads to the inactivation of Cdk1. Ser1126 phosphorylation is thought to induce a conformational change in separase, leading to the demasking of the actual MPF binding site (Boos et al., 2008) (Fig. 8). This site lies within the unstructured regulatory region of separase (amino acids 1276-1556), more precisely in a Cdc6-like domain (CLD, amino acid position 1342-

1400) exhibiting a weak homology to budding yeast Cdc6, which shows similar phosphorylation-dependent Cdk1 binding behavior (Mimura et al., 2004). MPF phosphorylates Thr1346 within this region, Polo like kinase (Plk) may further phosphorylate Thr1363 and Ser1399, and these phosphorylations are the basis for stable MPF binding to the CLD via the regulatory Cdk1 subunit cyclin B1 (Boos et al., 2008; Gorr et al., 2005; Stemmann et al., 2001).

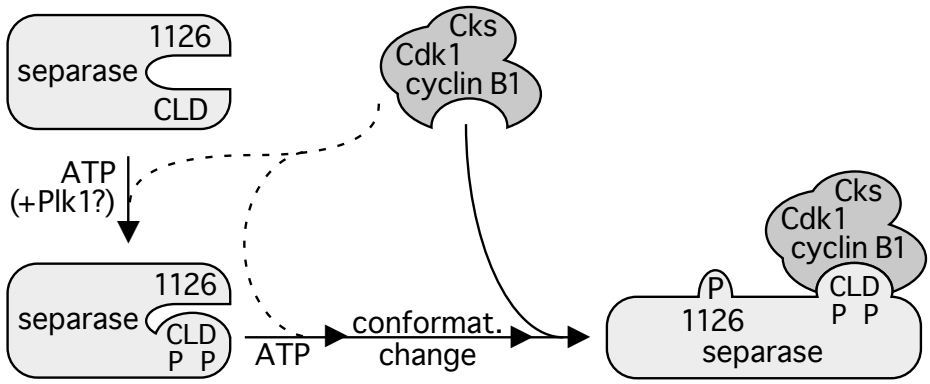

FIGURE 8. Model for the stepwise assembly of the separase-Cdk1 complex.

The phosphorylation of separase by cyclin B1-Cdk1 complex in mitosis is thought to induce a conformational change in separase that allows inhibitory binding of the kinase complex to the protease. See text for details. Figure taken from (Boos et al., 2008).

Several *in vivo* studies have highlighted the crucial importance of MPF for the regulation of vertebrate separase and demonstrate that in contrast to securin, MPF-mediated separase inhibition is essential for the viability of mammals (Holland and Taylor, 2006; Huang et al., 2008; Huang et al., 2005).

1.4. Cyclin-dependent kinase 1 (Cdk1) as the master regulator of mitosis

Reversible phosphorylation is one of the most important post-translational modifications of proteins, and is characterized by the protein kinase catalyzed transfer and covalent attachment of a phosphoryl group from ATP to the free hydroxyl groups of serine, threonine or, less commonly, tyrosine residues of proteins. Phosphorylation of a protein can alter such important attributes as its biological activity, localization, stability and interaction behavior.

Cdk1, one of 428 serine/threonine (Ser/Thr) protein kinases encoded in the human genome (Manning et al., 2002), is considered the master regulator of mitosis. In association with its regulatory subunits cyclin B1 or cyclin A2 it phosphorylates a series of mitotic targets containing (S/T-P-X-K/R) consensus sites, leading to mitotic entry (Fig. 1). Among these critical targets are lamins, which make up the nuclear lamina and are associated with the inner nuclear membrane. Once phophorylated by Cdk1-cyclin B1, nuclear lamins start depolymerizing and the nuclear envelope disassembles (Heald and McKeon, 1990). Furthermore, formation of the mitotic spindle depends on the phosphorylation of microtubule associated proteins (MAPs) by Cdk1-cyclin B1. Correspondingly, downregulation of Cdk1 activity at the end of mitosis is essential for the spindle to disassemble.

During S and G2 phase, cyclin B1 slowly accumulates in the cell and binds to Cdk1. This early Cdk1-cyclin B1 complex is phosphorylated at T161 in the so-called T-loop of Cdk1 by Cdk activating kinase (CAK), but remains inactive due to additional inhibitory phosphorylations on T14 and Y15 that block the active site of the kinase. These phosphorylations are imposed by the kinases Wee1 and Myt1 and have to be removed in late G2 by protein phosphatase Cdc25 before Cdk1 is fully activated. In a positive feedback loop, Cdk1-cyclin B1 activates its own activator, Cdc25, while simultaneously inhibiting its inhibitor Wee1 by phosphorylation.

Directly associated with active Cdk1-cyclin B1 complexes are small regulatory subunits of the Cks family (Cdc kinase subunit), although the exact function of these accessory proteins is still unknown (Bourne et al., 1996; Harper, 2001). Mammals have two paralogs, Cks1 and Cks2 (Richardson et al., 1990), although in contrast to the yeast Cks, neither appears to be crucial for Cdk function. Their possession of an anion binding pocket suggests that Cks proteins may function in recruiting Cdk1-cyclin B1 complexes to already phosphorylated targets (Bourne et al., 2000).

During interphase, cyclin B1 can shuttle between the nucleus and the cytoplasm but is primarily sequestered in the cytoplasm by a cytoplasmic retention signal (CRS). The active Cdk1-cyclin-B1 complex first concentrates at the centrosome in the cytoplasm, before being abruptly imported into the nucleus about 5 minutes before NEB (Gavet and Pines, 2010; Hagting et al., 1999; Ookata et al., 1992; Pines and

Hunter, 1991). This nuclear accumulation appears to be regulated in part by Plk1 (Jackman et al., 2003; Toyoshima-Morimoto et al., 2001; Yuan et al., 2002) and is dependent on cyclin A2 (De Boer et al., 2008; Fung et al., 2007; Gong et al., 2007). The Cdk1-Cyclin B1 complex then localizes to chromosomes and kinetochores early in mitosis (Bentley et al., 2007). At the metaphase-to-anaphase transition, cyclin B1 is degraded via the APC/C^{Cdc20} in a checkpoint-dependent manner (Clute and Pines, 1999; Jackman et al., 1995; Minshull et al., 1990; Pines and Hunter, 1991). Interestingly, the chromosomal and kinetochor-localized pools of cyclin B1 are the first to disappear as soon as the APC/C becomes active (Bentley et al., 2007; Clute and Pines, 1999). Cyclin B1 degradation leads to Cdk1 down-regulation and subsequently allows for dephosphorylation of nuclear lamins, DNA decondensation and disassembly of the mitotic spindle in preparation for mitotic exit.

Accumulation of cyclin B1 is necessary to trigger entry into mitosis, and degradation of cyclin B1 and thus Cdk1 inactivation is essential for mitotic exit (Murray and Kirschner, 1989; Murray et al., 1989). Accordingly, a nondegradable variant of cyclin B1 arrests cells in mitosis (Holloway et al., 1993; Wheatley et al., 1997).

Another important Cdk complex driving G2 phase and mitotic entry in vertebrate cells is Cdk2 (sometimes Cdk1) in association with cyclin A (Fig. 1). There are 2 subtypes of cyclin A in mammalian cells, A1 and A2, of which cyclin A1 expression is restricted to germ cells, while cyclin A2 is ubiquitously expressed (Sweeney et al., 1996). In mammalian cell lines, cyclin A2 is first detectable during S phase and is degraded independently of the SAC already during prometaphase (den Elzen and Pines, 2001; Geley et al., 2001; Pines and Hunter, 1991). Like cyclin B1, cyclin A2 shuttles dynamically between the cytoplasm and the nucleus during interphase (Jackman et al., 2002). Unlike cyclin B1 however, Cdk-cyclin A2 complexes are active and found entirely within the nucleus in early prophase, suggesting that mitotic entry events like DNA condensation that occur before NEB may rely on Cdk-cyclin A2 activity, while Cdk1-cyclin B1 becomes important at the end of prophase, when cyclin A2 starts being degraded, to initiate processes like NEB and mitotic spindle assembly. In support of this are findings by Gong and colleagues who demonstrated that knockdown of cyclin A2 and even more so of cyclin A2 and cyclin B1 together significantly delayed NEB, while cyclin B1 knockdown alone had only minor effects

on the timing of NEB in HeLa cells (Gong et al., 2007). Furthermore, cyclin A2 appears to play an important role in governing DNA condensation, as this process is severely delayed in cyclin A2 knockdown HeLa cells (Gong and Ferrell, 2010). Thus, it seems as though entry into mitosis is dependent on both cyclin A2 and B1-associated Cdk1 activity, with cylin A2 being able to substitue for cyclin B1, while progression through mitosis absolutely relies on Cdk1-cyclin B1 (Lindqvist et al., 2009).

1.5. Roles of protein phosphatase 2A (PP2A) in cell cycle progression

The level of phosphorylation of a protein is determined by the rates of its phosphorylation and dephosphorylation. Dephosphorylation is catalyzed by phosphatases, which counteract kinase activity by hydrolysing the phosphoester bonds between the hydroxyl groups of specific amino acids and phosphoryl groups.
There is a great discrepancy between the number of Ser/Thr kinases (428) and the corresponding number of catalytic subunits of Ser/Thr phosphatases (30) in the human genome (Johnson and Hunter, 2005; Lander et al., 2001; Venter et al., 2001). This is explained by the fact that many Ser/Thr phosphatase holoenzymes share a common catalytic subunit, and are distinguished by a large number of varying regulatory subunits. Protein phosphatase 2A (PP2A) belongs to the Ser/Thr phosphatase subgroup of phosphoprotein phosphatases, and is also one of the most abundant eukaryotic enzymes. Structurally, the PP2A holoenzyme is a heterotrimeric complex composed of three subunits: a 36 kDa catalytic (PP2A-C) and a 65 kDa scaffolding (PP2A-A) core subunit dimer, associated with a member of one of four families of regulatory subunits (PP2A-B). These regulatory subunit families (PP2A-B/B55, -B'/B56, -B'' and -B''') confer subcellular localization and substrate specificity to the PP2A holoenzyme. Each family can be further subcategorized into various isoforms that are encoded by different genes (the human PP2A-B'/B56 family can be subcategorized into B'/B56-α, -β, -γ, -δ and -ε for example). Including multiple splice variants of some isoforms, at least 16 different regulatory subunits have been characterized to date (Janssens and Goris, 2001; Shi, 2009; Xu et al., 2006; Yang and Phiel, 2010). Although cellular PP2A can generally exist either as a heterodimeric core enzyme (PP2A-A and -C subunits) or as a heterotrimeric holoenzyme, the relative stability of the three subunits seems to be co-regulated, at least in higher eukaryotes. Knockdown of either PP2A-A or -C subunits in *Drosophila*

S2 cells leads to the concomitant disappearance of the regulatory subunits, and vice versa (Silverstein et al., 2002). And also in mammalian cells the PP2A-C and most -B subunits are only stable when they complex with the A subunit (Li et al., 2002; Sablina and Hahn, 2007; Strack et al., 2004; Strack et al., 2002).

Several studies have suggested general roles for PP2A in regulating cell cycle progression and mitotic processes in particular. These include the regulation of the G2/M transition (Goris et al., 1989; Vigneron et al., 2009) as well as the metaphase-to-anaphase transition in both mitosis and meiosis (Chang et al., 2011; Vandre and Wills, 1992). All these studies are based on observations made after chemically inhibiting the catalytic subunit of PP2A using okadaic acid (OAA), a polyether fatty acid isolated from the marine sponge *Halichondria okadai*. OAA specifically inhibits Ser/Thr phosphatases 1 and 2A, the inhibitory effect being strongest for PP2A (with an inhibitory constant (IC_{50}) of 0.1 nM compared to 10 nM for PP1) (Bialojan and Takai, 1988; Cohen et al., 1990; MacKintosh et al., 1990).

PP2A-B'/B56 containing PP2A holoenzymes in particular have previously been shown to interact with shugoshin 1 (Sgo1) at centromeres and function in protecting centromeric cohesin in early mitosis (Kitajima et al., 2006; Riedel et al., 2006; Tang et al., 2006). In interphase, PP2A-B'/B56 family members are largely localized in the cytoplasm, but have the ability to shuttle between nucleus and cyctoplasm (Flegg et al., 2010). Interestingly, human separase can also interact with a PP2A holoenzyme comprising the PP2A-B'/B56 regulatory subunit (Holland et al., 2007). All five isoforms of the B'/B56 regulatory subunit family have the ability to associate with separase, and separase was shown to associate with similar amounts of active PP2A holoenzyme both in G1/S-arrested and mitotic cell populations (Holland et al., 2007). Furthermore, separase auto-cleavage negatively regulates PP2A association, as a non-cleavable separase variant was shown to recruit more PP2A than wild type separase (Holland et al., 2007). For human securin, a direct interaction with PP2A-B/B55 containing PP2A holoenzyme has been reported (Gil-Bernabé et al., 2006).

1.6. Specific characteristics of meiosis

Meiosis is characterized by two consecutive rounds of chromosome segregation, without an intermediate S phase. This leads to the generation of 4 haploid cells that each contain a single homolog (one chromatid) of each chromosome. During sexual reproduction, these haploid cells in the form of gamets (eggs and sperm) fuse to form a diploid zygote, containing one sister chromatid from the maternal and the homolog sister chromatid from the paternal parent. Initial meiotic S phase results in two sister chromatids per homolog, which are linked tightly by cohesins along their entire lengths. During the first meiotic division (MI), the homologous chromosomes are separated. This is achieved by pairing them in tetrads in prophase of MI. Homologous DNA recombination between homologous non-sister chromatids at this stage leads to crossovers that become visible as so-called chiasmata. These crossovers have an important impact on generating genetic variation. As in mitosis, cohesin is essential for mediating cohesion between sister chromatids. Cleavage of the meiotic Scc1 homolog Rec8 (Watanabe et al., 2001) by separase leads to the dissociation of arm cohesin at the metaphase-to-anaphase transition of MI, while centromeric cohesin is protected, thereby keeping sister chromatids together. This protection of centromeric cohesin in anaphase of MI is ensured by shugoshin 2 (Sgo2)-PP2A, similar to the protection of centromeric cohesin in prophase of mitosis by the Sgo1-PP2A complex. Mouse oocytes lacking Sgo2 display a premature release of the meiosis-specific Rec8 cohesin complexes from anaphase I centromeres (Llano et al., 2008). A special prerequisite for the segregation of homologous chromosomes in MI is that both kinetochors of each sister chromatid behave as one entity and attach to microtubules emanating from the same spindle pole. The second meiotic division (MII) then leads to the separation of the sister chromatids in a process very similar to mitosis.

Importantly, in order for cells to progress from meiosis I to meiosis II, Cdk1 must not be inactivated completely as at the end of mitosis. While some Cdk1 targets must be dephosphorylated to enable spindle disassembly, it is absolutety crucial that components of the replication origin for example remain phosphorylated to prevent a round of DNA replication between MI and MII.

During vertebrate spermatogenesis, meiosis results in four haploid spermatids. Due to the asymmetric nature of the cell divisions in vertebrate oogenesis on the other hand, only one oocyte is generated, while three so-called polar bodies are left to degenerate. The oocyte is arrested in metaphase of meiosis II until fertilization. This metaphase II arrest in *Xenopus* oocytes is called cytostatic factor (CSF) arrest and is imparted by xErp1/hEmi2-mediated APC/C^{Cdc20} inhibition (Haccard et al., 1993; Masui and Markert, 1971). In this state, cyclin B1 is stabilized and Cdk1-cyclin B1 activity is high. Fertilization leads to an influx of Ca^{2+} ions, and this triggers the SCF-dependent proteolytic degradation of xErp1/hEmi2. This activates the APC/C^{Cdc20} and oocytes can exit meiosis II (Rauh et al., 2005; Schmidt et al., 2005; Tung et al., 2005). This system can be put to use to study mitotic and meiotic events. Injecting females of the African clawed frog *Xenopus laevis* with the hormone chorionic gonadotropin causes them to lay eggs that are arrested in metaphase of meiosis II (CSF arrest). Extracts made from these eggs (CSF extracts) can be induced to cycle through mitosis-like metaphase II by the addition of Ca^{2+} ions that mimick fertilization. Addition of Ca^{2+} alone triggers progression into interphase. The prior addition of non-degradable cyclin B1Δ90 (cyclin B1 with an N-terminal deletion of 90 amino acids, which comprise its destruction box) maintains high Cdk1-cyclin B1 activity and thereby arrests the extracts in anaphase. Low concentrations of cyclin B1Δ90 merely block mitotic exit, while high concentrations additionally inhibit separase activity (Stemmann et al., 2001).

1.7. Aims of this study

The key issue to be solved after the identification of B'/B56 subunit containing PP2A as a novel interacting partner of human separase is how this phosphatase might be involved in regulating separase activity. Central to answering this question is the identification of PP2A substrate sites as well as a detailed characterization of the PP2A binding site on separase. In addition, the function of separase auto-cleavage has remained enigmatic to date, and this study aims at giving further insights into the nature and purpose of this mechanism, particularly in the light of the identified antagonistic relationship between separase auto-cleavage and PP2A binding (Holland et al., 2007). Furthermore, securin has been reported to interact with B/B55 subunit containing PP2A, and this interaction was reported to protect securin from

SCF-dependent degradation (Gil-Bernabé et al., 2006). In the present study, this reported function of securin as a PP2A substrate will be reassessed with regards to the regulatory PP2A subunit and the degradation mechanism involved. As a starting point towards approaching the above mentioned issues, a quantitative mass spectrometry approach was applied, identifying both separase and securin as substrates of separase-associated PP2A.

2. RESULTS

2.1. Characterization of the separase-securin-PP2A complex composition

Holland et al. (2007) had previously identified the B' (B56) regulatory subunit isoform of PP2A as an interaction partner of separase. On the other hand, Gil-Bernabé et al. (2006) had reported the B (B55) regulatory subunit isoform of PP2A to be a direct interaction partner of securin. It therefore remained to be unambiguously clarified whether PP2A interacts directly with separase or securin (or both), and which isoform of the phosphatase would do so.

2.1.1. Separase forms a heterotrimeric complex with securin and PP2A

To test if separase, securin and PP2A can form a heterotrimeric complex, a tandem affinity purification was performed from mitotic Hek293T cells co-expressing ZZ-TEV-separase and securin-FLAG (Fig. 9). The ZZ-TEV-tag comprises two IgG binding domains of protein A and a tobacco etch virus (Tev) protease cleavage site. In a first purification step, ZZ-TEV-tagged separase was isolated on IgG sepharose and eluted by treatment with Tev protease. From this eluate, securin-FLAG was isolated in a second step using anti-FLAG agarose. Bound proteins were subsequently detected by immunoblotting. As illustrated by the presence of its catalytic subunit, PP2A was present in the tandem affinity purified separase-securin complex (lane 3). This association was specific because in corresponding controls, PP2A did not bind unspecifically to either IgG sepharose (lane 4) or anti-FLAG agarose (lane 5). Thus, a heterotrimeric securin-separase-PP2A complex does indeed exist.

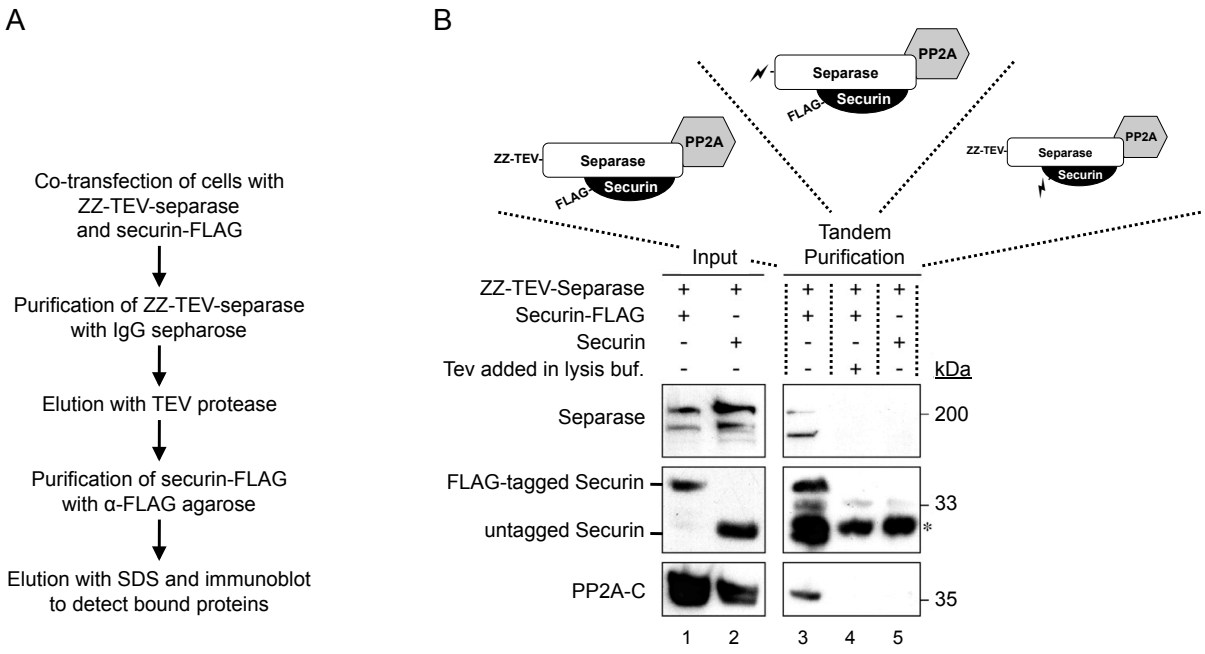

FIGURE 9. Separase forms a heterotrimeric complex with securin and PP2A.

(**A**) Schematic overview of the tandem affinity purification procedure. (**B**) Hek293T cells co-expressing ZZ-TEV-separase and securin-FLAG or untagged securin were synchronized in prometaphase of mitosis with nocodazole. In a first step, ZZ-TEV-separase was purified using IgG sepharose with subsequent Tev protease elution. Released proteins were then purified in a second step over anti-FLAG beads, and bound proteins were detected by immunoblotting. The catalytic subunit of PP2A (PP2A-C) was detected as a representative of the whole PP2A complex. As a control for unspecific binding to IgG sepharose, Tev protease was added already during cell lysis procedure (lane 4). Unspecific association with anti-FLAG agarose was excluded by tandem affinity purification from lysates of cells overexpressing untagged instead of FLAG-tagged securin (lane 5). The asterisk (*) corresponds to the IgG light chain.

2.1.2. PP2A interaction with securin is bridged by separase

To answer the question of whether PP2A within this complex interacts with separase, securin or both, PP2A's association with separase-securin complex *versus* separase-free securin was analyzed. For this purpose, HeLa cells were transfected with expression plasmids coding for untagged separase, securin and PP2A-B'-FLAG, and then arrested in early mitosis. From the corresponding lysate, all separase was removed by immunoprecipitation (IP) using anti-separase beads. Separase-free securin was then isolated from the supernatant of this IP by a second round of immunoprecipitation using anti-securin beads. Finally, proteins bound to immobilized

anti-separase, anti-securin or unspecific IgG (Ctrl) were analyzed by immunoblotting. (Fig. 10). A fraction of the PP2A-B' pool present in the lysate (input) was bound to the separase-securin complex (Sep IP). However, no PP2A-B' signal above background intensity (Ctrl IP) could be detected in the securin IP (Sec IP). Thus, free securin cannot bind PP2A. If they co-purify, then their interaction is indirect, mediated by separase.

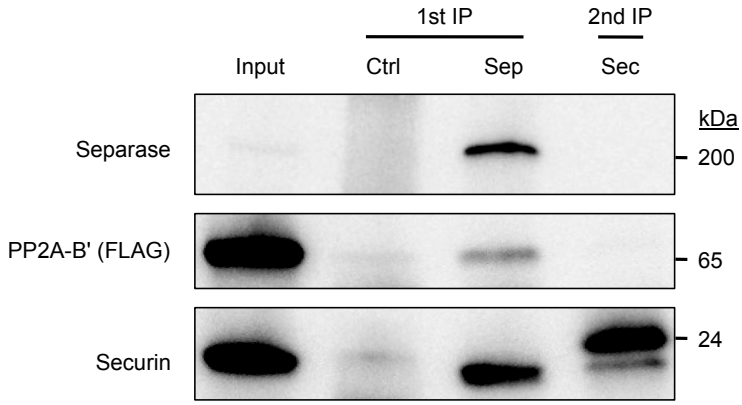

FIGURE 10. PP2A interaction with securin is bridged by separase.

HeLa cells co-expressing separase, securin and PP2A-B'-FLAG were synchronized with nocodazole. Separase-securin complex was precipitated from cell lysate using anti-separase coupled protein G sepharose beads (Sep). In a second step, free securin was precipitated from cell lysate depleted of separase-securin complex using anti-securin coupled protein G sepharose beads (Sec). Proteins were eluted by boiling in sample buffer and detected by immunoblotting. Rabbit unspecific antibody coupled to protein G sepharose beads was used as a control for unspecific binding (Ctrl). Note that free securin (2nd IP) exhibits decreased mobility relative to separase-associated securin (1st IP).

2.1.3. Separase interacts with PP2A-B’ but not -B subunit

The finding of a direct separase-PP2A interaction largely contradicts a previous study by Gil-Bernabé et al. (2006), which claims that securin directly interacts with the B (B55) isoform of PP2A. However, Fig. 10 clearly demonstrates that PP2A interaction with securin is actually bridged by separase, as free securin is not associated with PP2A at all. Furthermore, Holland et al. (2007) identified the B' (B56) as opposed to the B (B55) regulatory subunit isoform of PP2A in a mass spectrometric analysis of separase associated proteins. To ultimately clarify which of these two isoforms of PP2A interacts with separase, FLAG-tagged PP2A-B or -B' were overexpressed in

Hek293T cells together with securin and one of three variants of Myc-tagged separase. More specifically, wild-type (WT) separase was compared to non-cleavable (NC) separase, which binds PP2A more efficiently than WT (Holland et al., 2007), and to a PP2A-binding deficient separase variant (ΔEEEL), which will be described later (Fig. 17). As judged by Myc-immunoprecipitations followed by Western analysis, only PP2A-B' but not -B co-purified with separase, and it did so only with the WT and NC form, as expected (Fig. 11).

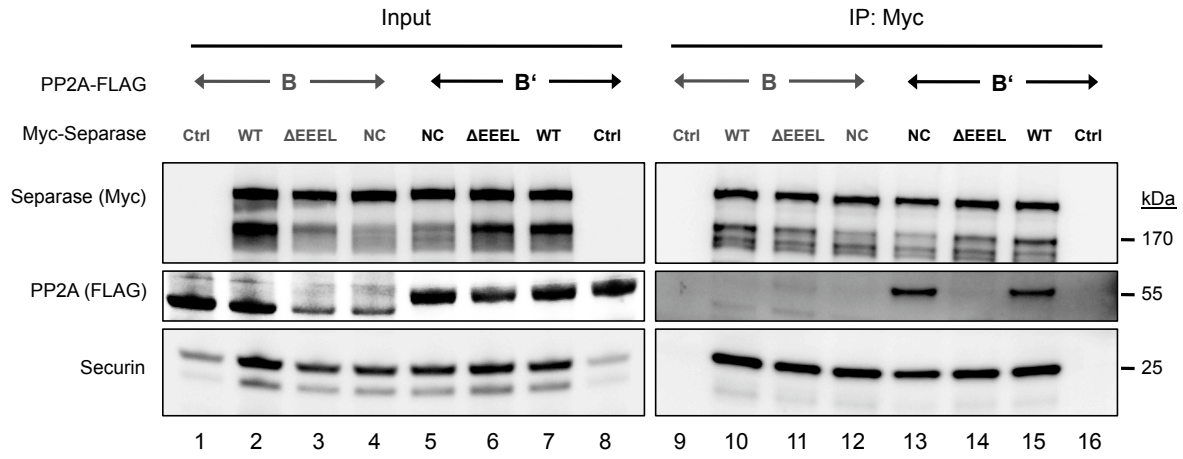

FIGURE 11. Separase interacts with the B' but not the B isoform of PP2A.

Hek293T cells co-expressing Myc-separase variants, untagged securin and PP2A-B-FLAG or PP2A-B'-FLAG were synchronized with nocodazole. An affinity purification was performed using anti-Myc agarose beads with subsequent elution by boiling in SDS sample buffer. For the control samples (Ctrl), the empty Myc expression vector was transfected together with securin and PP2A-B- or B'-FLAG encoding plasmids. Eluted proteins were detected by immunoblotting.

2.2. Identification of PP2A substrate sites on separase and securin

As established so far, separase directly interacts with securin on the one hand, and the B' isoform of PP2A on the other hand to form a heterotrimeric complex. Using a malachite green phosphatase assay, it had previously been shown that the PP2A associated with separase is catalytically active (Holland et al., 2007), raising the question of whether the associated separase and/or securin might be substrate(s) of the phosphatase. Holland et al. (2007) had described a small deletion within separase (amino acids 1419-1473) that resulted in greatly reduced binding of the protease to PP2A. A similar variant, which lacked amino acids 1408-1478 (described in Fig. 17), was now to be quantitatively compared to wild-type separase in terms of phosphorylation status of the protease and associated securin.

2.2.1. Both separase and securin are substrates of separase-bound PP2A

To map and quantitatively assess phosphorylation sites on separase and/or securin, a SILAC (Stable Isotope Labeling with Amino acids in Cell culture) mass spectrometric approach was embarked upon (Fig. 12A). For this technique, one group of cells was metabolically labeled through growth in medium supplemented with 'heavy' forms of particular amino acids, in this case arginine (R10: $^{13}C_6$,$^{15}N_4$) and lysine (K8: $^{13}C_6$, $^{15}N_2$). At the same time, a second group of cells was grown in the corresponding normal 'light' cell culture medium (R0/K0). After 6 cell doublings, the 'light' cells were transfected to overexpress ZZ-TEV-separase, while the 'heavy' cells were transfected to overexpress ZZ-TEV-separase$^{\Delta PP2A}$. Untagged securin was co-expressed in both cases. Following a cell cycle arrest in mitosis, the cells were lysed in the presence of phosphatase inhibitors to preserve phosphorylations. From these lysates the corresponding separase-securin complexes were purified over IgG sepharose and eluted by Tev protease treatment. The two eluates were characterized by Coomassie-staining and immunoblotting to ensure comparable amounts of separase and securin in both samples (Fig. 12B, C). The eluates were subsequently combined, resolved by SDS-PAGE and stained with Coomassie. The separase and securin bands were excised and digested in-gel using endoproteinases trypsin and AspN. Following an enrichment of phosphorylated peptides on a TiO_2 matrix, the peptides were analyzed by mass spectrometry. Owing to the fact that peptides of the ΔPP2A separase variant are heavier by 10 Da per arginine and by 8 Da per lysine residue, they could easily be distinguished from the chemically identical but lighter peptides of wild-type separase. Hence, the ratio of peak intensities for any given peptide pair in the resulting mass spectrum directly correlates with the abundance ratio of the two peptides. Generally, a 'heavy'-to-'light' ratio of ≥ 2 or ≤ 0.5 indicates a significant difference in the phosphorylation status under the two conditions.

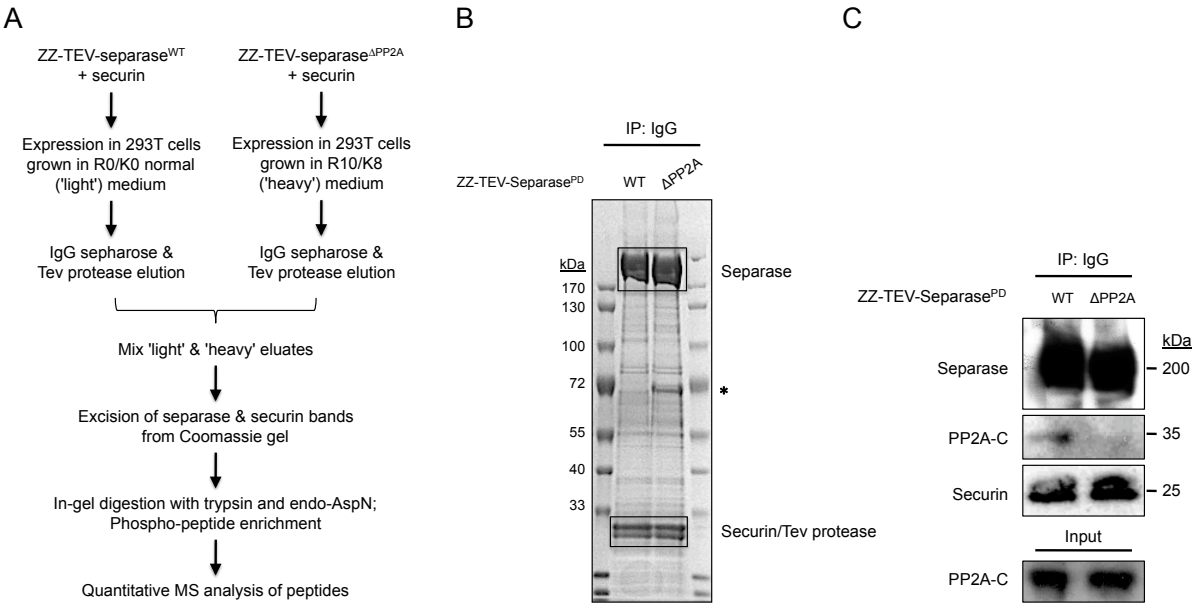

FIGURE 12. Isolation of differentially labeled, PP2A-less or -containing separase-securin complexes for comparative, quantitative mass spectrometry.

(**A**) Schematic overview of the SILAC (Stable Isotope Labeling with Amino acids in Cell culture) mass spectrometric approach. (**B**) Coomassie-stained gel of the two affinity purified separase-securin complexes before they were combined. Separase and securin bands that were later excised from the corresponding Coomassie gel of the mixed eluates are indicated (boxes). The asterisk (*) marks the height of the C-terminal auto-cleavage fragment of separase. (**C**) Immunoblot of the two affinity purified separase-securin complexes before they were combined. Note: the catalytic subunit of PP2A (PP2A-C) that was detected here as a representative of the whole PP2A complex is absent from the purified ΔPP2A (Δ1408-78) separase-securin complex as expected. The subsequent mass-spectrometric analysis was performed by C. Pan in the lab of M. Mann (MPI for Biochemistry, Martinsried).

This analysis identified both separase and securin as substrates of separase-bound PP2A, because for both proteins peptides whose phosphorylation status differed significantly within the two samples were found (Fig. 13 and 18). Phosphorylation sites within separase (Fig. 13) that were altered in their phosphorylation status between the ΔPP2A variant as compared to the wild-type cluster in two regions, i.e. the Cdc6-like domain (CLD, amino acids 1342-1400) and the vicinity of the main auto-cleavage site (ER1503/6). For securin (Fig. 18), the identified PP2A substrate residues largely mapped to the N-terminus, in close proximity to securin's KEN- and D-box. The following chapters will take a closer look at the identified PP2A substrate sites on both separase (chapter 2.2.2.) and securin (chapter 2.2.4.) and, with the help of appropriate follow-up experiments, will try to put these results into a functional context.

A SILAC results for separase

aa	ratio H/L (norm.)	Peptide sequence and phosphorylated residue	Phosphorylated residue (green: upregulated; red: downregulated in ΔPP2A mutant)
1387-1392	3.79	VQTRLK	T1389
1499-1506	2.45	KMSFEILR	S1501
1330-1341	2.22	LNNTSQKGLEGR LNNTSQKGLEGR	T1333 S1334
1500-1518	0.20	MSFEILRGSDGEDSASGGK MSFEILRGSDGEDSASGGK	S1508/S1513 S1508/1515
1519-1535	0.30	TPAPGPEAASGEWELLR	T1519

B

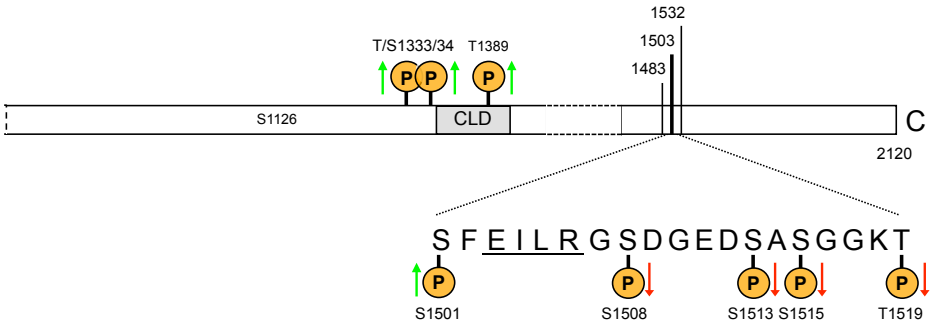

FIGURE 13. Separase is a substrate of separase-associated PP2A.

(**A**) PP2A substrate sites identified within separase by quantitative mass-spectrometric analysis (SILAC approach, see Fig. 12). Residues depicted in green represent sites that are hyper-phosphorylated in the absence of PP2A from separase-securin complexes. Residues depicted in red indicate a corresponding hypo-phosphorylation. (**B**) PP2A substrate sites within separase map to two locations: sites within or close to the Cdc6-like domain (CLD) and sites in proximity of separase's main auto-cleavage site (underlined). Green arrows show upregulated phosphorylation in the absence of PP2A. Correspondingly, red arrows show dephosphorylation in the absence of PP2A. This experiment was independently conducted two times. However, while the second experiment qualitatively confirmed most residues of the first experiment, the differences in phosphorylation were less pronounced overall. This might have been due to incomplete labeling of the cells prior to transfection and less material being used. Therefore, only results of one experiment are depicted here. H = 'heavy' peptides, L = 'light' peptides; ratios were normalized (norm.) to those of unrelated, unphosphorylated peptide pairs.

2.2.2. What is the role of PP2A-dependent dephosphorylation of separase?

An obvious possibility is that PP2A counteracts the phosphorylation-dependent binding and inhibition of separase by cyclin B1-Cdk1. Indeed, one separase residue within and two residues close to the Cdc6-like domain (CLD, amino acids 1342-1400) exhibited markedly increased phosphorylation in the absence of PP2A, i.e. in the ΔPP2A variant compared to wild-type separase (Fig. 13). The CLD constitutes the cyclin B1 binding site of separase and has previously been carefully mapped and extensively characterized (Boos et al., 2008). Although the binding of cyclin B1 occurs in a phosphorylation-dependent manner, the three residues identified here lie either just outside the CLD (Thr1333 and Ser1334) or have no measurable impact on cyclin B1 binding (Thr1389). Moreover, the phosphorylation status of Ser1126, whose Cdk1-dependent phosphorylation is an essential prerequisite for binding and inhibition of separase by cyclin B1-Cdk1, was not changed in the ΔPP2A variant compared to wild-type separase. Consistent with this, cyclin B1-Cdk1 binding to the ΔPP2A variant is not increased relative to wild-type separase (Holland et al., 2007). Thus, contrary to the intuitive model, PP2A does not seem to antagonize the phosphorylation dependent inhibition of separase by cyclin B1-Cdk1.

2.2.2.1. PP2A counteracts phosphorylation-dependent cleavage of separase

The phosphorylation status of a second region on separase appeared to be heavily influenced by PP2A. Ser1501, just 6 amino acids upstream of the major auto-cleavage site on separase (ER1503/6), was significantly hyper-phosphorylated in the ΔPP2A separase variant. To further characterize Ser1501 phosphorylation and identify relevant kinases, the AQUA (Absolute Quantification of proteins) method (Gerber et al., 2003) was applied. Briefly, two standard peptides were synthesized to resemble tryptic separase peptides containing Ser1501 in its phosphorylated or dephosphorylated state. A leucine residue at the C-terminal end of these peptides contained stable isotopes, enabling the distinction by mass-shift of these synthetic peptides from the corresponding native peptides formed by proteolysis. Affinity-purified separase was then incubated with different kinases or reference buffers in the presence of ATP. Following separation by SDS-PAGE, separase bands were digested in-gel with trypsin in the presence of defined amounts of the AQUA

peptides. Finally, peptides were extracted and quantitatively analyzed by mass spectrometry. In this manner, it was found that Ca^{2+}/calmodulin-dependent protein kinase (CaMKII) and protein kinase A (PKA) but not cyclin B1-Cdk1 or Polo kinase can phosphorylate separase at Ser1501 (Gerber et al., 2003). Consistently, this site indeed constitutes a consensus phosphorylation site for both CaMKII (R-X-X-S/T) as well as PKA (R-R/K-X-S/T), as annotated in the 'Phosphorylation Site Database' (PHOSIDA). In *S. cerevisiae* it is known that cleavage of cohesin subunit Scc1 by separase is enhanced by phosphorylation of a serine residue at the same relative position of -6 (Alexandru et al., 2001). To answer the question if auto-cleavage of human separase is also stimulated by phosphorylation, HA-tagged separases were expressed that lacked the first and third auto-cleavage sites (R1486A and R1535A) and were catalytically inactive (C2029S). One of two such variants additionally had Ser1501 replaced by Ala. The two variants were purified from Hek293T cells using anti-HA agarose beads, phosphorylated by PKA *in situ*, competitively eluted with HA peptide, and then used as substrates for active, untagged separase in a cleavage assay (Fig. 14A). Analysis by anti-HA immunoblot showed that auto-cleavage was more efficient when separase could still be phosphorylated at position 1501 (Fig. 14B). Thus, similar to the situation with *S. cerevisiae* Scc1, phosphorylation just upstream of the major cleavage site renders separase a better substrate for itself. Together with the fact that this site is a substrate for PP2A, one can conclude that PP2A antagonizes the auto-cleavage of separase by dephosphorylation of Ser1501.

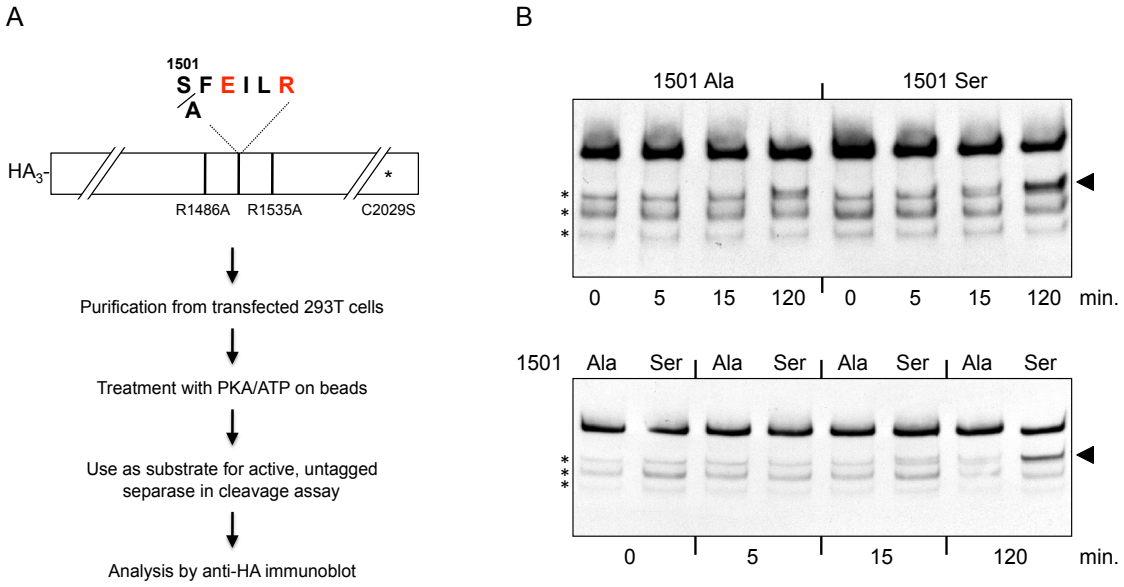

FIGURE 14. Phosphorylation of Ser1501 promotes separase auto-cleavage.

(**A**) Two HA_3-tagged separase variants (R1486A, R1535A, C2029S and either S1501A or S1501S) were purified from Hek293T cells using anti-HA agarose, treated with PKA and ATP on beads, and used as substrates for active, untagged separase in an *in vitro* cleavage assay. Proteins were eluted by boiling in SDS sample buffer and analyzed by anti-HA immunoblot. (**B**) The two blots contain the same samples, loaded in two different ways. Asterisks (*) show irrelevant bands, arrow heads (◀) mark separase's N-terminal cleavage fragment. This experiment was performed by O. Stemmann.

2.2.2.2. Separase-PP2A association is not phosphorylation-dependent

An unexpected result was obtained for a stretch of phosphorylation sites between the 2nd (ER1503/6) and 3rd (ER1532/5) auto-cleavage site on separase: here, the degree of phosphorylation decreased in the absence of PP2A. Ser1508, Ser1513, Ser1515 and Thr1519 are all significantly hypo-phosphorylated in the ΔPP2A variant relative to wild-type separase (Fig. 13A and B). This result seems counter-intuitive, as one would expect increased phosphorylation in the absence of the phosphatase. Interestingly, phosphorylation of xErp1/Emi2 has been reported to result in the association of PP2A with this meiotic inhibitor of APC/C (Wu et al., 2007). Importantly, the relevant phosphorylation sites are not substrates but rather part of the PP2A binding motif and, as such, protected from dephosphorylation. Assuming a similar scenario in separase, one could speculate that the region, which is less phosphorylated in the absence of PP2A, is, in fact, part of a larger PP2A binding site

of separase. It is possible that this cluster of phosphorylations is protected from dephosphorylation when covered by PP2A. To test this possibility, variants were generated, in which the corresponding Ser/Thr phosphorylation sites (Ser1508, Ser1513, Ser1515 and Thr1519) were mutated to Ala or Asp, to prevent or mimick their phosphorylation, respectively (Fig. 15B*;* 4xA and 4xD variant). After expression of the corresponding ZZ-TEV-separase variants together with securin and PP2A-B' and subsequent affinity purification over IgG sepharose, separase-associated proteins were analyzed by immunoblotting. However, none of the two variants showed an altered association with PP2A in comparison to wild-type separase.

It had been shown that mutation of the phosphorylation sites S335 and T336 or of a nearby SQSE motif in xErp1/Emi2 largely abrogated PP2A binding (Wu et al., 2007). Based on a sequence alignment of this characterized PP2A binding motif of xErp1/Emi2 with the auto-cleavage region of separase, another separase variant was designed and subsequently analyzed with regard to PP2A binding (Fig. 15C). First, four potentially important residues were replaced by alanines. In addition, the major auto-cleavage site was inactivated (ER1503/6AA) to ensure that potential alterations in the amount of bound PP2A were not due to auto-cleavage mediated loss of PP2A (see chapter 2.2.3. below). Finally, PP2A interaction with this 6xA separase variant was analyzed. However, similar amounts of PP2A co-immunoprecipitated with 6xA and wild-type separase. Therefore, the Ser/Thr residues around separase's main auto-cleavage site, which are less phosphorylated in the absence of PP2A, are nevertheless not involved in PP2A binding.

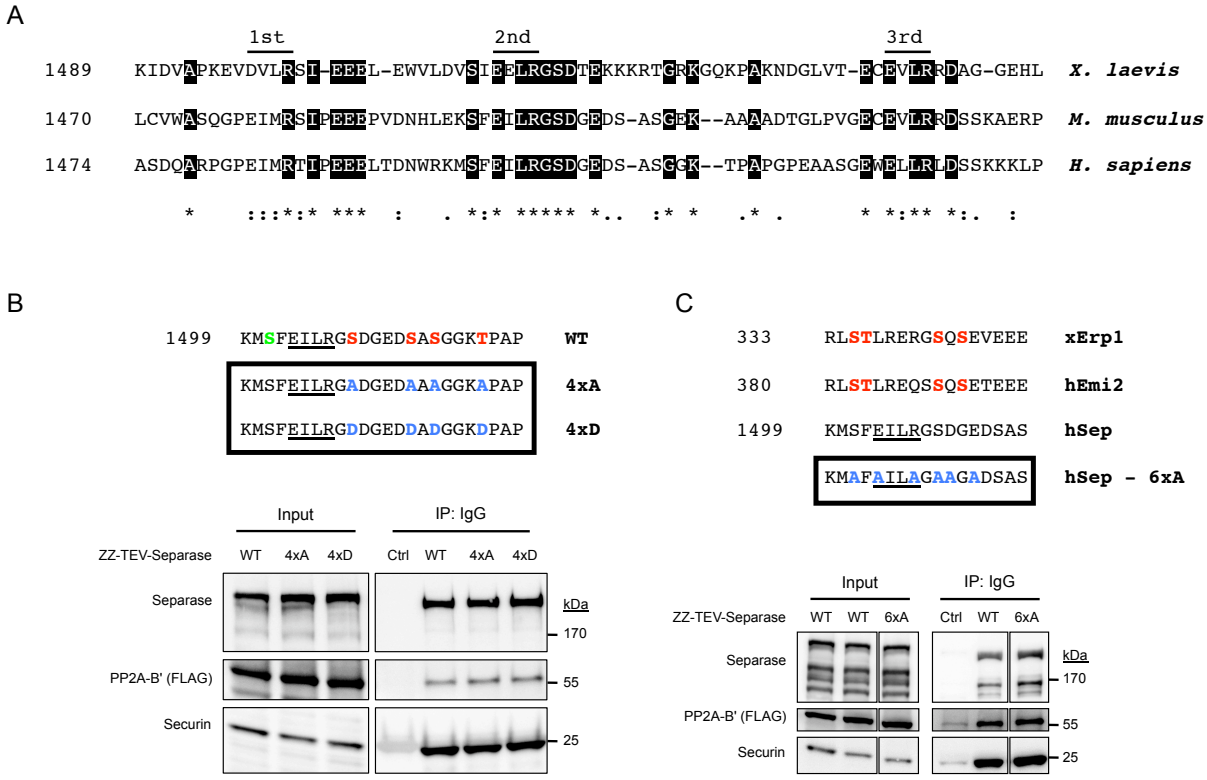

FIGURE 15. Ser/Thr residues around separase's main auto-cleavage site are not involved in PP2A binding.

(**A**) Alignment of *Xenopus*, mouse, and human separase sequences around the auto-cleavage region. Sequences were taken from the GenBank sequence database and alignment was carried out using the ClustalW sequence alignment program. The numbers on the left side show the positions of the corresponding amino acids. The conserved ExxR auto-cleavage motifs are marked (1st, 2nd and 3rd auto-cleavage site). Identical residues among all three species are shaded in black and marked (*), conserved substitutions are marked (:) and semi-conserved substitutions are marked (.) (**B**) The Ser/Thr residues downstream of separase's 2nd auto-cleavage site (underlined), which were collectively hypo-phosphorylated (red) in the ΔPP2A separase variant (SILAC experiment, Fig. 13), were mutated to Ala or Asp, respectively (blue). The upregulated Ser1501 residue is highlighted in green. Hek293T cells co-expressing these ZZ-TEV-separase variants, untagged securin and PP2A-B'-FLAG were synchronized with nocodazole. An affinity purification was performed using IgG sepharose with subsequent Tev protease elution. For the control sample (Ctrl), Tev protease was added already during cell lysis procedure. Eluted proteins were detected by immunoblotting. (**C**) Alignment of mapped PP2A binding motifs on xErp1/hEmi2 (red) and the corresponding residues on separase, which partially overlap with the stretch of downregulated Ser/Thr sites identified in the SILAC screen (Fig. 13). ST336AA and S342/344A mutations in xErp1/hEmi2 are impaired in their ability to bind PP2A (Wu et al., 2007). Hek293T cells co-expressing corresponding ZZ-TEV-separase variants, untagged securin and PP2A-B'-FLAG were synchronized with nocodazole. An affinity purification was performed using IgG sepharose with subsequent Tev protease elution. For the control sample (Ctrl), Tev protease was added already during cell lysis procedure. Eluted proteins were detected by immunoblotting.

2.2.3. Separase's PP2A-binding and auto-cleavage sites partially overlap

As established before (Holland et al., 2007) and now supported by data from the SILAC screen, PP2A binding and separase auto-cleavage exhibit an antagonistic relationship. This is further exemplified by the finding that ΔPP2A separase shows increased auto-cleavage (Fig. 12B**,** asterisk). *Vice versa*, Holland and colleagues could show that a non-cleavable (NC) separase variant showed increased PP2A binding. Accordingly, cleavage of separase might destroy the PP2A binding site and result in the release of the phosphatase from the protease. To test this prediction, the main cleavage site of separase (ER1503/6) was either rendered non-cleavable (NC, ExxR to RxxE) or replaced by a Tev protease cleavage site (NC^{TEV}). In addition, both variants had their first and third auto-cleavage sites destroyed and were expressed as Myc-tagged fusion proteins in Hek293T cells. While securin and PP2A-B'-FLAG were always co-expressed, Tev protease was either included or left out. Corresponding cell lysates were passed over anti-Myc agarose and captured proteins analysed by immunoblotting. As shown in Fig. 16, NC^{TEV} separase was very effectively cleaved by Tev protease (lanes 4 and 8), while NC separase remained unperturbed (lanes 2 and 6). As expected, cleavage by Tev protease indeed induces PP2A dissociation from separase (lane 8), although not to 100%. This is likely due to the fact that residual amounts of full-length separase are still present. This result is in accordance with findings by Holland and colleagues (Holland et al., 2007), which show that PP2A purified from cells is predominantly associated with full-length as opposed to cleaved separase, in contrast to securin and cyclin B1, which both also associate with a cleaved pool of separase.

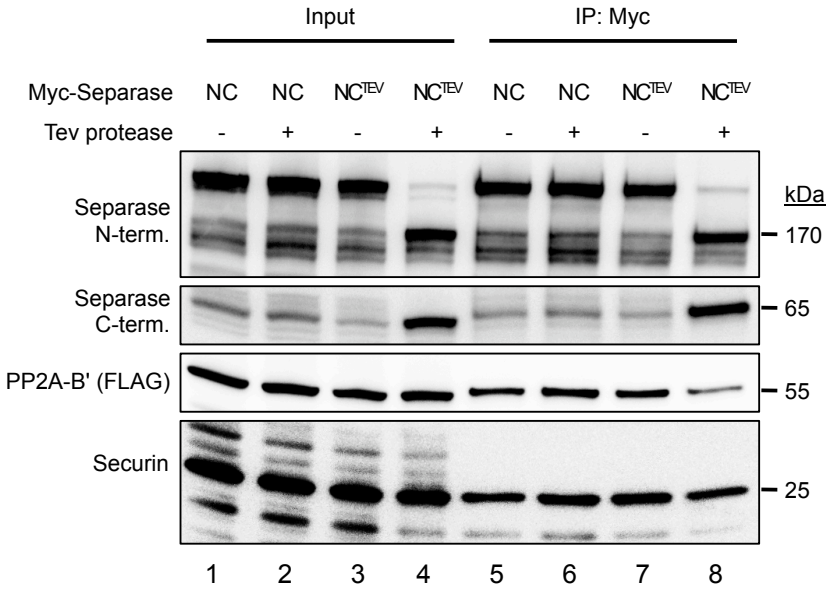

FIGURE 16. Separase cleavage induces partial PP2A dissociation.

Hek293T cells co-expressing non-cleavable (NC) Myc-separase^{3xNC} or Tev-protease cleavable (NC^{TEV}) Myc-separase$^{2xNC/1xTEV\ site}$, untagged securin, PP2A-B'-FLAG and untagged Tev protease were synchronized with nocodazole. An affinity purification was performed using anti-Myc agarose beads with subsequent elution by boiling in SDS sample buffer. Eluted proteins were detected by immunoblotting.

The hyper-recruitment of PP2A to NC separase was largely but not completely abolished by a 55 amino acid deletion (Δ1419-1473) upstream of the auto-cleavage sites (Holland et al., 2007). This suggests that additional sites on separase may be involved in PP2A association. In a quest to characterize the PP2A binding domain on separase to a more complete extent, a fine-mapping was conducted. To this end, ZZ-TEV separase variants were generated in which different amino acid stretches within the characterized 55 amino acid PP2A binding domain but also beyond this region were deleted. Due to the importance of the auto-cleavage sites in PP2A binding behavior, a small deletion between the 1st and 2nd major cleavage sites on separase was also tested (Fig. 17A). All ZZ-TEV-separase variants were co-expressed in Hek293T cells together with securin and PP2A-B'-FLAG. Purification of separase-securin-PP2A complexes from mitotic lysates was done by IgG sepharose and Tev-protease elution. Bound proteins were then detected by immunoblotting. In one sample, the ZZ-tag was removed from separase by addition of Tev protease prior to the affinity matrix (Fig. 17B, lane 10). Non-cleavable (NC) separase (lane 13) and protease-dead (PD) separase (lane 12), i.e. separase's with mutations that alleviate

separase auto-cleavage, show increased PP2A binding compared to wild-type separase (lane 11) as expected. A ΔCLD variant also showed increased PP2A binding (lane 19). Surprisingly, dissecting the characterized Δ55 amino acid domain (Δ1419-1473) even further (lanes 15 and 16) did not increase associated PP2A levels, and likewise, expansion of this domain by a few amino acids on either side (Δ1408-1478, lane 17) had no diminishing effect on PP2A binding. The same amount of residual PP2A was associated with all these variants, arguing for only an indirect involvement of this domain in binding PP2A. Strikingly, deleting only 4 amino acids (Δ1490-1493; ΔEEEL) between the 1st and 2nd auto-cleavage site completely abolished PP2A association with separase (lane 14). An alignment of this region on human separase with the corresponding *Xenopus* and mouse separase sequences (Fig. 17C) revealed a conservation of the EEE motif between species, suggesting that this may indeed constitute a relevant PP2A binding site on separase. As demonstrated by the enhanced cleavage after Ser1501 phosphorylation (Fig. 14) and the identification of this Ser1501 residue as a substrate of PP2A in the SILAC screen (Fig. 13), PP2A can catalytically disrupt separase auto-cleavage. Here it was now shown that on top of this catalytic block, there also seems to be a sterical hinderance of auto-cleavage by PP2A, owing to the fact that the PP2A binding and auto-cleavage sites partially overlap.

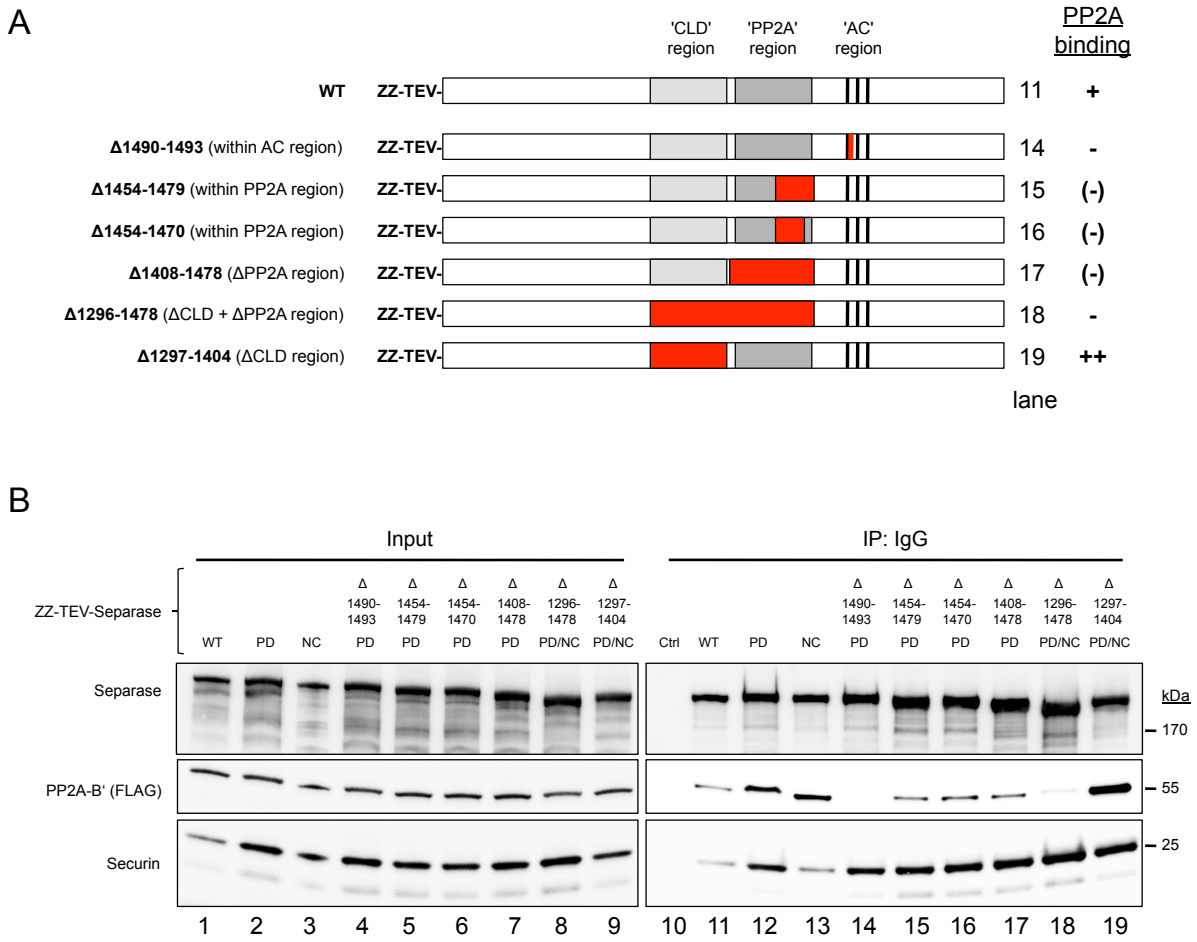

FIGURE 17. Fine-mapping of the PP2A-binding site on separase.

(**A**) Schematic representation of human separase variants, showing the CLD region, the PP2A binding region and the auto-cleavage sites (AC). Deleted regions are highlighted in red. (**B**) Hek293T cells co-expressing ZZ-TEV-separase variants, untagged securin and PP2A-B'-FLAG were synchronized with nocodazole. An affinity purification was performed using IgG sepharose with subsequent Tev protease elution. For the control sample (Ctrl), Tev protease was added already during cell lysis procedure. Eluted proteins were detected by immunoblotting. (**C**) Excerpt of alignment (Fig. 15A) around separase's 1st auto-cleavage site (ExxR motif underlined). Conserved residues between *Xenopus*, mouse, and human separase sequences are shaded in black. In an otherwise poorly conserved sequence stretch, the EEE motif (highlighted in red) which, when deleted (Δ1490-93, ΔEEEL) abolishes PP2A binding to separase (Fig. 17A, B), is conserved between species.

2.2.4. Implications of securin as a PP2A substrate

2.2.4.1. Separase stabilizes bound securin by PP2A-mediated de-phosphorylation

For securin, the PP2A substrate residues identified in the SILAC screen largely mapped to the N-terminus (Fig. 18A and B). The phosphorylation status of Ser31, Thr66 and Ser87/89 on securin bound to a ΔPP2A separase variant was significantly increased compared to securin in complex with wild-type separase. This seems coherent with observations made in previous experiments. Firstly, when separase-bound securin is compared to separase-free securin in mitotic cells (Fig. 10), securin in complex with separase indeed exhibits an increased electrophoretic mobility compared to the bulk of free securin (Sep IP vs. Sec IP), arguing that it is hypo-phosphorylated. Furthermore, when securin bound to wild-type separase is compared to securin bound to a ΔPP2A separase variant in lysates where phosphorylations are conserved by the addition of phosphatase inhibitors (Fig. 12C), a prominent second securin band with slower gel mobility (indicating hyper-phosphorylation) appears in the ΔPP2A separase-securin complex. These findings strongly argue that separase-bound PP2A keeps separase-associated securin dephosphorylated.

A SILAC results for securin

aa	ratio H/L (norm.)	Peptide sequence and phosphorylated residue	Phosphorylated residue (upregulated in ΔPP2A mutant)
22-35	4.25	DGLKLGSGP<u>S</u>IKAL	S31
62-69	3.76	KALG<u>T</u>VNR	T66
63-69	2.47	ALG<u>T</u>VNR	
83-91	2.25	QKQP<u>S</u>FSAK	S87
85-91	2.57	QP<u>S</u>F<u>S</u>AK	S87/89

B

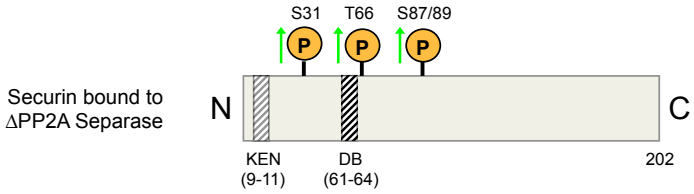

FIGURE 18. Securin is a substrate of separase-associated PP2A.

(**A**) PP2A substrate sites identified within securin by quantitative mass-spectrometric analysis (SILAC approach, see Fig. 12). Residues depicted in green represent sites upregulated in their phosphorylation status in the ΔPP2A separase variant over wild-type separase. (**B**) Schematic location of PP2A substrate sites on securin. Green arrows indicate upregulated phosphorylation in the absence of PP2A. This experiment was independently conducted two times. However, while the second experiment qualitatively confirmed most residues of the first experiment, the differences in phosphorylation were less pronounced overall. This might have been due to incomplete labeling of the cells prior to transfection and less material being used. Therefore, only results of one experiment are depicted here. H = 'heavy' peptides, L = 'light' peptides; ratios were normalized (norm.) to those of unrelated, unphosphorylated peptide pairs.

Securin's KEN- and D-box (amino acids 9-11 and 61-64, respectively) constitute the recognition motifs for the APC/C and are essential for securin's proteasomal degradation. Considering the proximity of the identified PP2A substrate residues on securin to these destruction motifs, one could imagine that separase plays a part in stabilizing bound securin via dephosphorylation by PP2A in this complex. To analyze if dephosphorylated, separase-bound securin is in fact stabilized over free, phosphorylated securin, a cycloheximide (CHX) shut-off experiment was conducted (Fig. 19A). To this end, stable HeLa FlpIn cell lines were generated that express FLAG-tagged securin upon tetracycline induction (Fig. 20). Stable wild-type securin

expressing cells were thymidine-nocodazole synchronized to quantitatively arrest them in prometaphase, when securin levels in the cell are highest, i.e. just before bulk APC/C activity is switched on. After addition of CHX to prevent re-synthesis of securin, cells were harvested in intervals of 2 hours over a 10 hour period. In a first round of immunoprecipitation, separase-securin complexes were depleted from the lysates by separase IP. From the remaining, separase-free supernatants, free securin was then purified by anti-FLAG IP. Heterogeneous phosphorylations can result in broadened migration behavior in SDS-PAGE and, consequently, be misinterpreted as degradation. Therefore, immunoprecipitated samples were treated with λ-phosphatase prior to analysis to ensure that securin would run as one distinct band. While separase-bound securin levels showed no alteration over 6 hours, free securin levels had already decreased to less than half the initial amount after 4 hours. Thus, the degradation kinetics of separase-bound securin were considerably slower than those of free securin (Fig. 19C). Owing to the cytotoxic effects of CHX, cells began to become apoptotic after 8 hours. This is mirrored in the rising sub-G1 phase cell content (Fig. 19B) and also in the declining separase levels after 10 hours (Fig. 19C). A similar stabilization of separase-bound securin was obtained for endogenous proteins in normal HeLa cells (data not shown; S. Hellmuth, master thesis in the lab of O. Stemmann, 2010). Here, free securin started being degraded already after 2 hours, and no free securin could be detected on the immunoblot after 8 hours. In contrast, separase-bound securin remained completely stable over 8 hours, and slowly started dissapearing only after 10 hours, probably as a consequence of apoptosis as judged by the accompanying DNA content profiles. Therefore, free securin is less stable than separase-associated securin and slowly proteolysed even in prometaphase-arrested cells.

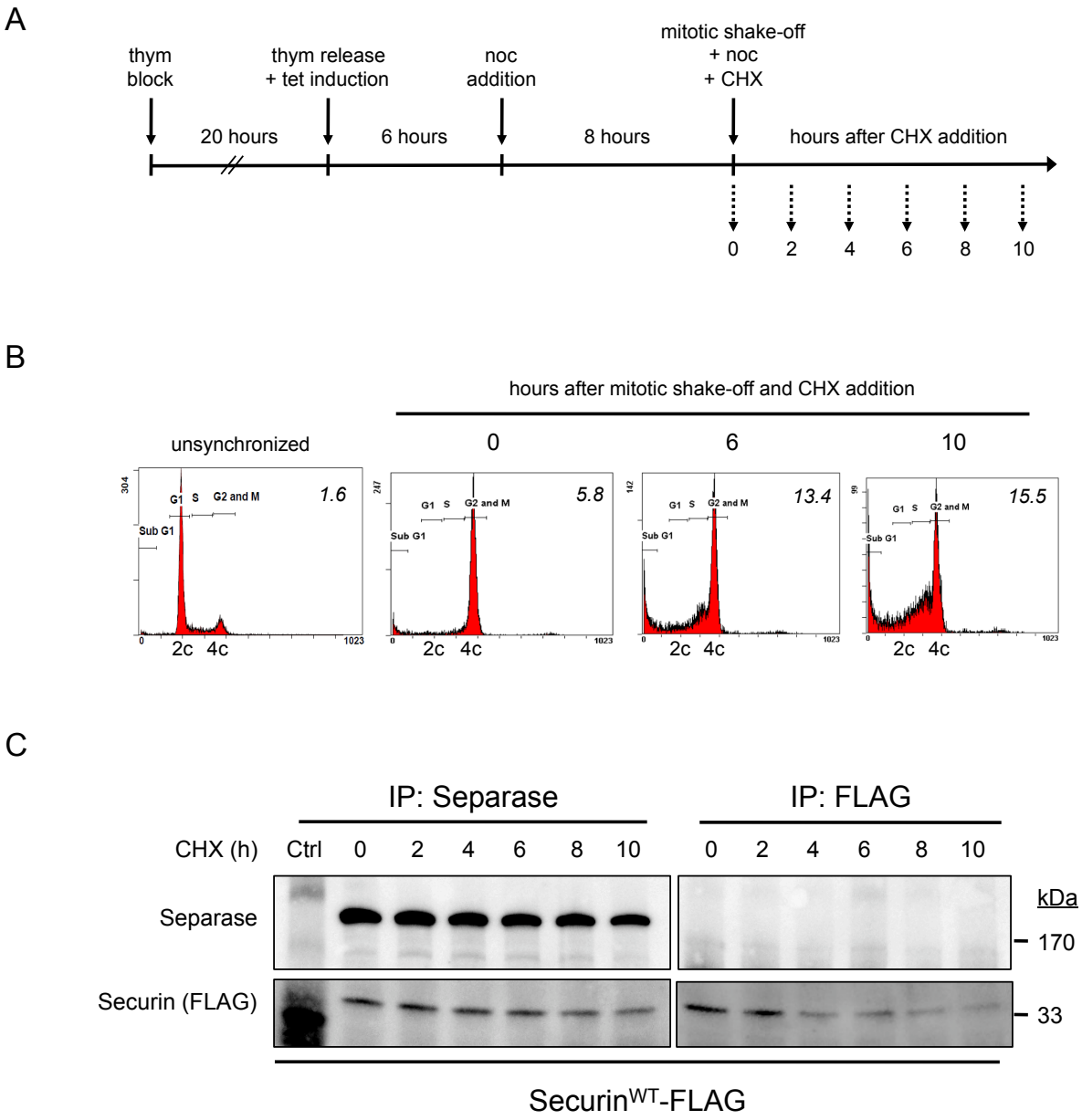

FIGURE 19. Free securin is degraded faster than separase-bound securin.

(**A**) HeLa FlpIn cell lines were synchronized in prometaphase with thymidine (thym) and nocodazole (noc) as indicated, and tetracycline (tet) induced to overexpress securin^{WT}-FLAG. After mitotic shake-off, cells were held in nocodazole and treated with cycloheximide (CHX) over 10 h. Cells were harvested at the indicated time points. (**B**) DNA content profiles of cells before and after synchronization and CHX treatment. *Numbers* represent the sub G1 population (%) as an indicator of apoptosis. c represents the DNA content. (**C**) Separase-securin complexes were isolated by anti-separase coupled to protein G sepharose beads and eluted by boiling in sample buffer. Free securin was isolated from lysates depleted of separase-securin complex by anti-FLAG coupled to protein G sepharose beads, λ-phosphatase treated and eluted by boiling in sample buffer. Proteins were detected by immunoblotting.

A

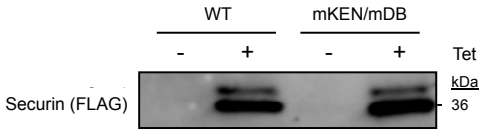
WT
mKEN/mDB
- + - +
Tet
Securin (FLAG)
kDa
36

B

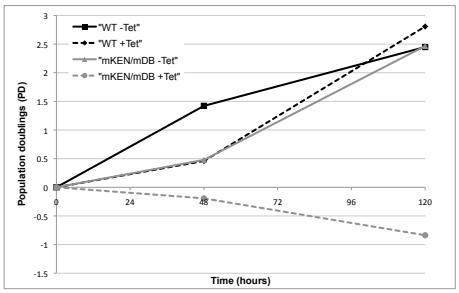
"WT -Tet"
"WT +Tet"
"mKEN/mDB -Tet"
"mKEN/mDB +Tet"
Population doublings (PD)
Time (hours)

C

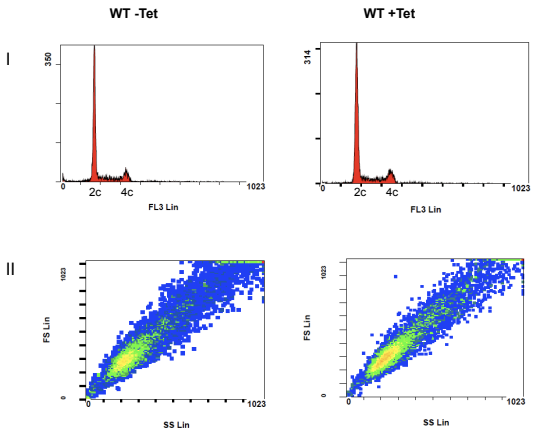
WT -Tet
WT +Tet
I
II
FL3 Lin
FS Lin
SS Lin

D

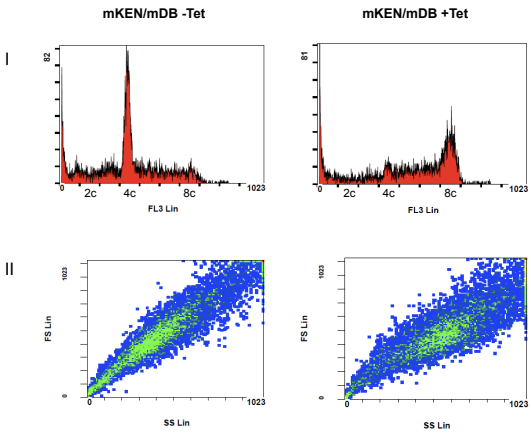
mKEN/mDB -Tet
mKEN/mDB +Tet
I
II
FL3 Lin
FS Lin
SS Lin

E

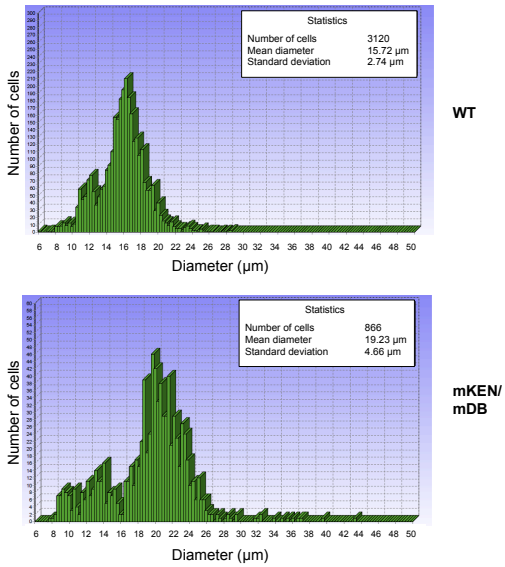
Statistics
Number of cells 3120
Mean diameter 15.72 µm
Standard deviation 2.74 µm
Number of cells
Diameter (µm)
WT
Statistics
Number of cells 866
Mean diameter 19.23 µm
Standard deviation 4.66 µm
Number of cells
Diameter (µm)
mKEN/
mDB

F

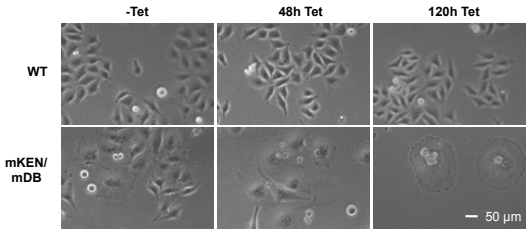
-Tet
48h Tet
120h Tet
WT
mKEN/
mDB
50 µm

FIGURE 20. Characterization of stable securin HeLa FlpIn cell lines.

(**A**) HeLa FlpIn cell lines were tetracycline (Tet)-induced for 14 h to overexpress securin^{WT}-FLAG or securin$^{mKEN/mDB}$-FLAG. Securin was purified from cell lysates using anti-FLAG beads, resolved by SDS-PAGE, and analysed by immunoblotting. (**B**) Growth curves of induced and uninduced HeLa FlpIn securin clones over 120 h. Population doubling (PD) times were calculated using the formula (log N-log N_0)/log 2, N being the final and N_0 the initial cell number for each time point. Similar growth behavior was observed in 2 independent experiments. (**C**) DNA content and granularity profiles of stable HeLa FlpIn clones overexpressing FLAG-securin^{WT} upon tetracycline (Tet) induction. Cells were fixed, stained with propidium iodide and analyzed by FACS. (**i**) DNA content profiles: *x* axis, fluorescence units; *y* axis, number of cells; c represents the DNA content (**ii**) Granularity profiles: *x* axis, granularity units; *y* axis, arbitrary cell size units. (**D**) DNA content and granularity profiles of stable HeLa FlpIn clones overexpressing FLAG-securin$^{mKEN/mDB}$ upon tetracycline (Tet) induction. Cells were fixed, stained with propidium iodide and analyzed by FACS. (**i**) DNA content profiles: *x* axis, fluorescence units; *y* axis, number of cells; c represents the DNA content. (**ii**) Granularity profiles: *x* axis, granularity units; *y* axis, arbitrary cell size units. (**E**) Viable cell diameter distribution of uninduced stable securin HeLa FlpIn clones (WT or mKEN/mDB securin) as calculated by Vi-CELL^{TM}XR Cell Viability Analyzer using the ViCELLXR 2.03 software. (**F**) Light microscopic pictures of stable securin HeLa FlpIn clones before and after Tet-induction.

2.2.4.2. Phosphorylation-dependent degradation of securin is APC/C-dependent

In an attempt to determine whether this faster degradation of separase-free securin over bound securin is dependent on the APC/C, stable HeLa cell lines were generated, which expressed a corresponding APC/C-resistant FLAG-tagged securin (with mutated KEN- and D-box) upon tetracycline induction (Fig. 20). However, these cells were *per se* polyploid (Fig. 20D and E). This is probably due to low basal expression of the highly toxic APC/C-resistant securin even in the absence of tetracycline, the accumulation of which blocks chromosome segregation and consequently also causes cytokinesis defects. A CHX shut-off experiment comparing the half-lifes of separase-bound vs. free securin in mitosis, as conducted for WT securin (Fig. 19), was not possible using this cell line. Induced HeLa FlpIn cells expressing APC/C-resistant securin$^{mKEN/mDB}$-FLAG started becoming extremely apoptotic already after 4 hours of CHX treatment (data not shown). Therefore, a different approach was embarked upon. Using unsynchronized HeLa FlpIn cell lines that express FLAG-tagged securin^{WT} or securin$^{mKEN/mDB}$ upon tetracycline induction, phosphorylation-dependent degradation of securin over a shorter period of time was analyzed, before variant securin expression rendered cells apoptotic. Cells were treated with CHX to prevent re-synthesis of securin, and with okadaic acid (OAA) to specifically inhibit PP2A (Fig. 21A). In a 3 hour CHX shut-off alone, wild-type securin levels were greatly diminished but residual amounts remained (lane 3). Concomitant OAA treatment on the other hand lead to complete securin degradation after 3 hours (lane 4). The levels of the APC/C-resistant securin also decreased slightly after a 3 hour CHX shut-off (lane 8) but, in contrast to wild-type securin, additional OAA treatment did not lead to complete degradation (lane 9). Instead, securin was hyper-phosphorylated, as demonstrated by an upward smear of the corresponding band in the immunoblot. After λ-phosphatase treatment, this phosphorylation induced shift was reversed (lane 10), clearly showing that a mutated KEN- and D-box renders securin fully resistant against this phosphorylation-dependent degradation. Similar results were obtained using *Xenopus* egg extracts that were arrested in metaphase and then released by Ca^{2+} addition in the presence of CHX and OAA. As predicted, wild-type securin was rapidly degraded, while variant securin was stabilized (Fig. 21B, top blots). OAA-treatment merely induced the afore seen phosphorylation

dependent change in electrophoretic migration behavior as revealed by λ-phosphatase treatment (Fig. 21B, bottom blots). Therefore, in contrast to wild-type securin, APC/C resistant securin is not degraded in a phosphorylation dependent manner in the pseudo-mitotic state mimicked here by OAA addition, arguing that this form of degradation is APC/C dependent. These results again contradict previous findings by Gil-Bernabé and colleagues (Gil-Bernabé et al., 2006), who not only argued that securin itself is associated with (the B55 isoform of) PP2A, but also that phosphorylated securin is degraded in an APC/C-independent but SCF-dependent manner.

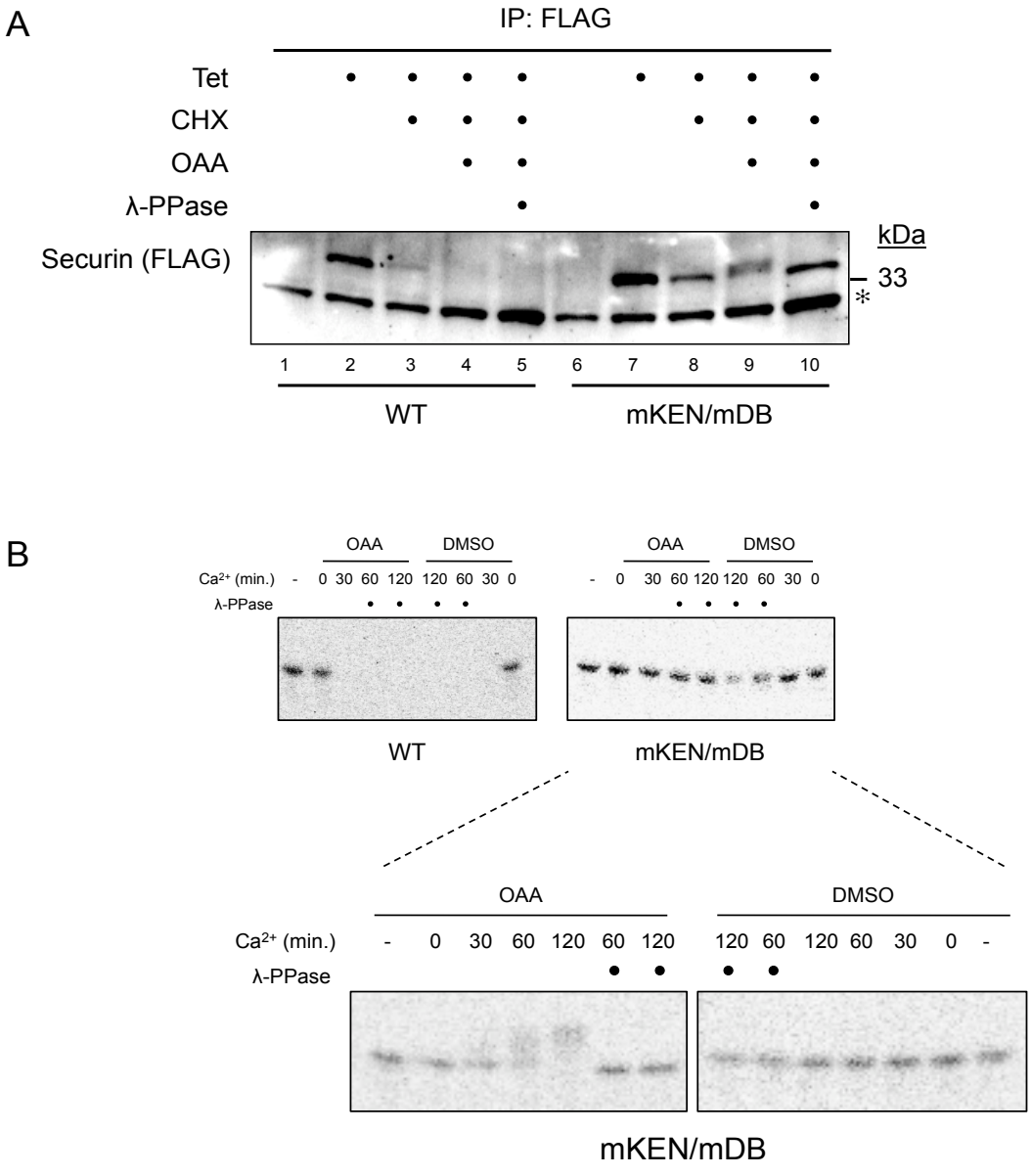

FIGURE 21. APC/C-resistant securin is not degraded in a phosphorylation-dependent manner.

(**A**) HeLa FlpIn cell lines were tetracycline (Tet)-induced to overexpress FLAG-tagged securin^{WT} or securin$^{mKEN/mDB}$. Cycloheximide (CHX) shut-off was done with or without simultaneous okadaic acid (OAA) treatment over 3h. Securin was purified from cell lysates using anti-FLAG beads. Where indicated, securin was treated with λ-phosphatase (λ-PPase) prior to elution from beads by boiling in sample buffer. The asterisk (*) corresponds to the IgG light chain. (**B**) ^{35}S-labelled securin was incubated in CHX-supplemented CSF-arrested *Xenopus* egg extract. The extract was released from metaphase-II-like arrest by Ca^{2+} addition with or without simultaneous OAA or DMSO control treatment. Where indicated, samples where treated with λ-phosphatase (λ-PPase) prior to boiling in sample buffer. Securin was detected by autoradiography.

In an attempt to specifically link the identified PP2A substrate sites on securin to the stabilizing effect of separase-associated PP2A, the appropriate serine and threonine residues (Ser31, Thr66 and Ser87/89) were mutated. The degradation behavior of the resulting variants (triple alanine or triple aspartate, respectively) was then analyzed in *Xenopus* egg extracts supplemented with CHX and released from metaphase arrest by Ca^{2+} addition. If the postulated theory holds true, one would expect the phosphorylation-resistant serine-to-alanine variant to be degraded with slower kinetics than wild-type securin. *Vice versa*, the serine-to-aspartate variant might be degraded faster if the negatively charged amino acids were to successfully mimick phosphorylation in this case. However, as Fig. 22 shows, no significant differences in the degradation kinetics could be detected with either variant. This could be due to the fact that often, when the regular phosphorylation residues are inaccessible or mutated, as is the case here, neighbouring sites are modified instead.

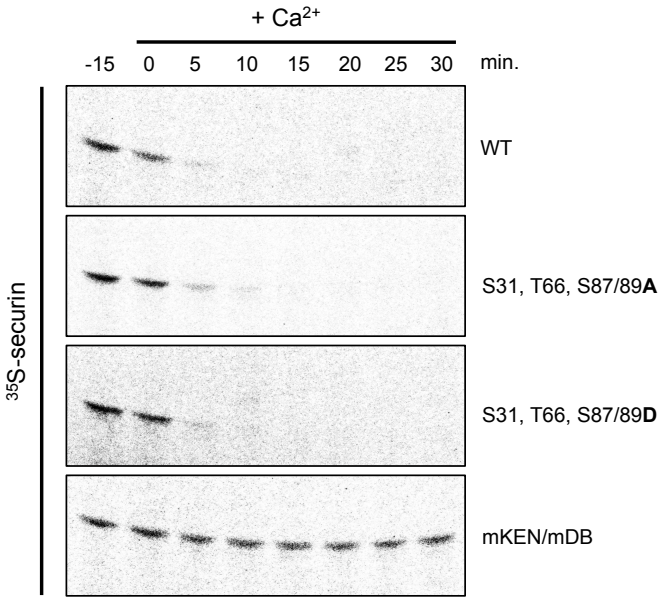

FIGURE 22. Securin variants, which have PP2A substrate sites mutated, are degraded with wild-type kinetics in *Xenopus* egg extract.

^{35}S-labelled *in vitro* expressed securin proteins were incubated in cycloheximide (CHX) supplemented CSF extracts. After 15 min. (at t=0 min.), the extracts were released by addition of Ca^{2+}. At the indicated time points, samples were taken for analysis by SDS-PAGE and autoradiography.

Even though the substrate-sites of separase-bound PP2A on securin could not be confirmed as being involved in phosphorylation-dependent degradation of securin using this approach, what seems clear from the data presented here so far is that within the separase-securin complex, securin not only acts as an inhibitor for the protease. At the same time separase also influences securin in a positive manner. More precisely, separase stabilizes bound securin, and this correlates with PP2A-mediated dephosphorylation. In contrast, free securin is degraded by the APC/C in a phosphorylation- and APC/C-dependent manner. Fitting to this model and the data presented herein, Holland and Taylor have previously shown that overexpression of separase results in elevated levels of securin (Holland and Taylor, 2006).

2.3. Securin has a positive effect on separase

2.3.1. Securin prevents aggregation of separase

The inhibitory function of securin on separase is well characterized (Cohen-Fix et al., 1996; Funabiki et al., 1996; Stemmann et al., 2001; Zou et al., 1999). It binds and thereby inhibits separase's protease activity until anaphase onset, when it is polyubiquitylated and rapidly degraded, releasing active separase. In organisms like *S. pombe* and *Drosophila* (Funabiki et al., 1996; Stratmann and Lehner, 1996), loss of securin function results in the same phenotype as loss of separase function, namely a failure to separate chromosomes. This exemplifies that securin, besides inhibiting separase, also exerts a positive effect on the protease. Even in mammals, where securin is not essential (Mei et al., 2001; Pfleghaar et al., 2005), this positive influence of securin on separase is nevertheless conserved. Separase levels and activity are greatly reduced in human securin -/- cells, albeit sufficiently high to still mediate normal execution of anaphase (Pfleghaar et al., 2005). A mere inhibitory function of securin on separase would predict that separase activity were increased upon loss of securin. How, then, does securin exert its positive effect on separase? Several theories have been proposed. Both in budding and fission yeast, securin may be involved in proper localization of separase (Hornig et al., 2002; Nagao et al., 2004). Several studies have also described securin as a transcriptional regulator (Bernal et al., 2002; Hamid and Kakar, 2004; Tong and Eigler, 2009). Using an electrochemical biochip (Pöhlmann, 2009; Wang et al., 2007), C. Pöhlmann and M. Sprinzl quantitatively compared the levels of separase mRNA from human securin knock-out relative to the parental HCT116 cells. This analysis revealed that separase mRNA levels are the same in both cell lines, arguing that securin does not influence separase on the level of transciption or mRNA stability. In an attempt to further characterize the positive effects of securin on separase, an aggregation assay was performed. This was to answer the question if securin might be required for separase to adopt a native, conformational state, ready to be activated as soon as securin is degraded. If this were the case, one would predict that without securin, separase becomes insoluble, as misfolded proteins tend to aggregate with each other via their exposed hydrophobic surfaces into insoluble complexes. Such a mechanism would ensure that separase is inhibited as soon as it has been translated, and that any

separase not associated with securin would aggregate, protecting the cell from premature separase activation and premature sister-chromatid separation. Therefore, Hek293T cells were transiently transfected to overexpress separase, thereby titrating out securin. The cells were mitotically arrested and the subsequent lysates cleared by centrifugation. Western analysis of soluble supernatant and insoluble pellet fractions revealed that the resulting level of soluble separase was low, as most separase accumulated in the pellet (Fig. 23, 'Sep.' lanes). Simultaneous overexpression of securin, however, greatly increased the level of soluble separase (Fig. 23, 'Sep. + Sec.' lanes). The overall level of separase was the same in both cases, as determined by analysis of whole cell extracts prior to centrifugation. This suggests that securin indeed functions as a chaperone for separase, preventing aggregation of the protease. A similar protection mechanism is known for the endonuclease CAD (caspase activated DNase), which aggregates when synthesised in the absence of its inhibitor I^{CAD} (Sakahira and Nagata, 2002). I^{CAD} ensures that CAD is correctly folded and ready to be activated as soon as I^{CAD} is degraded upon apoptosis.

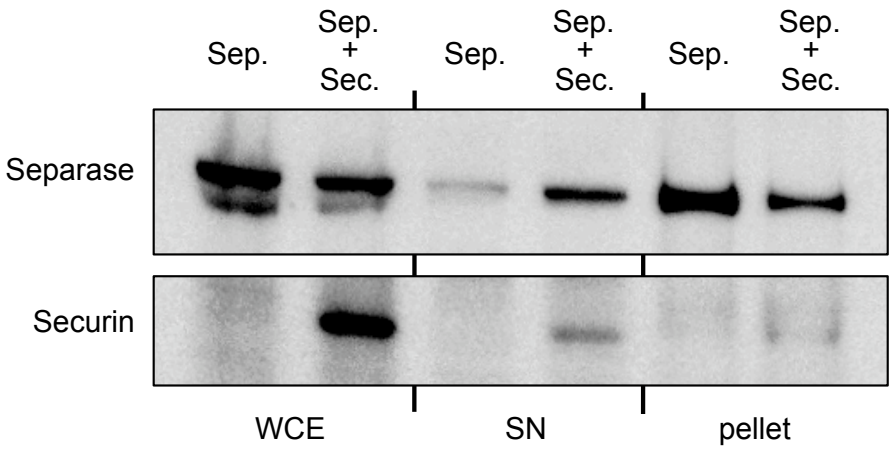

FIGURE 23. Association with securin keeps separase soluble.

Hek293T cells were transiently transfected to overexpress either separase alone or separase and securin together. Whole cell extracts (WCE) were centrifuged and the resulting soluble supernatants (SN) and insoluble pellet fractions (which were resolubilized in urea buffer) were analyzed by SDS-PAGE and immunoblotting.

2.3.2. Securin associates with separase co-translationally

Does securin associate with separase already as separase is being translated, i.e. co-translationally, or only after separase has been completely translated? To analyze the earliest steps in protein folding, the formation of so-called 'Ribosome Nascent Chain' (RNC) complexes is an appropriate method. It enables the isolation of a stable complex of mRNA, bound ribosome and a nascent polypeptide chain. In order for stable RNC complexes to form, the ribosome has to be stalled during translation. This can be achieved by expression of mRNA lacking a stop codon, thereby preventing the recruitment of termination factors. *In vitro* translation of N-terminal separase run-off transcripts of varying length in the presence of ^{35}S labeled securin lead to the isolation of RNC complexes that could subsequently be analyzed for the presence of securin (S. Hellmuth, master thesis in the lab of O. Stemmann, 2010). A nascent polypeptide fragment spanning the first 627 amino acids of separase formed an RNC complex that co-precipitated securin (S. Hellmuth, personal communication), confirming the assumption that securin indeed associates with separase as the protease is being translated. This provides the first biochemical evidence for the possible mechanism and time of action of securin's positive effect on the native state of separase.

2.4. Cyclin A2 cannot substitute for cyclin B1 in binding separase

Neither the possitive nor the negative effect of securin on separase is essential in higher eukaryotes. Since the phosphorylation-mediated inhibition of separase by cyclin B1-Cdk1 can only come into effect in mitosis, when this kinase is activated, the question remains as to how separase is held in check from the time of cohesion establishment in S phase until mitotic entry, especially in the absence of securin. Potential candidates here are cyclin A-Cdk complexes, because their activities first appear in early S phase, increase during G2 and are switched off soon after nuclear envelope breakdown due to APC/C^{Cdc20}-mediated degradation of cyclin A (Hu et al., 2001). To examine if cyclin A-Cdk complexes can associate with separase and potentially inhibit the protease, stable cyclin A2 and/or stable cyclin B1 were transiently overexpressed in Hek293T cells together with wild-type or non-phosphorylatable (PM) ZZ-TEV-tagged separase (Fig. 24). Cells were synchronized in prometaphase and treated with MG-262 to further stabilize the cyclins by inhibiting the proteasome. After purification of separase by IgG immunoprecipitation, associated cyclin levels were compared. As judged by protein levels in the input samples, cyclin A2 levels were comparable to cyclin B1 levels unter these cell synchronization conditions. However, while wild-type (but not PM) separase could interact with stable cyclin B1 (lanes 9, 10 and 14), no significant interaction with stable cyclin A2 could be detected (lanes 9, 10 and 12). Thus, cyclin A2 cannot substitute for cyclin B1 in binding and inhibiting separase in early phases of the cell cycle.

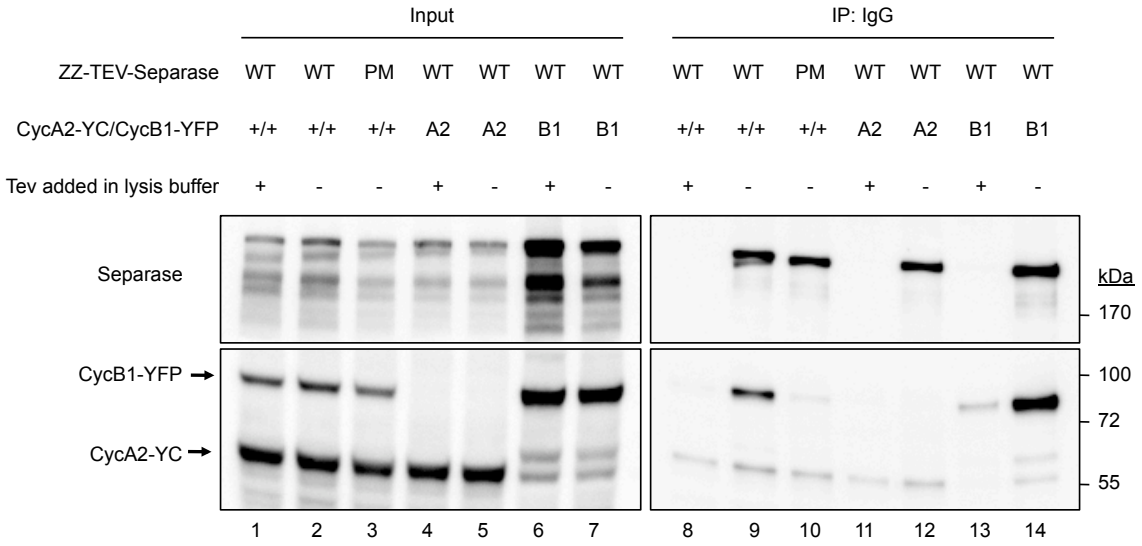

FIGURE 24. Cyclin A2 cannot associate with separase.

Hek293T cells were transfected with plasmids coding for wild-type (WT) or PM (S1126A, T1346A, ΔL1391-E1402) ZZ-TEV-tagged separase, together with plasmids coding for stable (ΔN) YC-tagged cyclin A2 and/or stable (ΔN) eYFP-tagged cyclin B1. Cells were arrested in prometaphase by nocodazole treatment and the proteasome was inhibited by MG-262 treatment for 2 hours prior to harvesting, thereby further stabilizing the cyclins. Separase-cyclin complexes were purified by IgG sepharose immunoprecipitation and subsequent Tev protease elution. To control for unspecific binding, Tev protease was already added to the appropriate lysates prior to immunoaffinity purification (lanes 8, 11 and 13). Eluted proteins were detected by immunoblotting. Note: both the eYFP- as well as the YC (amino acids 155-239 of eYFP)-tag are recognized by the same anti-eGFP antibody.

3. DISCUSSION

3.1. PP2A interaction with securin is bridged by separase

Both human securin and separase have previously been reported to associate with protein phosphatase 2A (PP2A) (Gil-Bernabé et al., 2006; Holland et al., 2007). This Ser/Thr protein phosphatase exists as a heterotrimer, consisting of a catalytic subunit (C), a scaffolding subunit (A) and one of four alternative regulatory subunits (B/B55, B′/B56, B″, or B‴). The nature of this regulatory subunit determines both substrate specificity and subcellular localization of the heterotrimeric PP2A complex. Importantly, in higher eukaryotes, monomeric PP2A subunits are unstable and degraded by the ubiquitin-proteasome protein degradation pathway (Li et al., 2002; Strack et al., 2004). Therefore, localization of the substrate-specificity determining regulatory subunits directly reflects the localization of the corresponding PP2A holoenzyme.

Based on yeast two-hybrid and co-immunoprecipitation experiments, an interaction of human securin with the B (B55)-containing PP2A holoenzyme has been proposed (Gil-Bernabé et al., 2006). Separase on the other hand has been shown to interact specifically with the B' (B56)-containing PP2A holoenzyme by mass-spectrometric analysis of separase associated proteins and subsequent co-immunoprecipitation experiments from Hek293 cell lysates (Holland et al., 2007). Furthermore, B'-containing PP2A was shown to associate with a GST-separase fragment (aa 1278-1556) *in vitro* even in the absence of securin, and a securin-binding deficient separase variant (lacking the first 325 amino acids) could still bind PP2A.

The present study now aimed to unambiguously clarify which of these two scenarios holds true. First, the existence of a heterotrimeric separase-securin-PP2A complex was clearly demonstrated (Fig. 9). Furthermore, while PP2A-B' co-precipitated with separase-securin complex from HeLa cell lysates, the isolation of separase-free securin did not yield any associated PP2A-B' (Fig. 10). The specificity of the PP2A-B' over a putative PP2A-B interaction was then demonstrated by co-immunoprecipitation experiments from Hek293T cells (Fig. 11). Here, no association

of PP2A-B with separase could be observed, while PP2A-B' readily co-precipitated with the protease. Lastly, deleting the PP2A binding site from separase removed all traces of PP2A from the separase immunoprecipitate, without effecting securin binding (Fig. 17). Therefore, both securin and the B'-containing isoform of PP2A directly interact with separase to form a heterotrimeric complex. Together with the above mentioned findings by Holland et al. (2007), the data presented herein strongly argue that PP2A directly interacts with separase, and that the securin-PP2A interaction characterized by Gil-Bernabé and colleagues is likely to be indirect and bridged by separase.

3.2. Positive effects of PP2A on securin

The observation that overexpression of separase in human cells leads to a concomitant elevation of securin levels (Holland and Taylor, 2006) suggests that separase might positively affect securin, for example, by promoting securin synthesis, or by preventing its degradation. However, the nature of such a potential positive regulation mechanism has remained enigmatic.

One important difference between free and separase-bound securin is that the former is phosphorylated in mitosis, whereas the latter is not (Fig. 10). This observation is coherent with the identification of securin as a substrate of separase-associated PP2A (Fig. 18). Therefore, separase-associated PP2A keeps securin dephosphorylated within this complex. This is accompanied by slower degradation kinetics of bound vs. free securin within a nocodazole-induced prometaphase arrest (Fig. 19). The established view is that APC/C^{Cdc20} can only mediate the destruction of securin at the metaphase-to-anaphase transition, when the spindle assembly checkpoint (SAC) is inactivated and Cdc20 can activate the APC/C. Because the SAC is activated in nocodazole arrested cells, APC/C^{Cdc20} activity is inhibited. While this explains why separase-bound securin is stable in prometaphase, the turnover of free securin under these conditions implies that there might be an alternative securin degradation mechanism operating in early mitosis that defies the spindle checkpoint. Considering the hyper-phosphorylated nature of free securin over separase-bound securin, this mechanism is likely to be phosphorylation dependent.

There are several candidate kinases that have been reported to phosphorylate human securin. Of the PP2A substrate sites identified on securin in this study (Ser31, Thr66 and Ser87/89), Ser31 and its preceeding residues match the consensus site (S-X-X-S/T) for CK1 (casein kinase 1) phosphorylation, according to the PHOSIDA database. Experimentally, both Cdk1 and DNA-dependent protein kinase (DNA-PK) have been shown to phosphorylate human securin (Ramos-Morales et al., 2000; Romero et al., 2001). Cdk1 has also been shown to phosphorylate budding yeast securin, and interestingly, this correlates with slower APC/C-dependent degradation compared to unphosphorylated securin (Holt et al., 2008). This mode of regulation is contrary to the one proposed in this study, and budding yeast securin shows no sequence similarity to human securin. Nevertheless, this example still demonstrates that APC/C-dependent degradation of securin can, in principle, be regulated by phosphorylation at the substrate level.

Interestingly, several APC/C^{Cdc20} substrates have been identified in recent years that are degraded in prometaphase despite an active spindle checkpoint. The most prominent of these early mitotic APC/C^{Cdc20} substrates is cyclin A. In mammalian somatic cells, cyclin A forms complexes with either Cdk1 or Cdk2 and is required for S phase and passage through G2 phase (Furuno et al., 1999; Pagano et al., 1992). Cyclin A-Cdk associates with Cdc20 already in late G2 phase, and is then degraded in mitosis right after nuclear envelope breakdown in an APC/C^{Cdc20}-dependent manner. Critical in this process is the recruitment of cyclin A-Cdk-Cdc20 complex to the (phosphorylated) APC/C by the small Cdk subunit Cks (den Elzen and Pines, 2001; Geley et al., 2001; Wolthuis et al., 2008). Importantly, the checkpoint component Mad2 does not coimmunoprecipitate with cyclin A-Cdc20 complexes, arguing that Cdc20 is protected from mitotic checkpoint complex (MCC)-mediated inactivation by interaction with cyclin A (Wolthuis et al., 2008). Importantly, Cks interaction with cyclin A-Cdc20 must be bridged by Cdk to ensure timely degradation of the cyclin (den Elzen and Pines, 2001). Cks proteins can bind to phosphorylated proteins via their anion-binding pocket (Bourne et al., 2000). This raises the question of whether phosphorylation-dependent securin degradation may be mediated by Cks? Affinity purification of securin from nocodazole arrested HeLa cells, which had additionally been treated with the proteasome inhibitor MG-132 and the phosphatase inhibitor OAA, did not result in co-purification of either Cks1 or Cks2 (data not

shown). Therefore, a Cks-dependent recruitment of phosphorylated securin to the APC/C is unlikely.

Another APC/C^{Cdc20} substrate, Nek2A (NIMA [never in mitosis in *Aspergillus nidulans*]-related kinase 2A), is also degraded in prometaphase in a checkpoint-independent manner. This depends on an exposed carboxy-terminal methionine-arginine (MR) dipeptide tail, which is involved in direct, Cdc20-independent, binding of Nek2A to the core APC/C complex (Hayes et al., 2006). A similar C-terminal dipeptide tail mediates direct interaction of Cdc20 and Cdh1 to the APC/C (Vodermaier et al., 2003). Securin does not possess such an APC/C interacting motif. However, a direct interaction of securin with APC/C activating subunit Cdh1 has been observed in early mitosis (Jeganathan et al., 2006). In addition, mRNA export factor Rae1 and nucleoporin Nup98 were shown to complex with both APC/C^{Cdh1} and securin in prometaphase. In cells with low levels of Rae1 and Nup98, APC/C^{Cdh1} was shown to mediate the premature destruction of securin already in prometaphase (Jeganathan et al., 2006; Jeganathan et al., 2005). It is generally accepted that APC/C^{Cdh1} activity is associated with late mitotic and early G1 phase events (Kotani et al., 1999; Kramer et al., 2000). However, there is evidence that APC/C^{Cdh1} may have earlier functions as well. In mouse oocyctes, for example, Cdh1-activated APC/C has been assigned essential roles in maintaining prophase I arrest (Reis et al., 2006; Reis et al., 2007). Thus, one possibility is that Rae1 and Nup98 specifically prevent the APC/C^{Cdh1}-dependent degradation of separase-bound, dephosphorylated securin but not of free, phosphorylated securin.

Finally, a recent study demonstrated that human anti-apoptotic protein Mcl-1 can be degraded in prometaphase-arrested cells in a phosphorylation- and APC/C^{Cdc20}-dependent manner (Harley et al., 2010), although the accompanying mechanism is still unclear.

It cannot be completely excluded that free, hyperphosphorylated securin is degraded in an APC/C-independent manner. The second big group of E3 ubiquitin ligases regulating cell cycle control besides the APC/C complex are SCF ligases, which are active throughout the cell cycle and are known for specifically recognizing phosphorylated substrates. Indeed, such a mechanism has previously been proposed for securin degradation (Gil-Bernabé et al., 2006). Gil-Bernabé and

colleagues claim that B subunit-containing PP2A protects securin from SCF-dependent degradation by direct interaction of PP2A with securin. However, this statement is clearly contradicted by the findings in this study. First of all, PP2A interaction with securin is not direct, but bridged by separase (Fig. 10). Secondly, not the B but the B' containing regulatory PP2A subunit is associated with this complex (Fig. 11). And finally, chemical PP2A inhibition by OAA treatment lead to the stabilization of an APC/C-resistant securin variant (mutated KEN- and D-boxes) compared to wild-type securin (Fig. 21), strongly arguing in favour of an APC/C-dependent degradation mechanism. To confirm this, the degradation behavior of separase-free securin in a prometaphase-arrest is currently being investigated in a Cdc20 and/or Cdh1 knock-down background. Additionally, to confirm the increased stability of the SILAC phosphorylation site securin variant (Fig. 22) and thereby characterize separase-bound PP2A action on securin to a more complete extent, stable cell lines will be established which will inducibly express wild-type securin or the phosphorylation site variant. Following brief induction of transgene expression, the half-lifes of these securins will be determined by CHX shut-off experiments analogous to those conducted in Fig. 19 and 21.

Summarizing the results of this section gives rise to a model in which separase-associated PP2A keeps bound securin dephosphorylated to protect it from premature degradation by an APC/C-dependent mechanism that has yet to be fully characterized (Fig. 25). Thereby, the cell makes sure that excess free securin is removed prior to anaphase onset. This would permit a more rapid, switch-like induction of sister-chromatid separation because as soon as bulk APC/C activity is switched on, the degradation of separase-bound securin would immediately start. In fact, securin has been shown to not only be a substrate of the APC/C but to also function as an inhibitor of APC/C, possibly modulating the activity of the E3 ligase in early mitosis (Marangos and Carroll, 2008; Solomon and Burton, 2008). Excess of securin will keep the APC/C^{Cdc20} busy, thereby delaying anaphase onset. Furthermore, separase might be repeatedly activated and re-inhibited in the presence of excessive securin, which might result in asynchronous separation of sister-chromatids, missegregation and aneuploidy. It might be for these reasons that securin is frequently overexpressed in tumor cells (Pei and Melmed, 1997; Zou et al., 1999).

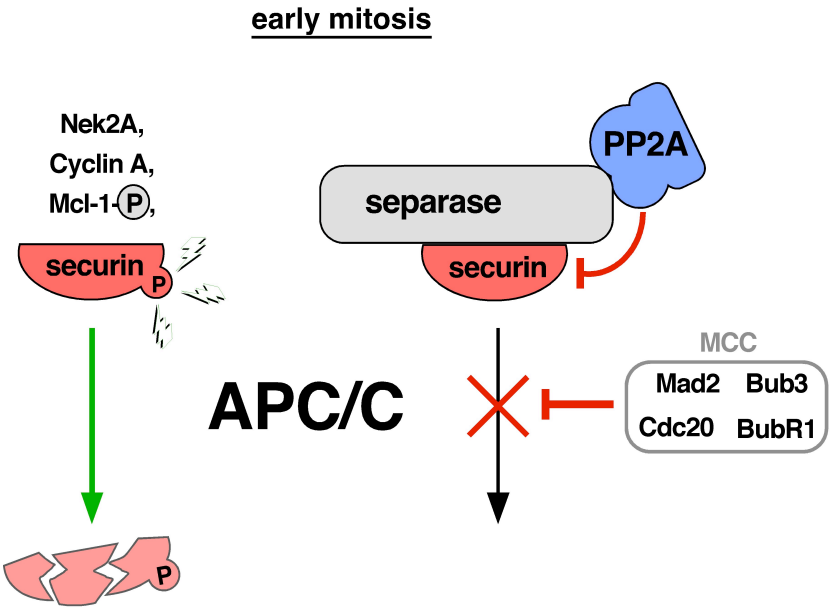

FIGURE 25. Model for the APC/C-dependent degradation of separase-free securin in prometaphase.

Separase-free securin can be phosphorylated upon mitotic entry, making it a substrate for basal APC/C activity in early mitosis. Separase-associated securin is protected from this degradation mechanism by separase-bound PP2A mediated dephosphorylation. Model with modifications from O. Stemmann.

3.3. Positive effects of securin on separase

A universal feature of all securin proteins is that they act as inhibitors of separase activity. However, based on several genetic studies, securin also seems to exert a positive, chaperone-like function on separase (Hornig et al., 2002; Jallepalli et al., 2001; Nagao et al., 2004). This observation was confirmed and further characterized in this (chapter 2.3.) and a parallel study (S. Hellmuth, master thesis). Overexpression of wild-type separase under conditions where securin was limiting lead to the precipitation of bulk separase. Co-overexpression of securin, on the other hand, kept separase soluble. This indicates that newly synthesized separase aggregates in the absence of enough stabilizing securin. This is mirrored in the observation that when inhibitory securin is enzymatically removed from separase, the protease is very instable, highly prone to aggregation and only active for a short time *in vitro*. Together with results by S. Hellmuth (master thesis), which suggest that securin interacts with separase as soon as the protease is translated (chapter 2.3.2.), this offers new insights into the nature of securin's dual regulation of separase.

Generally, the primary structure (i.e. the amino acid sequence) of a protein carries the instructions that determine the correct tertiary conformation necessary for a protein to be fully functional (Anfinsen, 1973). During the folding process of a newly synthesized polypeptide, hydrophobic side chains are exposed that have a propensity to associate with each other and form aggregates. While this can be an ordered process (known as 'hydrophobic collapse') and is hypothesized to be a natural intermediate step in the folding process of many proteins (the so-called 'molten globule' structure), it can also lead to inappropriate protein aggregations. To counteract misfolding and aggregation into non-functional structures, molecular chaperones play an important role in stabilizing nascent polypeptide chains co-translationally. Typically, chaperones stabilize exposed hydrophobic residues of their substrates through rounds of ATP-dependent binding and release, until the substrate protein has achieved its native state (Netzer and Hartl, 1998).

Securin may function as such a chaperone for separase, recognizing and binding to nascent polypeptide separase chains, thereby preventing their misfolding and aggregation. Functionally such a mechanism would ensure that separase, whose premature activation would pose a great threat for genome stability, is associated with its inhibitor from the time of its synthesis until timely activation of APC/C^{Cdc20}. Because of its dual function as chaperone and inhibitor, securin, contrary to typical chaperones, remains asociated with its substrate after synthesis and folding are completed, and is only dissociated at the metaphase-to-anaphase transition of mitosis, when it is degraded and releases active separase. A similar mechanism is known for caspase-activated DNase (CAD) and its inhibitor I^{CAD}. CAD causes chromosomal DNA fragmentation during apoptosis, and is kept in check until then by its association with I^{CAD}. When cysteine caspases are activated in apoptosis, I^{CAD} is cleaved and active CAD released. It could be shown that I^{CAD} associates with CAD co-translationally and assists folding of CAD. In addition to I^{CAD}, heat shock proteins Hsc70/Hsp70 and Hsp40 are essential for the refolding of *in vitro* denatured CAD (Sakahira and Nagata, 2002). In this context it is interesting to note that human securin has also been reported to interact with another heat shock related chaperone, the DnaJ (Hsp40) homolog HSJ2 in a yeast two-hybrid screen (Pei, 1999).

Securin itself is known as a natively unfolded or intrinsically unstructured protein (IUP), with no well-defined 3-dimensional structure. While the N-terminal half (containing the KEN- and D-box destruction motifs) is totally disordered, the C-terminal half contains a few segments (aa150-159, aa113-S127 and aa174-178) that might adopt secondary structure elements (Csizmok et al., 2008). Interestingly, structural disorder has been described as an important functional feature of protein chaperones (Bhattacharyya and Das, 1999; Kim et al., 2002; Tompa and Csermely, 2004). Both for protein and especially for RNA chaperones, the incidence of disorder predicted by PONDR (predictor of natural disordered regions) is extremely high. Mechanistically, structurally disordered chaperone regions may serve as molecular recognition elements that solubilize partially misfolded proteins through direct binding (Tompa and Csermely, 2004).

What is the fate of separase that aggregates in the absence of stabilizing securin? Generally, proteins that are unable to adopt their native state are targeted for degradation by the ubiquitin-proteasome pathway (Hershko and Ciechanover, 1998; Hirsch and Ploegh, 2000). If the concentration of misfolded proteins in the cell becomes too high, aggregates are sequestered into so-called aggresomes and subsequently degraded throught the aggresome pathway (Garcia-Mata et al., 2002; Kopito, 2000; Rodriguez-Gonzalez et al., 2008). This involves the transport of aggresomal particles along microtubules towards the microtubule organizing center (MTOC), where they accumulate into a single aggresome that surrounds the MTOC. This is thought to activate the autophagic clearance mechanism, that ultimately terminates in lysosomal degradation. Such a mechanism is conceivable for the large amounts of separase that presumably accumulate in the cell when overexpressed in the absence of securin. To test for this, the localization behavior GFP-tagged separase in the presence or absence of securin could be analyzed by fluorescence microscopy.

3.4. Intrinsic regulation of separase auto-cleavage and PP2A association

In higher eukaryotes, separase cleaves not only cohesin's Scc1 subunit upon activation at the metaphase-to-anaphase transition, but also itself. Human separase has three well conserved auto-cleavage sites (Fig. 15A), which are characterized by ExxR consensus sequences also found on Scc1. Although separase auto-cleavage was recognized and initially characterized almost 10 years ago (Waizenegger et al., 2002; Zou et al., 2002), its functional relevance remains enigmatic. In marked contrast to the related caspases, separase does not depend on self-cleavage for catalytic activity. *In vitro*, non-cleavable variants are as active in cleaving cohesin as wild-type separase (Waizenegger et al., 2002; Zou et al., 2002). In *Drosophila*, separase is encoded by two separate genes, one encoding a small protein containing the catalytic domain (SSE) and another encoding an N-terminal separase domain (THR). Based on genetic data, cleavage of THR by SSE after the metaphase-to-anaphase transition results in degradation of the C-terminal cleavage product and has been proposed to help inactivate separase in telophase (Herzig et al., 2002; Jager et al., 2001). Furthermore, the C-terminal cleavage product of budding yeast Scc1 is rapidly degraded by the N-end rule pathway (Rao et al., 2001). Thus, one might assume that the cleavage fragments of human separase are also turned over more quickly than the uncleaved, full-length protease. However, the auto-cleavage fragments of human separase not only remain physically associated and catalytically active (Zou et al., 2002), they can also be readily detected as long as prometaphase of the next cell cycle (data not shown). In a CHX shut-off after nocodazole-induced mitotic arrest of HeLa cells, the degradation kinetics of full length separase were compared to those of separase cleavage fragments over a 10 hour period. Both separase species were similarly stable over this time period (data not shown). Thus, auto-cleavage does not mediate the rapid destruction of human separase. Support for this conclusion comes from Papi and colleagues. Introduction of cleavage-site mutations into the endogenous separase locus of human HCT116 cells by a knock-in approach generated clones, in which five of the six auto-cleavage sites in the genome were mutated (Papi et al., 2005). These cells delayed entry into mitosis and exhibited chromosome alignment defects, but demonstrated unperturbed mitotic exit and cytokinesis progression, suggesting a positive role for cleaved separase products during G2 and early mitosis of the next cell cycle. These functions of

separase cleavage products in G2/M transit and prometaphase progression are likely to be independent of separase's catalytic activity, since separase is inhibited by securin during these stages.

Strikingly, regulation of auto-cleavage of human separase is closely linked to separase's ability to interact with PP2A. Non-cleavable separase variants are associated with more PP2A than wild-type separase (this study, Fig. 17B, lanes 13 and 11; Holland et al., 2007). *Vice versa*, cleavage of separase prevents PP2A binding or even induces its dissociation from separase (Fig. 16). It could be shown that the nature of this mutual regulation is both steric and catalytic. More precisely, the PP2A binding site on separase was mapped to a small EEE(L) motif right between separase's first and second auto-cleavage site (Fig. 17C). Deletion of these four residues (aa 1490-93) lead to a quantitative loss of separase-PP2A association. Furthermore, phosphorylation of a well conserved serine residue (Ser1501) just prior to separase's second main cleavage site (ER1503/6) promotes separase auto-cleavage *in vitro*. Intriguingly, this Ser1501 residue is one of the main substrate sites of separase associated PP2A (Fig. 13A, B). Holland and colleagues could show that the phenotype associated with overexpression of a non-cleavable (NC) separase variant was premature loss of sister chromatid cohesion and a prolonged mitotic arrest (Holland et al., 2007). This phenotype was fully rescued by additional deletion of the PP2A binding site, indicating that the hyper-activity of NC separase is a direct consequence of the increased PP2A interaction.

The most obvious explanation for the premature loss of cohesion observed in NC separase expressing cells is that the accompanying increased PP2A association antagonizes Ser1126 phosphorylation and cyclin B1-mediated inhibition. Some observations support such a mutually exclusive action of PP2A and cyclin B1-Cdk1 on separase. Firstly, when endogenous cyclin B1 was purified from mitotic HeLa lysates, separase but neither PP2A-A nor PP2A-C could be co-precipitated (Holland et al., 2007). Additionally, PP2A bound to separase has been shown to be catalytically active, and, using a phosphorylation-specific antibody, an increased level of Ser1126 phosphorylation was observed when PP2A binding to separase was inhibited (Holland et al., 2007). Finally, when PP2A-B' association with different separase variants was analyzed in this study, a NC/ΔCLD separase variant, which is

unable to interact with the cyclin B1-Cdk1 complex, showed significantly higher levels of associated PP2A than NC separase (Fig. 17B). On the other hand, several strong lines of evidence argue against the possibility that PP2A antagonizes Cdk1-dependent regulation of separase. Equal amounts of cyclin B1 associate with wild-type and ΔPP2A separase variants. *Vice versa*, a Ser1126Ala variant of separase, which cannot bind cyclin B1-Cdk1 complex, does not show elevated levels of PP2A association compared to wild-type separase (Holland et al., 2007). Furthermore, Ser1126 can be efficiently dephosphorylated when cyclin B1 is bound to separase, and this does not disrupt cyclin B1 binding (Holland and Taylor, 2006). Finally, compromising separase's PP2A binding ability does not result in increased phosphorylation of Ser1126 or the critical CLD residues Thr1346, Thr1363 and Ser1399 as judged by SILAC (Fig. 13A, B). Based on these conflicting results, it can therefore not be unambiguously clarified if the respective actions of PP2A and cyclin B1-Cdk1 on separase antagonize each other. To shed more light onto the relative actions of cyclin B1-Cdk1 and PP2A on separase function, an appropriate future experiment will be discussed later (end of chapter 3.6.).

3.5. Relative importance of securin and MPF in the timely regulation of anaphase onset

When a Cdk1-resistant Ser1126Ala separase variant is overexpressed in Hek293 cells, sister chromatids separate prematurely and the SAC is activated (Holland and Taylor, 2006). This phenotype can be suppressed by simultaneous overexpression of securin, indicating that securin becomes limiting when separase alone is heavily overexpressed. Interestingly, under cyclin B1-Cdk1 and securin limiting conditions, sister chromatids separate just 5 minutes earlier than they normally do. Similarly, mouse embryonic stem (ES) cells of the genotype securin$^{-/-}$/separase$^{WT/S1121A}$ (Ser1121 of mouse separase corresponds to Ser1126 of human separase) were viable and largely displayed normal mitotic timing but failed to maintain sister chromatid cohesion only in response to the microtubule poison nocodazole (Huang et al., 2005). In ES cells that only lacked securin or only expressed the Cdk1-resistant separase, no premature sister chromatid separation was observed. Therefore, securin and Cdk1 can compensate each other in inhibiting separase, at least in

human Hek293 and ES cells. And even when separase is activated prematurely due to the loss of both these inhibitory mechanisms, the timing of sister separation is still not significantly disrupted in a normal, undisturbed cell cycle. This hints at a third mechanism that limits the activation of separase even when securin and the inhibitory phosphorylation are taken out of the equation. Alternatively, mechanisms may be in place that prevent prematurely activated separase from targeting its substrate. In budding yeast, for example, sister chromatid separation is positively influenced by phosphorylation of Scc1, which renders it a better substrate for separase (Alexandru et al., 2001). Separase-dependent cleavage of human Scc1 is also enhanced by phosphorylation of the substrate (Hauf et al, 2005). Therefore, it would be interesting to see whether mutations that prevent or mimick phosphorylation of Scc1 would alleviate or aggravate, respectively, the effect of separase deregulation.

Importantly, while securin-mediated inhibition of separase is dispensable, inhibitory phosphorylation is crucial in embryonic germ cell development and in early embryogenesis. A mouse strain carrying the aforementioned Ser1121Ala point mutation is characterized by infertility of both sexes as well as complete primordial germ cell depletion in male mice (Huang et al., 2009; Huang et al., 2008; Xu et al., 2011). This argues that the cyclin B1-Cdk1 inhibition mechanism is superior to securin in inhibiting separase, at least in some cell types.

An interesting observation was made regarding separase regulation by cyclin B1-Cdk1 in stable Hek293 cell lines. While bulk wild-type separase aggregated in mitosis in the absence of additionally transfected securin, most non-phosphorylatable Ser1126Ala separase did not (S. Hellmuth, master thesis and personal communication). This argues that securin-free separase aggregates because it is phosphorylated in mitosis. In interphase, neither wild-type separase nor the phosphorylation site variant aggregated under conditions of limiting amounts of securin, probably because of lack of phosphorylations in interphase. It is therefore possible that cyclin B1-Cdk1, much like securin, simultaneously acts as an inhibitor and as a chaperone for separase. Phosphorylation of separase by cyclin B1-Cdk1 in mitotis would therefore lead to aggregation unless it is immediately followed by binding of the Cdk1 complex. This model would also account for the fact that the

securin inhibiting mechanism is not essential, by demonstrating that in principle, cyclin B1-Cdk1 on its own can make sure that separase is kept in check until the spindle checkpoint is satisfied (Fig. 26).

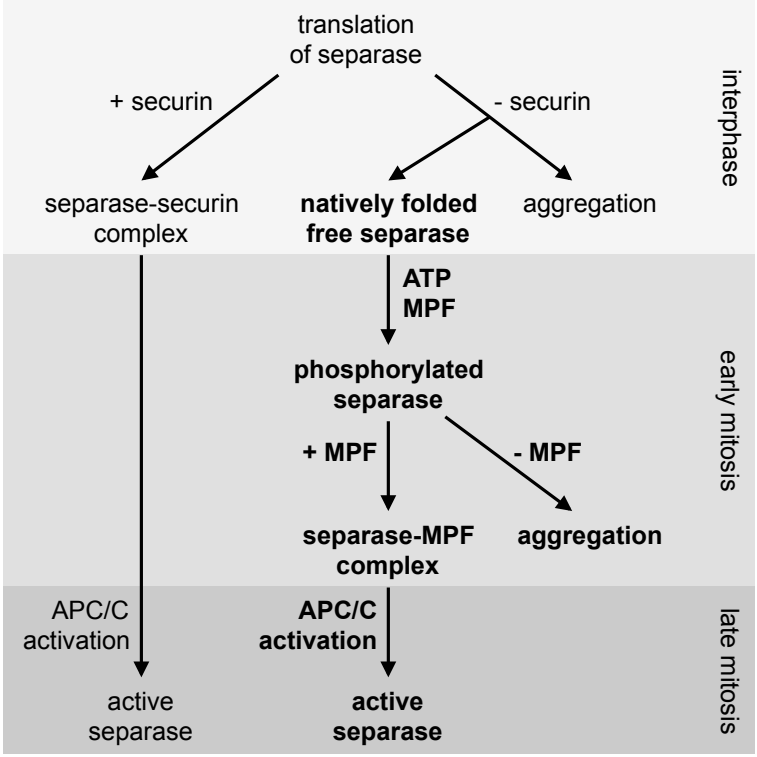

FIGURE 26. Putative chaperone function of cyclin B1-Cdk1 complex for separase may explain why securin is not essential in humans.

Co-translational association of securin with separase ensures that separase can correctly fold into its native conformation and at the same time inhibits the protease (left branch). In the absence of securin, most separase aggregates (right branch). Any separase that does manage to natively fold in the absence of securin will be phosphorylated upon entry into mitosis by the cyclin B1-Cdk1 (MPF) complex. This phosphorylation would lead to an increased tendency to aggregate and thereby to inactivation of separase (right branch), unless MPF binds phosphorylated separase (middle branch). This physical association prevents aggregation and ensures separase activation upon APC/C activation.

If securin is not essential, then what inhibits separase in earlier stages of the cell cycle, when cyclin B1-Cdk1 is not yet active? In this study, cyclin A-Cdk complexes were ruled out, as they cannot associate wih separase (chapter 2.4.). It is possible that in a securin$^{-/-}$ scenario, the spatial separation of separase and cohesin in cytoplasm and nucleus, respectively, suffices to prevent loss of cohesion prior to accumulation of cyclin B1 and entry into mitosis.

In conclusion, backed by the results of this study the regulation of anaphase onset can be outlined as follows. In a normal, unpertubed cell cycle, securin probably acts to support separase folding and mediates separase inhibition throughout interphase. Apart from binding securin, nuclear exclusion of separase prevents it from gaining access to its chromosomal substrate. In early mitosis, excess, free securin is phosphorylated by mitotic kinases and removed by basal APC/C activity, making the cell vulnerable for sudden increases in separase levels. Here, cyclin B1-mediated phosphorylation of separase takes over and removes any separase not associated with securin (and PP2A) by promoting its aggregation or re-inhibition by cyclin B1-Cdk1 complex binding.

3.6. How may PP2A contribute to orderly mitotic progression?

The antagonistic relationship between separase-Cdk1 and separase-PP2A complex formation is further exemplified by the fact that Cdk1 is largely associated with cleaved separase (in which PP2A association is lost), whereas securin preferentially associates with uncleaved, full-length separase, as demonstrated by Cks2 *versus* securin immunoprecipitation experiments from mitotic Hek293T cell lysates (Gorr et al., 2005). These experiments also revealed a co-existence of separase-securin and separase-Cdk1 complexes in prometaphase cells.

Therefore, separase-associated PP2A may fulfill two functions in early mitosis: one is to protect separase-bound securin from being degraded together with free securin, and the other is to mediate between securin and cyclin B1 binding to separase. In G2 phase, securin-separase-PP2A complexes, as well as cleaved separase from the previous cell cycle in complex with securin exist. Upon entry into mitosis, free securin and securin bound to cleaved separase (i.e. securin not protected by separase-bound PP2A) is phosphorylated and degraded by basal APC/C activity. Any free separase as well as cleaved separase freed from securin is phosphorylated by cyclin B1-Cdk1 and either bound and inhibited by this complex or left to aggregate. Therefore, in early mitosis, securin-separase-PP2A and separase-cyclin B1-Cdk1 complexes coexist. When securin and cyclin B1 are degraded at the metaphase-to-anaphase transition by the APC/C, both already cleaved and uncleaved separase are released from their cyclin B1- and securin-mediated inhibitions, respectively, releasing active separase (Fig. 27).

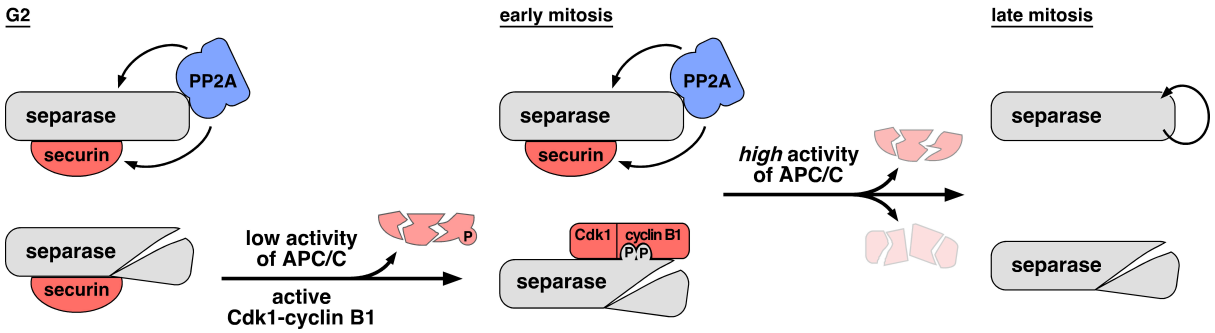

FIGURE 27. Model for the role of separase-bound PP2A in regulating anaphase onset.

In interphase, securin-separase-PP2A and cleaved separase from the previous cell cycle in complex with securin exist. Upon entry into mitosis, securin not protected by PP2A activity is phosphorylated and degraded by basal APC/C activity. Therefore, in early mitosis, only the securin-separase-PP2A complexes persist. In addition, cleaved separase freed from its inhibitor securin can be phosphorylated and bound by its second inhibitor, the cyclin B1-Cdk1 complex. The burst of APC/C activity at the metaphase-to-anaphase transition leads to concomitant degradation of securin and cyclin B1, thereby activating separase.

Considering the fatal consequences of premature sister chromatid separation for the cell, the aquisition of such a complex framework of intrinsic regulation for separase is perhaps not surprising. A critical experiment in further defining the role PP2A plays in mediating orderly anaphase onset will be the generation of Hek293 cell lines stably overexpressing a separase variant displaying a moderate level of premature sister chromatid separation (PSCS). The effects of concomitantly deleting the PP2A-binding sites on this variant (ΔPP2A), or of concomitantly mutating the auto-cleavage sites on this variant (NC), on the extent of PSCS will be determined by FACS analysis and chromosome spreading. In order to be able to observe effects both ways, i.e. an aggrevation or an alleviation of PSCS, a LAG (Ala1380*L*eu, Pro1381*A*la and Arg1386*G*ly) separase variant will be used, which is only partially Cdk1-resistant and shows a weaker level of PSCS than Ser1126Ala and ΔCLD (aa 1342-1400) separase variants. If PP2A antagonizes Cdk1 regulation of separase, a ΔPP2A mutation should alleviate the PSCS phenotype of LAG separase, while a mutation which renders separase non-cleavable should aggravate the PSCS phenotype.

4. MATERIALS AND METHODS

If not indicated otherwise, companies are situated in Germany.

4.1. Materials

4.1.1. Hard- and software

This work was written on an "Apple MacBook2,1" (Apple Computer Inc., Cupertino, CA, USA) using "Microsoft® Word 2008" (Microsoft Corporation, Redmond, WA, USA). "Microsoft® Excel 2008" (Microsoft Corporation, Redmond, WA, USA) was used for generation of diagrams. Chemiluminescence signals of immunoblots as well as Coomassie stained gels were digitized using an "LAS-4000" system (Fuji Film Europe, Düsseldorf). Autoradiographies were digitized using an "FLA-7000" phosphorimager (Fuji Film Europe, Düsseldorf). The image analysis software MultiGauge (Fuji Film Europe, Düsseldorf) was used to visualize chemiluminescence signals from immunoblots and digitized autoradiographies. Processing of all images and generation of figures was done using "Microsoft® Powerpoint® 2008" (Microsoft Corporation, Redmond, WA, USA) and "Canvas 9.0.4" (ACD Systems International Inc., Victoria, B.C., Canada). "DNASTAR Lasergene" (GATC Biotech, Konstanz) was used for analysis of DNA and protein sequences. Literature and database searches were done with electronic online services provided by the "National Center for Biotechnology Information" (http://www.ncbi.nlm.nih.gov/). A service of the European Bioinformatics Institute was used for sequence aligments ("EMBOSS Pairwise alignment" algorithm, http://www.ebi.ac.uk/Tools/emboss/align/index.html).

4.1.2. Protocols

The methods described in this section are based on standard techniques (Ausubel and Struhl, 1998; Sambrook, 1989; Sambrook and Russell, 2001) or follow the manufacturer’s instructions. Where protocols have been modified, detailed information is provided. For all methods, de-ionized sterile water and, when appropriate, sterile solutions and sterile flasks were used.

4.1.3. Chemicals and reagents

Unless otherwise stated, chemicals and reagents (pro analysis grade) were purchased from AppliChem (Darmstadt), Biomol (Hamburg), Biorad (Munich), GE Healthcare (Munich), Fermentas (St. Leon-Rot), Invitrogen (via Fisher Scientific, Schwerte), Merck/Calbiochem (Darmstadt), Millipore (Schwalbach), New England Biolabs (NEB, Frankfurt a. M.), Pierce/Fisher Scientific (Schwerte), Promega (Mannheim), Qiagen (Hilden), Roche Diagnostics (Mannheim), Roth (Karlsruhe), Serva (Heidelberg) and Sigma-Aldrich (Steinheim).

4.1.4. Antibodies

Commercial antibodies and affinity matrices used in this study were as follows: mouse monoclonal anti-securin (clone DCS-280, Abcam, Cambridge, UK), mouse monoclonal anti-separase (clone XJ11-1B12, Abcam, against C-terminal residues 1866-1996 of human separase), rabbit polyclonal anti-separase (A302-214A, Bethyl, Montgomery, TX, USA, against residues 1100-1150 of human separase), mouse monoclonal anti-PP2A, C'α subunit (clone 1D6, Millipore), mouse monoclonal anti-Myc (clone 4A6, Millipore), rabbit polyclonal anti-Myc (clone A-14, Santa Cruz Biotechnology, CA, USA), mouse monoclonal anti-Flag (clone M2, Sigma-Aldrich), rabbit polyclonal anti-FLAG (Sigma-Aldrich), mouse monoclonal anti-α-tubulin (clone 12G10, Developmental Studies Hybridoma Bank), unspecific rabbit (Bethyl) IgG (Sigma-Aldrich) and IgG sepharose (4 Fast Flow; GE Healthcare). Polyclonal goat anti-rabbit-IgG, rabbit anti-goat-IgG, goat anti-mouse-IgG coupled to peroxidase (Sigma-Aldrich) or goat anti-mouse IgG (γ) coupled to peroxidase (KPL, Gaithersburg, MD, USA, heavy-chain specific) were used as secondary antibodies in immunoblotting.

Non-commercial antibodies used were: rabbit polyclonal anti-pSX104 (against His_6-hSecurin), rabbit polyclonal anti-pSX38 (against His_6-tagged human separase residues 1305-1573), rabbit polyclonal anti-hSeparase-N (against N-terminal residues 2-16 of human separase, Stemmann et al., 2001), rabbit polyclonal anti-hSeparase-M (against residues 1507-1521 of human separase) and mouse monoclonal anti-eGFP (against the C-terminal 3rd of eGFP; hybridoma cell line was kindly provided by D. van Essen & S. Saccani, MPI Freiburg).

4.1.5. Plasmids

Vector	Origin
pCS2	Turner and Weintraub (1994), with modified MCS (FseI/AscI sites inserted)
pcDNA5-FRT-TO	Invitrogen
pET28a	Novagen, with modified MCS (FseI/AscI sites inserted)

Plasmids	Insert	Tag	Vector
Separase			
pSX38	hSep$^{S1305\text{-}T1573}$ fragment	N-His_6	pET28a
pOS22	hSep	N-ZZ-TEV_4-	pCS2
pOS41	hSep^{PD}	N-ZZ-TEV_4-	pCS2
pSX136	hSep	-	pCS2
pOS337	hSep $^{PM\ (S1126A,\ T1346A,\ \Delta L1391\text{-}E1402)}$	N-ZZ-TEV_4-	pCS2
pAS1228	hSep$^{3xNC\ (R>A),\ \Delta 1297\text{-}1404}$	N-ZZ-TEV_4-	pCS2
pAS1229	hSep$^{3xNC\ (R>A),\ \Delta 1296\text{-}1478}$	N-ZZ-TEV_4-	pCS2
pAS1272	hSep$^{PD,\ \Delta 1408\text{-}1478}$	N-ZZ-TEV_4-	pCS2
pAS1273	hSep$^{PD,\ \Delta 1454\text{-}1470}$	N-ZZ-TEV_4-	pCS2
pAS1274	hSep$^{PD,\ \Delta 1454\text{-}1479}$	N-ZZ-TEV_4-	pCS2
pAS1275	hSep$^{PD,\ \Delta 1490\text{-}1493}$	N-ZZ-TEV_4-	pCS2
pFB1681	hSep$^{PD,\ S1508\text{-}19A\ 4xA}$	N-ZZ-TEV_4-	pCS2
pFB2056	hSep$^{3xNC\ (R>A)}$	N-ZZ-TEV_2-	pCS2
pFB2118	hSep$^{2xNC\ (R>A),\ 1501\text{-}11\ 6xA}$	N-ZZ-TEV_4-	pCS2
pFB2490	hSep$^{PD,\ S1508\text{-}19D\ 4xD}$	N-ZZ-TEV_4	pCS2
pOS182	hSep$^{PD,\ 2xNC\ (R>A),\ S1501A}$	N-HA_3-	pCS2
pOS184	hSep$^{PD,\ 2xNC\ (R>A),\ S1501S}$	N-HA_3-	pCS2
pFB2577	hSep	N-Myc_6-	pcDNA5-FRT-TO
pFB2603	hSep$^{\Delta EEEL\ (\Delta 1490\text{-}93)}$	N-Myc_6-	pcDNA5-FRT-TO
pFB2609	hSep$^{3xNC\ (ER>RE)}$	N-Myc_6-	pcDNA5-FRT-TO
pFB2700	hSep$^{2xNC\ (ER>RE),\ 1503\text{-}09:\ ENLYFQG\ (TEV)}$	N-Myc_6-	pcDNA5-FRT-TO

Securin			
pSX104	hSecurin	N-His_6	pET28a
pSX100	hSecurin	-	pCS2
pOS237	hSecurin	-His_6-Flag-His_6-Flag-C	pCS2
pOS238	hSecurin$^{mKEN/mDB}$	-His_6-Flag-His_6-Flag-C	pCS2
pFB2234	hSecurin	-His_6-Flag-His_6-Flag-C	pcDNA5-FRT-TO
pFB2235	hSecurin$^{mKEN/mDB}$	-His_6-Flag-His_6-Flag-C	pcDNA5-FRT-TO
pFB2570	hSecurin$^{3xA\ (S31A,\ T66A,\ S87/89A)}$	-His_6-Flag-His_6-Flag-C	pCS2
pFB2571	hSecurin$^{3xD\ (S31D,\ T66D,\ S87/89D)}$	-His_6-Flag-His_6-Flag-C	pCS2
PP2A			
pFB2470	hPP2A Bα subunit	-His_6-Flag-His_6-Flag-C	pCS2
pFB2471	hPP2A B'α subunit	-His_6-Flag-His_6-Flag-C	pCS2
Others			
pLG2256	Tev protease^{S219V}	-	pCS2
pFB2340	hCyclin B1$^{\Delta N\ (\Delta 1\text{-}75)}$	-YFP-C	pCS2
pFB2341	hCyclin A2$^{\Delta N\ (\Delta 1\text{-}86)}$	-YC-C	pCS2

Source: pFB – this study; others – Stemmann laboratory plasmid collection

PD: protease-dead (C2029S)

NC (R>A): non-cleavable (R1486A, R1506A, R1535A)

NC (ER>RE): non-cleavable (ER1483/6RE, ER1503/6RE & ER1532/5RE)

mKEN/mDB: KEN to RDQ & RxxL to AxxA

4.1.6. DNA oligonucleotides

Plasmid	Primer	Sequence
pFB2118	hSep_PP2A_6xA_W	5'- GGCCTTTGCGATCCTCGCGGGCGCTGCCGGGGCAGACTCAGCCTCAGGTGG-3'
	hSep_PP2A_6xA_C	5'- CCGGCAGCGCCCGCGAGGATCGCAAAGGCCATTTTTCTCCAGTTGTCAGTC-3'
pFB2490	hSepS1508-19D+FB	5'- TCCTTCCCACCATCGGCATCGTCTTCCCCGTCATCGCCCCTGAGGATCTC-3'
	hSepS1508-19D-FB	5'- GATGACGGGGAAGACGATGCCGATGGTGGGAAGGATCCAGCTCCGGG-3'
pFB1681	hSepPM1508-19-FB	5'- GCTGACGGGGAAGACGCAGCCGCAGGTGGGAAGGCTCCAGCTCCG-3'
	hSepPM1508-19+FB	5'- CCTTCCCACCTGCGGCTGCGTCTTCCCCGTCAGCGCCCCTGAGGATCTC-3'
pFB2700	dbsep_1503-10_TEV_rev	5'- GAGGCTGAGTCTTCCCCCTGAAAGTAGAGGTTCTCAAAGCTCATTTTT-3'
	dbsep_1503-10_TEV_for	5'- AAAAATGAGCTTTGAGAACCTCTACTTTCAGGGGGAAGACTCAGCCTC-3'

pFB2570	hSecS31A hSecT66A hSecS87/89A	5'- GGTCTGGACCTGCAATCAAAGCC-3' 5'- AGGCTTTGGGAGCTGTCAACAGAG-3' 5'- ACAAAAACAGCCAGCCTTTGCTGCCAAAAAGATG-3'
pFB2571	hSecS31D hSecT66D hSecS87/89D	5'- GTCTGGACCTGATATCAAAGCCT-3' 5'- GCTTTGGGAGATGTCAACAGA-3' 5'- AAAACAGCCAGACTTTGATGCCAAAAAG-3'
pFB2470	hPP2A_Balpha_5'F hPP2A_Ba_3'open	5'- TAAGGCCGGCCCATGGCAGGAGCTGGAGGA-3' 5'- GGCGCGCCAATTCACTTTGTCTTGAAAT-3'
pFB2471	hPP2A_B'a_5'F hPP2A_B'a_3'open	5'- TAAGGCCGGCCCATGTCGTCGTCGTCGCCG-3' 5'- GGCGCGCCATTCGGCACTTGTATTGCTG-3'
pFB2340	5'F_hCycB1_D76 hCycB1_3Aop_OS	5'- GCTGGCCGGCCAATCATGGATAAAAAACTACCAAAACCT-3' 5'- TTAGGCGCGCCTTAACACCTTTGCCACAGCC-3'
pFB2341	5'F_hCycA2_V87 hCycA2_3'opA	5'- ATGGGCCGGCCATCATGGTTCCTCCTTGGAAAGCAAACA-3' 5'- GGCGCGCCACAGATTTAGTGTCTCTGGTGGGTTGAGGA-3'

4.2. Microbiological techniques

If not indicated otherwise, percentages in buffer recipes are given as v/v.

4.2.1. *E. coli* strains

Strain	Description and origin
XL1-Blue	*E. coli sup*E44, *hsd*R17, *rec*A1, *end*A1, *gyr*A46, *thi*, *rel*A1, *lac*$^-$ [F' *pro* AB *lac*I^q, *Lac* ZdM15, Tn10 (*Tet*^{r})] Stratagene/AgilentvTechnologies, Santa Clara, CA, USA
Rosetta DE3	*E. coli* F^-, *ompT, hsdS*$_B$ (r_B^- m_B^-), *gal, dcm,* λ (*DE3* [*lacI, lacUV5-T7 gene 1, ind1, sam7, nin5*]) *Cam*^{R} Novagen/Merck

4.2.2. *E. coli* media

LB medium
1% (w/v) Tryptone (Difco, BD Biosciences, Heidelberg)
0.5% (w/v) yeast extract (Difco)
1% NaCl (w/v)
dissolved in ddH_2O and sterilized by autoclaving

LB agar
LB-medium with 1.5% agar (Roth)

4.2.3. Cultivation and storage of *E. coli*

E. coli strains were grown in LB medium by shaking at 200 rpm at 37°C, LB agar plates were incubated at 37°C. Antibiotics for selection of transformed bacteria were added to media at 100 µg/ml (ampicillin), 30 µg/ml (kanamycin) or 34 µg/ml (chloramphenicol) final. Culture densities were determined by measuring the absorbance at a wavelength of 600 nm (OD_{600}). Cultures on agar plates were stored at 4°C for up to 30 days. For long-term storage, liquid cultures were supplemented with glycerol to 20% final concentration, subsequently snap frozen and stored at -80°C.

4.2.4. Preparation of chemically competent *E. coli*

Tbf1 buffer	30 mM KAc
	50 mM $MnCl_2$
	100 mM KCl
	15% Glycerol
	pH adjusted to 5.8
Tbf2 buffer	10 mM MOPS/NaOH
	75 mM $CaCl_2$
	10 mM KCl
	15% Glycerol
	pH adjusted to 7.0

For preparation of chemical-competent bacteria, 300 ml LB medium was inoculated with 4 ml of an overnight culture derived from a single *E. coli* colony and grown at 37°C to an OD_{600} of 0.5. After chilling the culture flask on ice for 15 min, cells were harvested by centrifugation (4°C, 5000 g, 15 min). All following steps were performed with prechilled sterile materials and solutions at 4°C. Sedimented bacteria were carefully resuspended in 90 ml Tbf1 buffer and chilled on ice for 15 min. After a second centrifugation (4°C, 5000 g, 15 min), bacteria were resuspended in 15 ml Tbf2 buffer and chilled on ice for 5 min. Finally, suspension of bacteria was aliquoted, snap-frozen and stored at -80°C.

4.2.5. Transformation of plasmid DNA into chemically competent *E. coli*

Competent bacteria were thawed on ice. For chemical transformation, 50 µl of competent bacteria were mixed with 1 µl of plasmid DNA or 10 µl ligation reaction and incubated on ice for 20 min. A heat shock at 42°C was performed for 45 s. Subsequently, the cell suspension was incubated on ice for 2 min and after addition of 1 ml LB medium without antibiotics incubated on a shaker at 37°C for 45 min. After recovery, transformed cells were selected by streaking out the bacteria suspension on LB agar plates containing the respective antibiotic(s) and incubated overnight at 37°C.

4.2.6. Expression of proteins in *E. coli*

For expression of recombinant proteins from pET28a expression plasmids, the *E. coli* strain Rosetta DE3 was used. LB medium was inoculated with a dilution of 1:100 of an overnight culture from a freshly transformed colony. The culture was grown at 37°C and expression of protein(s) was induced by addition of IPTG (1 mM final concentration) at an OD_{600} of 0.5-0.8. After shaking for 3 h at 37°C, cells were harvested by centrifugation (4°C, 5000 g, 10 min). Pellets were either processed directly or stored at -80°C after snap-freezing.

4.3. Molecular biological methods

4.3.1. Isolation of plasmid DNA from *E. coli*

2.5 ml of LB medium containing the appropriate antibiotic was inoculated with a single *E. coli* XL1-Blue colony harboring the DNA plasmid of interest and shaken for 8-14 h at 37°C. Plasmid-DNA was purified via alkaline lysis of the bacteria and subsequent isolation by anion exchange columns according to the manufacturer's instructions (Qiagen, "Plasmid Purification Handbook, Plasmid Mini Kit"). Larger amounts of DNA for transfection of human cells were isolated from a 250 ml overnight culture according to the manufacturer's protocol (Qiagen, "Plasmid Purification Handbook, Plasmid Maxi Kit").

4.3.2. Determination of DNA/RNA concentration in solution

DNA or RNA concentrations were determined by measuring the absorbance at a wavelength of 260 nm (OD_{260}) with a ND-1000 Spectrophotometer (Peqlab, Erlangen). An OD_{260} = 1 equals a concentration of either 50 µg/ml double-stranded DNA or 40 µg/ml RNA.

4.3.3. Restriction digestion of DNA

Sequence-specific cleavage of DNA with restriction enzymes was performed according to standard protocols (Sambrook and Russell, 2001) and the instructions of the manufacturer (New England Biolabs, NEB). Usually, 5-10 units of restriction enzyme were used for digestion of 1 µg DNA. Reaction samples were incubated in appropriate buffer at the recommended temperature for 1 h. Restriction digestion was then stopped by addition of DNA loading buffer.

4.3.4. Dephosphorylation of DNA fragments

To avoid religation of linearized vectors, the 5' end of vector DNA was dephosphorylated by adding 0.1 units of shrimp alkaline phosphatase and the appropriate buffer (Roche, Mannheim) and incubating for 1 h at 37°C. Subsequently, shrimp alkaline phosphatase was heat-inactivated 15 min at 70°C.

4.3.5. Separation of DNA fragments by gel electrophoresis

TBE buffer	90 mM Tris Base
	90 mM Boric acid
	2.5 mM EDTA
DNA loading buffer	0.5% (w/v) SDS
(5x)	0.25% (w/v) Orange G
	25% Glycerol
	25 mM EDTA (pH 8.0)

For analytical analysis and preparative isolation, DNA fragments were electrophoretically separated on agarose gels (0.8-2.0% of agarose in TBE buffer) containing ethidium bromide (0.5 µg/ml final concentration). DNA samples were mixed with DNA loading buffer and separated at 100 V in TBE buffer. DNA fragments could be visualized by intercalation of ethidium bromide into DNA by using a UV transilluminator (324 nm). The size of the fragments was estimated by standard size markers (O'GeneRuler 1kb or 100 bp DNALadder, Fermentas).

4.3.6. Isolation of DNA from agarose gels

TE buffer	5 mM Tris (pH 8.0)
	1mM EDTA

After gel electrophoresis DNA fragments were isolated by excising the respective piece of agarose using a scalpel. DNA was extracted from the agarose using QiaExII Gel Extraction kit (Qiagen) according to manufacturer's instructions and eluted with 50 µl TE buffer.

4.3.7. Ligation of DNA fragments

Amounts of isolated DNA fragments ("inserts") and linearized vectors were estimated on an ethidium bromide-containing agarose gel. For ligation reaction a molar ratio of 2.5:1 of insert to vector was used. The reaction sample with a total volume of 10 µl usually contained 100 ng of vector DNA and 4 units of T4 DNA Ligase (Fermentas) and was incubated for 2 h at RT or overnight at 16°C in recommended amounts of reaction buffer (Fermentas).

4.3.8. Sequencing of DNA

Sequencing PCR and sample preparation were performed with the DYEnamic ET Terminator Cycle Sequencing Premix kit according to the manufacturer's instructions (GE Healthcare). One sample usually contained 1 µg of plasmid DNA and 20 pmol of primer. DNA sequencing was then carried out by the core facility MPI for biochemistry (Martinsried) with an Abi-Prism 377 sequencer (Perkin Elmer) or by an external commercial provider (SeqLab, Göttingen).

4.3.9. Site-directed mutagenesis of DNA

Site directed mutagenesis was usually perfomed using a fusion PCR based approach using two reverse complementary oligonucleotides harboring the desired mutation(s). In two separate PCR reactions, each oligonucleotide was used to create an upstream and a downstream fragment, respectively. The outer primers for these reactions were designed to terminate at useful restriction sites. After gel purification the two products were combined and fused in a PCR reaction with the two outer primers. The resulting fragments were restriction cloned into the desired vector. Verification was done by sequencing.

For the introduction of multiple specific point mutations within a gene sequence the GeneEditor *in vitro* Site-directed Mutagenesis System (Promega) was used according to the manufacturer's instructions. The underlying principle is the use of at least two oligonucleotides, one introducing a mutation into the *Amp*R gene leading to resistance against the “GeneEditor” antibiotic and the others containing the desired point mutation(s). After denaturation of the plasmid of interest, the oligonucleotides were allowed to anneal and the second strand was completed by PCR. Subsequently, the double stranded plasmid was transformed into bacteria that were then selected on “GeneEditor” antibiotic containing agar plates. Introduced mutations were verified by sequencing.

4.3.10. Polymerase chain reaction (PCR)

PCRs were usually performed in a total volume of 50 µl with 50-200 ng of plasmid DNA, 0.25 µl of the respective forward and reverse oligonucleotide primer (100 mM), 1 µl deoxynucleotide mix (10 mM, New England Biolabs, NEB) and 0.5 µl of Phusion DNA polymerase (Finnzymes, Espoo, Finland) in the corresponding PCR buffer (5x Phusion HF or GC buffer, Finnzymes). Amplification was carried out in a TC-512 temperature cycler (Techne, Burlington, NJ, USA). The reaction profile was adjusted according to quantity and quality of template DNA, the length and G/C content of the oligonucleotides as well as the length of the amplified sequences. Usually, the denaturing step was done for 20 s at 98°C, annealing for 20 s at a temperature optimized for the individual primer pairs, and elongation at 72°C for 20 s/kbp.

4.4. Cell biological methods

4.4.1. Mammalian cell lines

Cell line	Description and origin
Hek293T	human embryonic kidney cell line transformed with SV40 large T antigen
HeLa L	human cervix epithelial adenocarcinoma transformed by humanpathogene Papilloma virus, subclone L
HeLa FlpIn	human cervix epithelial cells modified by stable integration of a pFRT/*lac*Zeo plasmid (Invitrogen) carrying the FRT recognition site for transgene integration by Flp-recombinase (mediates zeocin resistance), and stable integration of a pcDNA6/TR plasmid (Invitrogen; modified by replacing the *blast*R gene with a *puro*R gene), for constitutive expression of the Tet-repressor (mediates puromycin resistance); This host cell line was kindly provided by Thomas U. Mayer (University of Konstanz)

4.4.2. Cultivation of mammalian cells

1x PBS	137 mM NaCl
	2.7 mM KCl
	10 mM Na_2HPO_4
	2 mM KH_2PO_4, pH 7.4

Cells were cultured in Dulbecco's Modified Eagle Medium (DMEM, PAA, Pasching, Austria). Media were supplemented with 10% heat inactivated (40°C, 10 min) fetal bovine serum (Biochrom, Berlin), 100 units/ml penicillin and 0.1 mg/ml streptomycin (PAA). Medium for HeLa FlpIn cells was additionally supplemented 4 µg/ml puromycine (Enzo Life Sciences, Plymouth Meeting, PA, USA) and 62.5 µg/ml zeocin (Invitrogen). Monolayer cultures were grown in cell culture dishes (Greiner Bio-One, Kremsmünster, Austria) at 37°C in a 5% CO_2 atmosphere and were split at a ratio of 1:4 to 1:8 twice a week. To split cells, medium was removed, cells were washed once

with PBS and subsequently incubated with 16 µl/cm^2 Trypsin/EDTA solution (PAA) at 37°C for 1 min (Hek293T cells) or 5 min (HeLa/HeLa FlpIn cells). By repeated pipetting in fresh medium, cells were detached from each other as well as from the culture dish. Subsequently, the cell suspension was diluted in medium and distributed on new cell culture dishes. Cell concentrations of suspensions were determined with a Vi-Cell counter (Beckman Coulter, Krefeld).

4.4.3. Storage of mammalian cells

Freezing medium 10% DMSO
90% Fetal bovine serum

Cells were harvested at 80% confluence by trypsination as described above, resuspended in freezing medium and aliquoted in cryo vials (SARSTEDT, Nümbrecht). The cell suspension was then cooled to -80°C in an insulated container or cardboard box at a rate of about 1°C/min. For long-term storage cryo vials were transferred to a liquid nitrogen tank.

For thawing, cryo-stocks were quickly removed from the liquid nitrogen freezer and placed into a 37°C water bath. To remove DMSO, tubes were briefly centrifuged (300 g, 3 min). The supernatant was discarded and the cell pellet resuspended in DMEM and transferred to an appropriate cell culture dish containing DMEM.

4.4.4. Transfection of Hek293T cells with plasmid DNA

2x HBS (50 ml) 800 mg NaCl
37 mg KCl
10.65 mg Na_2HPO_4
100 mg Glucose
500 mg HEPES
pH 7.05 adjusted with NaOH, sterile filtered (0.2 µm pore size)

Hek293T cells were transfected by the calcium phosphate method. 2.5·10^6 cells per cell culture dish (100 mm) were spread and grown overnight. Shortly before transfection the next day, chloroquin was added to the medium to a final

concentration of 20 µM. For one transfection mix, 5-20 µg (depending on the construct) of plasmid DNA were mixed first with 680 µl water and then with 99.2 µl sterile 2 M $CaCl_2$. Then 800 µl of 2x HBS solution were slowly added in small drops while gently vortexing. The transfection mix was immediately added to the cells by careful dripping onto the entire surface of the medium. 12 h later medium was exchanged. 24 h after transfection, nocodazole was added to the medium at a final concentration of 0.2 µg/ml to arrest cells in mitosis (unless interphase samples were prepared). 36 h after transfection, cells were harvested by rinsing the plate with the used cell culture medium. Following centrifugation (300 g, 3 min) cell pellets were washed once with PBS. Cell pellets were subsequently either lysed directly or snap frozen in liquid nitrogen and stored at -80°C for further use.

4.4.5. Transfection of HeLa cells with plasmid DNA

HeLa cells were either transfected using the cationic lipid reagent Lipofectamine 2000 (Invitrogen/Fisher Scientific) or by polyethylenimine (PEI, linear, MW 25,000, Polysciences, Inc., Warrington, PA, USA), a cationic polymer. In the case of Lipofectamine 2000 a 1:2 ratio of DNA (µg):Lipofectamine (µl) was used. Cells were seeded in six-well plates at $0.5 \cdot 10^6$ cells/well in 1 ml DMEM medium supplemented with fetal bovine serum only. Transfection mixes were prepared in two steps. First, 1.6 µg of DNA were diluted in 100 µl OptiMEM (Invitrogen/Fisher Scientific). In a separate tube, 3.2 µl of Lipofectamine 2000 were mixed well with 100 µl of OptiMEM by flicking the tube 20 times. After a 5 min incubation at RT, the DNA solution was pipetted to the Lipofectamine solution and mixed well. Following another incubation for 20 min at RT, the transfection mix was added to the cells. To limit cytotoxicity, medium was changed after 6 h, again using antibiotics-free DMEM medium. For PEI transfections, the ratio of DNA (µg):PEI (µl of 1 µg/µl stock solution) was 1:3. Cells were seeded at 10^6 cells per cell culture dish (100 mm). 1 µg/ml plasmid DNA was incubated in 1 ml DMEM medium without fetal bovine serum or antibiotics for 2 min at RT. After PEI addition, the transfection mix was vortexed, incubated at RT for 10 min and added to the cells for 48 h.

4.4.6. Generation of stable cell lines

HeLa FlpIn cell lines with stable, inducible transgenic expression were generated using the HeLa FlpIn host cell line (chapter 4.4.1.) from Invitrogen according to the manufacturer's instructions. Briefly, transgene plasmid DNA (His_6-Flag-His_6-Flag epitope tagged securin constructs in pcDNA5-FRT-TO vector background) and Flp integrase expression plasmid DNA (pOG44, Invitrogen) were transfected at a ratio of 1:10 using Lipofectamine 2000 (Invitrogen/Fisher Scientific) or polyethylenimine (PEI, linear, MW 25,000, Polysciences, Inc., Warrington, PA, USA). 36 h after transfection, cells were split to a lower density, left to settle onto the cell culture dish for 6 h and selected for site-specific integration of the transgene with 400 µg/ml hygromycin (PAA). Once hygromycin resistant colonies were large enough to see by eye, they were re-plated and inducible expression of the transgene was tested by 5 µg/ml tetracycline (Serva) addition for 12-16 h.

4.4.7. Synchronization and drug treatment of mammalian cells

Synchronization of cells at the G1/S boundary of the cell cycle was done using thymidine. 2 mM thymidine (Sigma-Aldrich) was added to the culture medium for 20 h. Cells were then released from the block by washing twice with medium followed by a 15 min incubation in the cell culture incubator and another medium change. In the case of a double thymidine block, 2 mM thymidine was readded 9 h after release from an 18 h thymidine block. 17 h later cells were released as described above. Synchronization of cells in prometaphase of mitosis was done using nocodazole. 200 ng/ml nocodazole were added either to an asynchronous cell population for 12-16 h or 6 h after release from thymidine block for another 8 h. Purity of the cell cycle phases was confirmed by flow cytometry.

For some experiments, cells were treated with the proteasome inhibitor MG-262 (0.45 µM, Enzo Life Sciences), the serine/threonine protein phosphatase inhibitor okadaic acid (1 µM; Sigma) or the protein biosynthesis inhibitor cycloheximide (10 µg/ml, Sigma) for 2 h, up to 4 h or up to 10 h prior to harvesting, respectively.

4.4.8. Flow cytometry

To confirm the cell cycle phase of synchronized cells, cells were trypsinated from the cell culture dish, pelleted (300 g, 3 min) and transferred to a 15 ml Falcon (Greiner Bio-One) tube with 1x PBS. Cells were subsequently fixed with 70% ethanol (-20°C), washed twice with PBS/0.2% (w/v) BSA and passed through the 35 µm nylon mesh cap of a FACS tube (BD Biosciences). DNA staining was done using a 69 µM propidium iodide solution (in 38 mM tri-sodium citrate, Sigma-Aldrich). RNA was digested by simultaneously treating the cells with 100 µg/ml RNase A (Qiagen) for 1 h at 37°C. DNA content was determined using a Beckman Coulter Cytomics FC 500 flow cytometry device and the program CXP Analysis (Beckman).

4.4.9. Stable Isotope Labeling with Amino acids in Cell culture (SILAC)

SILAC labeling of Hek293T cells was carried out based on the protocol previously described (Ong and Mann, 2007). DMEM medium without arginine and lysine amino acids (Invitrogen) was supplemented with either 13C/15N labeled arginine and 13C/15N labelled lysine (R10/K8), or with unlabeled arginine and lysine amino acids (R0/K0) (Sigma). Cells that were to be transfected with wild-type separase (plasmid pOS41, see chapter 4.1.5.) were cultured in R0/K0 medium, while cells that were to be transfected with ΔPP2A separase variant (plasmid pAS1272, see chapter 4.1.5.) were grown in R10/K8 medium over 6 generations. Labeled cells were transfected with the appropriate separase constructs together with wild-type securin (pSX100, see chapter 4.1.5.) using the calcium phosphate method (see chapter 4.4.4.) and arrested in prometaphase by nocodazole. The ZZ-TEV$_4$-tagged separase was immunoprecipitated from cell lysates of the labeled and unlabeled cells by IgG-IP (see chapter 4.5.8.), before eluates were mixed at a 1:1 ratio. Proteins were separated using SDS-PAGE and subsequently digested by in-gel digestion using trypsin and AspN according to standard protocol (Shevchenko et al., 2006). Phosphorylated peptides were then enriched by Titansphere chromatography. Sample analysis was done by reversed phase LC-MS/MS using the Agilent Technologies 1200 nanoflow system connected to an LTQ Orbitrap XL system (Thermo Electron, Bremen, Germany) with a nanoelectrospray ion source (Proxeon Biosystems, Odense, Denmark) as described (Olsen et al., 2005). Peptides were identified using the Mascot-MatrixScience LLC software and quantified using MSQuant.

4.4.10. Preparation of cytoplasmic extracts from *Xenopus laevis* eggs

MMR (25x)	2.5 M NaCl 50 mM KCl 25 mM $MgCl_2$ 50 mM $CaCl_2$ 2.5 mM EDTA/NaOH (pH 8.0) 125 mM HEPES/NaOH (pH 7.8) pH 7.8, adjusted with NaOH
XB-salts (20x)	2 M KCl 2 mM $CaCl_2$ 20 mM $MgCl_2$
Dejellying solution	2% (w/v) Cysteine (free base) 0.5x XB-salts pH 7.8, adjusted with KOH
CSF-XB (Murray, 1991)	100 mM KCl 0.1 mM $CaCl_2$ 2 mM $MgCl_2$ 10 mM HEPES/KOH (pH 7.7) 50 mM Sucrose 5 mM EGTA/KOH (pH 8.0) pH 7.7, adjusted with KOH
Cytochalasin B	10 mg/ml in DMSO *(1000x)*
Sperm dilution buffer	5 mM HEPES/KOH (pH 7.7) 100 mM KCl 150 mM Sucrose 1 mM $MgCl_2$
Ca^{2+} (25x)	15 mM $CaCl_2$ in sperm dilution buffer
Cycloheximide (100x)	10 mg/ml in H_2O (Calbiochem)

Laid eggs of *Xenopus laevis* are arrested in metaphase of meiosis II by cytostatic factor (CSF), a calcium-sensitive activity. Prior to extract preparation, all glasware used for buffers or extract preparation was therefore rinsed twice with ddH_2O to remove contaminating calcium ions. Work with frogs and frog eggs was performed at 18°C. Prepared extracts were kept on ice and were exclusively pipetted with cut tips. To induce egg laying, female frogs were injected with human chorionic gonadotropin (hCG, 1000 U/ml in ddH_2O, Sigma). Depending on the size of the frog, about 0.7-1.0 ml of hCG solution were injected into the dorsal lymph sac using a 27-gauge needle (B. Braun, Melsungen). 6-8 h later frogs were transferred to 1x MMR buffer. About 20-24 h after injection, the laid eggs were collected in flat-bottomed glas dishes and washed briefly with 1 x MMR. The jelly coats of the eggs were removed by incubation in dejellying solution for 5-10 min. The procedure was terminated by extensive washing in CSF-XB. After all eggs with abnormal morphology had been removed, eggs were transferred to prepared 12 ml centrifuge tubes (Beckman Coulter) containing 1 ml CSF-XB and 10 µl cytochalasin B to block actin polymerization and thereby prevent cytokinesis. By centrifugation in a JS 13.1 swing-out rotor (Beckman) for 1 min at 200 g and 1 min at 600 g, eggs were tightly packed. Surplus of buffer on top of the packed eggs was removed. Eggs were then crushed and fractionated by centrifugation at 13,000 g for 10 min. Subsequently, the centrifugation tube was punctured with a 18-gauge needle at the lower end of the middle layer and the cytoplasmic fraction was transferred to a cooled eppendorf tube. Cytochalasin B was added to the cytoplasmic extract at a final concentration of 10 µg/ml. For the applications in this study, extracts were further supplemented with cycloheximide at a final concentration of 100 µg/ml to inhibit protein synthesis and recombinant human cyclin B1Δ90 (kindly provided by L. Schöckel) at a final concentration of 10 ng/µl to obtain "low Δ90" extracts that exhibit APC/C, Cdk1 and separase activity after release from metaphase II arrest by Ca^{2+} addition.

4.5. Protein methods

4.5.1. SDS-polyacrylamide gel electrophoresis (SDS-PAGE)

Laemmli running buffer
25 mM Tris
192 mM Glycine
3.5 mM SDS

Sample buffer (4x)
250 mM Tris-HCl (pH 6.8)
40% Glycerol
8% (w/v) SDS
0.04% (w/v) Bromphenol blue
2 M β-Mercaptoethanol

For the separation of proteins under denaturing conditions, SDS-PAGE was performed using commercially available "SERVAGel^{TM} Neutral pH 7.4" gradient gels (Serva). Prior to loading, protein samples were mixed with sample buffer and denatured at 95°C for 5 min. As a molecular weight standard, PageRuler Prestained Protein Ladder (Fermentas) was used. Electrophoresis was carried out at 25 mA per gel in Laemmli running buffer.

4.5.2. Immunoblotting

Blotting buffer
25 mM Tris
192 mM Glycine
20% Methanol

TBS-w
25 mM Tris (pH 7.5)
137 mM NaCl
2.6 mM KCl
0.05% Tween-20

After separation via SDS-PAGE, proteins were transferred electrophoretically to a polyvinylidene fluoride (PVDF) membrane (Immobilon P, Millipore) using blotting buffer in a "semi-dry" blotting apparatus (Peqlab or Biorad). Prior to blotting, the hydrophobic PVDF membrane was briefly coated in 100% methanol. Protein transfer

was carried out at a constant voltage of 15 V for 45-60 min at RT. The membrane was blocked for unspecific binding with 5% skim milk in TBS-w for 40 min at RT. Subsequent incubation in primary antibody diluted in RotiBlock (Roth) was done at RT for 1-2 h or at 4°C o/n. The membrane was then washed three times with TBS-w for 5 min each. The appropriate horseradish peroxidase (HRP)-coupled secondary antibody was diluted in TBS-w and added to the membrane for 45 min at RT. Afterwards, the membrane was washed as before. Chemiluminescence detection was carried out using the protocol provided with the kit (ECL, GE Healthcare or HRP-Juice, PJK GmbH, Kleinblittersdorf) and a CCD-based LAS-4000 camera system (Fuji).

4.5.3. Coomassie staining

Coomassie solution	0.4% (w/v) Coomassie Billiant Blue R250
	0.4% (w/v) Coomassie Billiant Blue G250
	40% Methanol (reagent grade)
	10% Acetic Acid
Destaining solution	30% Methanol
	7% Acetic acid

For coomassie staining, gels were incubated in coomassie solution after SDS-PAGE for at least 2 h. To remove unspecific stain, gels were subsequently transferred to destaining solution for 5-12 h. For long-term storage, coomassie-stained gels were dried on Whatman blotting paper (GE Healthcare) in a slab gel dryer (GD2000, Hoefer).

4.5.4. Autoradiography

After SDS-PAGE, gels were incubated in destaining solution for 20 min and subsequently washed with water. Gels were then dried on Whatman blotting paper (GE Healthcare) in a slab gel dryer (GD2000, Hoefer) and exposed to a film (BioMax MR, Kodak) for 3 h to 3 days, depending on the intensity of the expected signals. Autoradiographies were digitized using an FLA-7000 phosphorimager (Fuji Film Europe, Düsseldorf).

4.5.5. Coupled *in vitro* transcription/translation (IVT)

In vitro transcription/translation in reticulocyte lysate supplemented with SP6 RNA polymerase was carried out using "TNT Quick Coupled Transcription/Translation System" (Promega, Mannheim). For a single reaction, 20 µl TNT Quick Master Mix, 1 µl of pCS2 plasmid DNA (500 ng/µl), 1 µl of [^{35}S] methionine (Hartmann Analytic GmbH, Braunschweig) and 3 µl of RNase free water were combined and incubated for 90 min at 30°C.

4.5.6. Ni^{2+}-NTA affinity purification of 6x-Histidine-tagged proteins

Lysis buffer	400 mM NaCl
	1x PBS

Ni^{2+}-NTA affinity purification was used to isolate recombinant His_6-tagged separase and securin fragments from *E. coli* lysates for use as antigens in subsequent antibody purifications (see chapter 4.5.7.). Protein expression was done as described in chapter 4.2.6. Pelleted bacteria were resuspended in 10 ml of ice cold lysis buffer per g pellet. Cells were lysed in a high pressure homogenizer (Avestin, Ottawa, Canada) by cycling the cell suspension for 10 min. The lysate was cleared from debris by centrifugation in a JA- 25.50 rotor (Beckman Coulter) at 25,000 g for 30 min, supplemented with 10 mM imidazole and subsequently incubated with 25 µl Ni^{2+}-NTA agarose (Qiagen) per ml lysate for 2 h at 4°C on a turning wheel. Beads were washed with lysis buffer supplemented with 10 mM imidazole and 0.02% Tween-20. Bound protein was eluted from beads with 2 times 1 ml lysis buffer supplemented with 250 mM imidazole and 5 mM β-mercaptoethanol. Protein containing fractions were identified by SDS-PAGE and Coomassie staining. Peak fractions were pooled and dialyzed in part against 1x PBS (for rabbit injection) or coupling buffer (0.2 M $NaHCO_3$/0.5 M NaCl pH 8.3) for coupling of NHS columns, see chapter 4.5.7.). Purified protein was aliquoted, snap-frozen using liquid nitrogen and subsequently stored at -80°C.

4.5.7. Purification of specific antibodies from rabbit serum

For the generation of polyclonal antibodies against human separase and human securin, His_6-tagged protein fragments of the desired epitope (see anti-pSX38 and anti-pSX104 antibodies chapter 4.1.4., non-commercial antibodies) were expressed in *E. coli* Rosetta DE3 and purified by Ni^{2+}-NTA agarose pull downs. Rabbits were immunized three times with 0.5-1 mg of antigen in 1x PBS buffer mixed with TiterMax™ Gold Adjuvant (Sigma) at a time over a ten week period (CovalAb, Villeurbanne, France). Antibodies raised against the antigen were purified by pumping the obtained rabbit serum over a HiTrap N-hydroxy-succinimide (NHS)-activated column (GE Healthcare) coupled with the antigen according to the instructions of the manufacturer at a rate of 0.5 ml/min. After washing with 1x PBS and 5 mM Tris-HCl (pH 6.8), antibodies were eluted from the column with 100 mM Glycine/100 mM NaCl (pH 2.5). Fractions containing antibodies were identified by SDS-PAGE and Coomassie staining. Peak fraktions were pooled, dialyzed against PBS/50% glycerine, snap-frozen in aliquots and stored at -80°C.

4.5.8. Co-Immunoprecipitation (Co-IP) experiments from transfected Hek293T cells

Lysis buffer 2 (LP2)	20 mM Tris-HCl (pH7.7) 100 mM NaCl 10 mM NaF 20 mM β-Glycerophosphate 5 mM $MgCl_2$ 0.1% Triton X-100 5% Glycerol 1 mM EDTA
*LP2**	LP2 supplemented with 1x protease inhibitior cocktail (Roche)

Cells were harvested by scraping (HeLa cells) or rinsing (Hek293T cells) from a 100 mm cell culture dish. After centrifugation for 3 min at 300 g at RT, cells were washed once with 1x PBS and centrifuged again. From here on all steps were

performed on ice. The cell pellets were resuspended in 500 µl LP2*, Dounce-homogenized (using a glass dounce homogenizer, Wheaton, Millville, NJ, USA) and left on ice for 10 min. Lysates were centrifuged at 16,000 g for 30 min and the supernatant was transferred to a new tube. An input sample of 20 µl was extracted and mixed with SDS-PAGE sample buffer. Concomitantly, the appropriate affinity matrix was equilibrated by washing once with PBS/0.01% Tween-20 and once with LP2. For ZZ-TEV tagged separase, 25 µl IgG-Sepharose™ 6 Fast Flow beads (GE Healthcare) were used. For Myc_6 epitope tagged separase, 5 µl anti-c-myc Agarose from rabbit (Sigma) were used. For His_6-FLAG-His_6-FLAG-tagged securin, 5 µl anti-FLAG M2-Agarose from mouse (Sigma) were used. Subsequently, the supernatants were incubated with the equilibrated beads at 4°C for 3-4 h (FLAG IPs) or o/n (IgG IPs). Beads were then washed three times with LP2*. Elution of ZZ-TEV tagged separase from IgG-Sepharose beads was done with 1/2 bead volume His_6-tagged Tev protease (12,000 U/ml, Core facility, MPI Martinsried; in the following referred to as His-Tev-protease) for 45 min at 18°C. As a negative control, 1/2 bead volume His-Tev-protease was added during the incubation procedure. Beads were removed by passing the sample over a Mobicol microcolumn (Mobitec, Göttingen). The eluted protein samples were boiled for 5 min at 95°C. Elution of His_6-FLAG-His_6-FLAG- and Myc-tagged proteins was done by shaking the beads with 2x SDS-PAGE sample buffer (without β-mercaptoethanol) for 15 min at 80°C. Beads were removed by passing the sample over a Mobicol microcolumn before the eluted protein sample was supplemented with 0.5 M β-mercaptoethanol and boiled for 10 min at 95°C.

For tandem affinity purification of overexpressed ZZ-TEV_4-separase and securin-His_6-FLAG-His_6-FLAG constructs from Hek293T cells, His-Tev-protease separase eluates from 10 ml LP2* lysates were expanded to 1 ml with LP2* and rotated for 4 h at 4°C together with anti-FLAG M2-agarose beads (Sigma). Subsequently, antibody-beads were washed and eluted as before.

4.5.9. Co-IP experiments of endogenous proteins

CSF-XB washing buffer	CSF-XB ((Murray, 1991); see chapter 4.4.10.)
	0.01% Triton X-100
	250 mM NaCl

10 µl protein G sepharose (4 Fast Flow, GE Healthcare) beads were washed twice with PBS/1% (w/v) BSA prior to coupling with approximately 5 µg of specific antibody for 90 min at RT. For standard IPs of endogenous separase, anti-pSX38 separase antibody was used. For analysis of endogenous separase-PP2A interaction specifically, anti-separase antibody from Bethyl (A302-214A), which binds to residues 1100-1150 of human separase, was used. Coupled beads were washed three times with LP2 and incubated with LP2* lysates from confluent 100 mm cell culture dishes (see chapter 4.5.8.) at 4°C for 4 h or o/n. Protein G sepharose coupled unspecific rabbit IgG served as negative controls. Beads were washed three times with CSF-XB washing buffer and bound proteins were eluted by boiling 25 µl beads and buffer volume with 25 µl 2x SDS-PAGE sample buffer for 10 min at 95°C. Beads were removed by passing the sample over a Mobicol microcolumn. For some experiments, the separase depleted lysates were subjected to another round of immuno-depletion with protein G sepharose coupled anti-pSX104 securin antibody. IP and elution of beads was done as before.

4.5.10. Lambda phosphatase treatment

This method was used to determine whether differential migration behavior of proteins in SDS-PAGE or on autoradiography was caused by phosphorylation. For Lambda phosphatase treatment of immunoprecipitated proteins, proteins were left on beads after immunoprecipitation, washed three times with LP2* (see chapter 4.5.8., omitting NaF, β-glycerophosphate and EDTA) and incubated with 400 units Lambda phosphatase (NEB) per 50 µl beads suspension. 1x NEBuffer for Protein MetalloPhosphatases (PMP, NEB) was added and $MnCl_2$ was set to a final concentration of 1 mM. Samples were incubated for 30 min at 30°C. Subsequently, proteins were eluted from beads as described (see chapter 4.5.8.). For Lambda phosphatase treatment of *in vitro* transcribed/translated proteins incubated in 50 µl CSF-extract for degradation studies, 3 µl sample were treated with 400 units Lambda phosphatase (NEB), 1x NEBuffer for PMP (NEB) and 1 mM $MnCl_2$.

5. ABBREVIATIONS

°C	degree Celsius
A	ampere
aa	amino acid(s)
APC/C	anaphase promoting complex/cyclosome
APS	ammonium peroxodisulfate
AQUA	absolute quantification of proteins
ARM	armadillo (protein domain)
ATP	adenosine 5'-triphosphate
bp	base pairs
BSA	bovine serum albumin
Bub	budding uninhibited by benzimidazole
ca.	circa
CAK	cdk-activating kinase
CaMKII	Ca^{2+}/calmodulin-dependent protein kinase
Cdc	cell division cycle
Cdk	cyclin-dependent kinase
CHX	cycloheximide
CLD	Cdc6-like domain
CMV	cyto megalo virus
CSF	cytostatic factor
CSF-extract	*X. laevis* egg extract arrested in metaphase II by CSF activity
C-terminus	carboxy terminus (C-terminal: carboxyterminal)
Ctrl	control
Da	dalton
D-box	destruction box (aa sequence RxxL; x: any amino acid)
dd	double distilled
Δ	delta (deletion of a protein binding domain, eg. of the PP2A binding domain on separase in a separase$^{\Delta PP2A}$ variant)
D. melanogaster	*Drosophila melanogaster*
DMSO	dimethylsulfoxide
DNA	deoxyribonucleic acid
dNTP	deoxynucleotide
DTT	dithiothreitol
E. coli	*Escherichia coli*
EDTA	ethylendiamine tetraacetic acid
EGTA	ethylen glycol tetraacetic acid
Emi	early mitotic inhibitor
Erp	Emi related protein
Fig	figure
FLAG	epitope tag (aa sequence: DYKDDDDK)
g	gram or gravitational constant (9.81 m/sec^2)
GFP	green fluorescent protein

GST	glutathione S transferase
h	hour or human
HA	hemagglutinin, epitope tag (aa sequence: YPYDVPDYA)
HAc	acetic acid
HBS	HEPES buffered saline
HEAT	huntingtin, elongation factor 3, PP2A subunit A, TOR1 (protein domain)
HEPES	4-(2-hydroxyethyl)-1piperazineethansulfonic acid
His	histidine
HRP	horse radish peroxidase
H. sapiens	*Homo sapiens*
IgG	immunoglobulin G
IP	immunoprecipitation
IPTG	isopropyl-β-D-thiogalactopyranoside
IVT	*in vitro* transcription/translation
k	kilo
kb	kilo base pairs
l	liter
LB	Luria-Bertani
µ	micro
m	milli, meter, mouse or mutated
M	mega or molar (mol/l)
Mad	mitotic arrest deficient
MCAK	mitotic centromere associated kinesin
MCC	mitotic checkpoint complex
MCS	multiple cloning site
MG-262	proteasome inhibitor (MyoGenetics)
min	minute(s)
MMR	Marc's modified Ringer
M. musculus	*Mus musculus*
MPF	mitosis/maturation promoting factor
mRNA	messenger RNA
MT	microtubules
Myc	c-Myc oncogene, epitope tag (aa sequence: EQKLISEEDL)
n	nano
NC	non-cleavable
NHS	N-hydroxysuccinimid
noc	nocodazole (MT poison)
NTA	nitrilo tri-acetic acid
N-terminus	amino terminus (N-terminal: aminoterminal)
OAA	okadaic acid (phosphatase inhibitor)
OD	optical density
o/n	over night
ORF	open reading frame
p.a.	*pro analysi*
PAGE	polyacrylamide gel electrophoresis
PBS	phoshate buffered saline
PCR	polymerase chain reaction

PD	protease-dead
PEI	polyethylenimine
PKA	protein kinase A
Plk	polo-like kinase
PPase	phosphatase
PP2A	protein phosphatase 2A
PVDF	polyvinylidene fluoride
RING	really interesting new gene
RNA	ribonucleic acid
RNAi	RNA interference
RNase	ribonuclease
rpm	revolutions per minute
RT	room temperature
SAC	spindle assembly checkpoint
SAP	shrimp alkaline phosphatase
S. cerevisiae	*Saccharomyces cerevisiae* (budding yeast)
SDS	sodium dodecylsulfate
sec	seconds
Ser/Thr	serine and threonine residues
Sgo	shugoshin
SILAC	stable isotope labeling with amino acids in cell culture
SMC	structural maintenance of chromosomes
SN	supernatant
S. pombe	*Schizosaccharomyces pombe* (fission yeast)
TBS	Tris buffered saline (TBS-w: TBS with 0.05 % Tween-20)
TEMED	N,N,N',N'-tetramethylethylendiamine
Tet	tetracycline
Tev	protease of tobacco etch virus
TEV	Tev protease recognition sequence (aa sequence: EXXYXQG/S)
Tris	tris(hydroxymethyl)aminomethane
U	unit
V	volt
v/v	volume per volume
Wapl	wings apart-like
WCE	whole cell extract
w/v	weight per volume
WT	wild-type
XB	extract buffer
x	any amino acid
X. laevis	*Xenopus laevis*
YC	C-terminal fragment of YFP
YFP	yellow fluorescent protein
ZZ	IgG binding domain of protein A

6. TABLE OF FIGURES

7. REFERENCES

Alexandru, G., Uhlmann, F., Mechtler, K., Poupart, M.A., and Nasmyth, K. (2001). Phosphorylation of the cohesin subunit Scc1 by Polo/Cdc5 kinase regulates sister chromatid separation in yeast. Cell 105, 459-472.

Anderson, D.E., Losada, A., Erickson, H.P., and Hirano, T. (2002). Condensin and cohesin display different arm conformations with characteristic hinge angles. J Cell Biol 156, 419-424.

Anfinsen, C.B. (1973). Principles that govern the folding of protein chains. Science 181, 223-230.

Ausubel, F.M., Brent, R., Kingston, R. E., Moore, D. D., Seidman, J. G., Smith, J. A., und, and Struhl, K. (1998). Current protocols in molecular biology. Greene publishing associates.

Bai, C., Sen, P., Hofmann, K., Ma, L., Goebl, M., Harper, J.W., and Elledge, S.J. (1996). SKP1 connects cell cycle regulators to the ubiquitin proteolysis machinery through a novel motif, the F-box. Cell 86, 263-274.

Bentley, A.M., Normand, G., Hoyt, J., and King, R.W. (2007). Distinct sequence elements of cyclin B1 promote localization to chromatin, centrosomes, and kinetochores during mitosis. Mol Biol Cell 18, 4847-4858.

Bernal, J.A., Luna, R., Espina, A., Lazaro, I., Ramos-Morales, F., Romero, F., Arias, C., Silva, A., Tortolero, M., and Pintor-Toro, J.A. (2002). Human securin interacts with p53 and modulates p53-mediated transcriptional activity and apoptosis. Nat Genet 32, 306-311.

Bhattacharyya, J., and Das, K.P. (1999). Molecular chaperone-like properties of an unfolded protein, alpha(s)-casein. J Biol Chem 274, 15505-15509.

Bialojan, C., and Takai, A. (1988). Inhibitory effect of a marine-sponge toxin, okadaic acid, on protein phosphatases. Specificity and kinetics. Biochem J 256, 283-290.

Boos, D., Kuffer, C., Lenobel, R., Korner, R., and Stemmann, O. (2008). Phosphorylation-dependent binding of cyclin B1 to a Cdc6-like domain of human separase. J Biol Chem 283, 816-823.

Bourne, Y., Watson, M.H., Arvai, A.S., Bernstein, S.L., Reed, S.I., and Tainer, J.A. (2000). Crystal structure and mutational analysis of the Saccharomyces cerevisiae cell cycle regulatory protein Cks1: implications for domain swapping, anion binding and protein interactions. Structure 8, 841-850.

Bourne, Y., Watson, M.H., Hickey, M.J., Holmes, W., Rocque, W., Reed, S.I., and Tainer, J.A. (1996). Crystal structure and mutational analysis of the human CDK2 kinase complex with cell cycle-regulatory protein CksHs1. Cell 84, 863-874.

Carretero, M., Remeseiro, S., and Losada, A. (2010). Cohesin ties up the genome. Curr Opin Cell Biol 22, 781-787.

CellSignalingTechnology (2010). http://www.cellsignal.com/reference/pathway/Ubiquitin_Proteasome.html.

Chang, H.Y., Jennings, P.C., Stewart, J., Verrills, N.M., and Jones, K.T. (2011). Essential role of protein phosphatase 2A in metaphase II arrest and activation of mouse eggs shown by okadaic acid, dominant negative protein phosphatase 2A, and FTY720. J Biol Chem 286, 14705-14712.

Ciosk, R., Shirayama, M., Shevchenko, A., Tanaka, T., Toth, A., and Nasmyth, K. (2000). Cohesin's binding to chromosomes depends on a separate complex consisting of Scc2 and Scc4 proteins. Mol Cell 5, 243-254.

Clute, P., and Pines, J. (1999). Temporal and spatial control of cyclin B1 destruction in metaphase. Nat Cell Biol 1, 82-87.

Cohen, P., Holmes, C.F., and Tsukitani, Y. (1990). Okadaic acid: a new probe for the study of cellular regulation. Trends Biochem Sci 15, 98-102.

Cohen-Fix, O., Peters, J.M., Kirschner, M.W., and Koshland, D. (1996). Anaphase initiation in Saccharomyces cerevisiae is controlled by the APC-dependent degradation of the anaphase inhibitor Pds1p. Genes Dev 10, 3081-3093.

Csizmok, V., Felli, I.C., Tompa, P., Banci, L., and Bertini, I. (2008). Structural and dynamic characterization of intrinsically disordered human securin by NMR spectroscopy. J Am Chem Soc 130, 16873-16879.

De Antoni, A., Pearson, C.G., Cimini, D., Canman, J.C., Sala, V., Nezi, L., Mapelli, M., Sironi, L., Faretta, M., Salmon, E.D., et al. (2005). The Mad1/Mad2 complex as a template for Mad2 activation in the spindle assembly checkpoint. Curr Biol 15, 214-225.

De Boer, L., Oakes, V., Beamish, H., Giles, N., Stevens, F., Somodevilla-Torres, M., Desouza, C., and Gabrielli, B. (2008). Cyclin A/cdk2 coordinates centrosomal and nuclear mitotic events. Oncogene 27, 4261-4268.

den Elzen, N., and Pines, J. (2001). Cyclin A is destroyed in prometaphase and can delay chromosome alignment and anaphase. J Cell Biol 153, 121-136.

Fang, G., Yu, H., and Kirschner, M.W. (1998). The checkpoint protein MAD2 and the mitotic regulator CDC20 form a ternary complex with the anaphase-promoting complex to control anaphase initiation. Genes Dev 12, 1871-1883.

Finley, D. (2009). Recognition and processing of ubiquitin-protein conjugates by the proteasome. Annu Rev Biochem 78, 477-513.

Flegg, C.P., Sharma, M., Medina-Palazon, C., Jamieson, C., Galea, M., Brocardo, M.G., Mills, K., and Henderson, B.R. (2010). Nuclear export and centrosome targeting of the protein phosphatase 2A subunit B56alpha: role of B56alpha in nuclear export of the catalytic subunit. J Biol Chem 285, 18144-18154.

Funabiki, H., Kumada, K., and Yanagida, M. (1996). Fission yeast Cut1 and Cut2 are essential for sister chromatid separation, concentrate along the metaphase spindle and form large complexes. EMBO J 15, 6617-6628.

Fung, T.K., Ma, H.T., and Poon, R.Y. (2007). Specialized roles of the two mitotic cyclins in somatic cells: cyclin A as an activator of M phase-promoting factor. Mol Biol Cell 18, 1861-1873.

Furuno, N., den Elzen, N., and Pines, J. (1999). Human cyclin A is required for mitosis until mid prophase. J Cell Biol 147, 295-306.

Gandhi, R., Gillespie, P.J., and Hirano, T. (2006). Human Wapl is a cohesin-binding protein that promotes sister-chromatid resolution in mitotic prophase. Curr Biol 16, 2406-2417.

Garcia-Mata, R., Gao, Y.S., and Sztul, E. (2002). Hassles with taking out the garbage: aggravating aggresomes. Traffic 3, 388-396.

Gavet, O., and Pines, J. (2010). Activation of cyclin B1-Cdk1 synchronizes events in the nucleus and the cytoplasm at mitosis. J Cell Biol 189, 247-259.

Geley, S., Kramer, E., Gieffers, C., Gannon, J., Peters, J.M., and Hunt, T. (2001). Anaphase-promoting complex/cyclosome-dependent proteolysis of human cyclin A starts at the beginning of mitosis and is not subject to the spindle assembly checkpoint. J Cell Biol 153, 137-148.

Gerber, S.A., Rush, J., Stemman, O., Kirschner, M.W., and Gygi, S.P. (2003). Absolute quantification of proteins and phosphoproteins from cell lysates by tandem MS. Proc Natl Acad Sci U S A 100, 6940-6945.

Gil-Bernabé, A.M., Romero, F., Limon-Mortes, M.C., and Tortolero, M. (2006). Protein phosphatase 2A stabilizes human securin, whose phosphorylated forms are degraded via the SCF ubiquitin ligase. Mol Cell Biol 26, 4017-4027.

Gong, D., and Ferrell, J.E., Jr. (2010). The roles of cyclin A2, B1, and B2 in early and late mitotic events. Mol Biol Cell 21, 3149-3161.

Gong, D., Pomerening, J.R., Myers, J.W., Gustavsson, C., Jones, J.T., Hahn, A.T., Meyer, T., and Ferrell, J.E., Jr. (2007). Cyclin A2 regulates nuclear-envelope breakdown and the nuclear accumulation of cyclin B1. Curr Biol 17, 85-91.

Goris, J., Hermann, J., Hendrix, P., Ozon, R., and Merlevede, W. (1989). Okadaic acid, a specific protein phosphatase inhibitor, induces maturation and MPF formation in Xenopus laevis oocytes. FEBS Lett 245, 91-94.

Gorr, I.H., Boos, D., and Stemmann, O. (2005). Mutual inhibition of separase and Cdk1 by two-step complex formation. Mol Cell 19, 135-141.

Gruber, S., Haering, C.H., and Nasmyth, K. (2003). Chromosomal cohesin forms a ring. Cell 112, 765-777.

Haccard, O., Sarcevic, B., Lewellyn, A., Hartley, R., Roy, L., Izumi, T., Erikson, E., and Maller, J.L. (1993). Induction of metaphase arrest in cleaving Xenopus embryos by MAP kinase. Science 262, 1262-1265.

Haering, C.H., Lowe, J., Hochwagen, A., and Nasmyth, K. (2002). Molecular architecture of SMC proteins and the yeast cohesin complex. Mol Cell 9, 773-788.

Hagting, A., Jackman, M., Simpson, K., and Pines, J. (1999). Translocation of cyclin B1 to the nucleus at prophase requires a phosphorylation-dependent nuclear import signal. Curr Biol 9, 680-689.

Hamid, T., and Kakar, S.S. (2004). PTTG/securin activates expression of p53 and modulates its function. Mol Cancer 3, 18.

Harley, M.E., Allan, L.A., Sanderson, H.S., and Clarke, P.R. (2010). Phosphorylation of Mcl-1 by CDK1-cyclin B1 initiates its Cdc20-dependent destruction during mitotic arrest. EMBO J 29, 2407-2420.

Harper, J.W. (2001). Protein destruction: adapting roles for Cks proteins. Curr Biol 11, R431-435.

Hauf, S., Roitinger, E., Koch, B., Dittrich, C.M., Mechtler, K., and Peters, J.M. (2005). Dissociation of cohesin from chromosome arms and loss of arm cohesion during early mitosis depends on phosphorylation of SA2. PLoS Biol 3, e69.

Hauf, S., Waizenegger, I.C., and Peters, J.M. (2001). Cohesin cleavage by separase required for anaphase and cytokinesis in human cells. Science 293, 1320-1323.

Hayes, M.J., Kimata, Y., Wattam, S.L., Lindon, C., Mao, G., Yamano, H., and Fry, A.M. (2006). Early mitotic degradation of Nek2A depends on Cdc20-independent interaction with the APC/C. Nat Cell Biol 8, 607-614.

Heald, R., and McKeon, F. (1990). Mutations of phosphorylation sites in lamin A that prevent nuclear lamina disassembly in mitosis. Cell 61, 579-589.

Heidinger-Pauli, J.M., Unal, E., and Koshland, D. (2009). Distinct targets of the Eco1 acetyltransferase modulate cohesion in S phase and in response to DNA damage. Mol Cell 34, 311-321.

Hershko, A., and Ciechanover, A. (1998). The ubiquitin system. Annu Rev Biochem 67, 425-479.

Herzig, A., Lehner, C.F., and Heidmann, S. (2002). Proteolytic cleavage of the THR subunit during anaphase limits Drosophila separase function. Genes Dev 16, 2443-2454.

Hirsch, C., and Ploegh, H.L. (2000). Intracellular targeting of the proteasome. Trends Cell Biol 10, 268-272.

Holland, A.J., Bottger, F., Stemmann, O., and Taylor, S.S. (2007). Protein phosphatase 2A and separase form a complex regulated by separase autocleavage. J Biol Chem 282, 24623-24632.

Holland, A.J., and Taylor, S.S. (2006). Cyclin-B1-mediated inhibition of excess separase is required for timely chromosome disjunction. J Cell Sci 119, 3325-3336.

Holloway, S.L., Glotzer, M., King, R.W., and Murray, A.W. (1993). Anaphase is initiated by proteolysis rather than by the inactivation of maturation-promoting factor. Cell 73, 1393-1402.

Holt, L.J., Krutchinsky, A.N., and Morgan, D.O. (2008). Positive feedback sharpens the anaphase switch. Nature 454, 353-357.

Hornig, N.C., Knowles, P.P., McDonald, N.Q., and Uhlmann, F. (2002). The dual mechanism of separase regulation by securin. Curr Biol 12, 973-982.

Howell, B.J., McEwen, B.F., Canman, J.C., Hoffman, D.B., Farrar, E.M., Rieder, C.L., and Salmon, E.D. (2001). Cytoplasmic dynein/dynactin drives kinetochore protein transport to the spindle poles and has a role in mitotic spindle checkpoint inactivation. J Cell Biol 155, 1159-1172.

Hu, B., Mitra, J., van den Heuvel, S., and Enders, G.H. (2001). S and G2 phase roles for Cdk2 revealed by inducible expression of a dominant-negative mutant in human cells. Mol Cell Biol 21, 2755-2766.

Huang, X., Andreu-Vieyra, C.V., Wang, M., Cooney, A.J., Matzuk, M.M., and Zhang, P. (2009). Preimplantation mouse embryos depend on inhibitory phosphorylation of separase to prevent chromosome missegregation. Mol Cell Biol 29, 1498-1505.

Huang, X., Andreu-Vieyra, C.V., York, J.P., Hatcher, R., Lu, T., Matzuk, M.M., and Zhang, P. (2008). Inhibitory phosphorylation of separase is essential for genome stability and viability of murine embryonic germ cells. PLoS Biol 6, e15.

Huang, X., Hatcher, R., York, J.P., and Zhang, P. (2005). Securin and separase phosphorylation act redundantly to maintain sister chromatid cohesion in mammalian cells. Mol Biol Cell 16, 4725-4732.

Ivanov, D., Schleiffer, A., Eisenhaber, F., Mechtler, K., Haering, C.H., and Nasmyth, K. (2002). Eco1 is a novel acetyltransferase that can acetylate proteins involved in cohesion. Curr Biol 12, 323-328.

Jackman, M., Firth, M., and Pines, J. (1995). Human cyclins B1 and B2 are localized to strikingly different structures: B1 to microtubules, B2 primarily to the Golgi apparatus. EMBO J 14, 1646-1654.

Jackman, M., Kubota, Y., den Elzen, N., Hagting, A., and Pines, J. (2002). Cyclin A- and cyclin E-Cdk complexes shuttle between the nucleus and the cytoplasm. Mol Biol Cell 13, 1030-1045.

Jackman, M., Lindon, C., Nigg, E.A., and Pines, J. (2003). Active cyclin B1-Cdk1 first appears on centrosomes in prophase. Nat Cell Biol 5, 143-148.

Jager, H., Herzig, A., Lehner, C.F., and Heidmann, S. (2001). Drosophila separase is required for sister chromatid separation and binds to PIM and THR. Genes Dev 15, 2572-2584.

Jager, H., Herzig, B., Herzig, A., Sticht, H., Lehner, C.F., and Heidmann, S. (2004). Structure predictions and interaction studies indicate homology of separase N-terminal regulatory domains and Drosophila THR. Cell Cycle 3, 182-188.

Jallepalli, P.V., Waizenegger, I.C., Bunz, F., Langer, S., Speicher, M.R., Peters, J.M., Kinzler, K.W., Vogelstein, B., and Lengauer, C. (2001). Securin is required for chromosomal stability in human cells. Cell 105, 445-457.

Janssens, V., and Goris, J. (2001). Protein phosphatase 2A: a highly regulated family of serine/threonine phosphatases implicated in cell growth and signalling. Biochem J 353, 417-439.

Jeganathan, K.B., Baker, D.J., and van Deursen, J.M. (2006). Securin associates with APCCdh1 in prometaphase but its destruction is delayed by Rae1 and Nup98 until the metaphase/anaphase transition. Cell Cycle 5, 366-370.

Jeganathan, K.B., Malureanu, L., and van Deursen, J.M. (2005). The Rae1-Nup98 complex prevents aneuploidy by inhibiting securin degradation. Nature 438, 1036-1039.

Jensen, S., Segal, M., Clarke, D.J., and Reed, S.I. (2001). A novel role of the budding yeast separin Esp1 in anaphase spindle elongation: evidence that proper spindle association of Esp1 is regulated by Pds1. J Cell Biol 152, 27-40.

Johnson, S.A., and Hunter, T. (2005). Kinomics: methods for deciphering the kinome. Nat Methods 2, 17-25.

Kim, T.D., Paik, S.R., and Yang, C.H. (2002). Structural and functional implications of C-terminal regions of alpha-synuclein. Biochemistry 41, 13782-13790.

King, R.W., Peters, J.M., Tugendreich, S., Rolfe, M., Hieter, P., and Kirschner, M.W. (1995). A 20S complex containing CDC27 and CDC16 catalyzes the mitosis-specific conjugation of ubiquitin to cyclin B. Cell 81, 279-288.

Kitajima, T.S., Sakuno, T., Ishiguro, K., Iemura, S., Natsume, T., Kawashima, S.A., and Watanabe, Y. (2006). Shugoshin collaborates with protein phosphatase 2A to protect cohesin. Nature 441, 46-52.

Kopito, R.R. (2000). Aggresomes, inclusion bodies and protein aggregation. Trends Cell Biol 10, 524-530.

Kotani, S., Tanaka, H., Yasuda, H., and Todokoro, K. (1999). Regulation of APC activity by phosphorylation and regulatory factors. J Cell Biol 146, 791-800.

Kramer, E.R., Scheuringer, N., Podtelejnikov, A.V., Mann, M., and Peters, J.M. (2000). Mitotic regulation of the APC activator proteins CDC20 and CDH1. Mol Biol Cell 11, 1555-1569.

Kueng, S., Hegemann, B., Peters, B.H., Lipp, J.J., Schleiffer, A., Mechtler, K., and Peters, J.M. (2006). Wapl controls the dynamic association of cohesin with chromatin. Cell 127, 955-967.

Kumada, K., Nakamura, T., Nagao, K., Funabiki, H., Nakagawa, T., and Yanagida, M. (1998). Cut1 is loaded onto the spindle by binding to Cut2 and promotes anaphase spindle movement upon Cut2 proteolysis. Curr Biol 8, 633-641.

Kumada, K., Yao, R., Kawaguchi, T., Karasawa, M., Hoshikawa, Y., Ichikawa, K., Sugitani, Y., Imoto, I., Inazawa, J., Sugawara, M., et al. (2006). The selective continued linkage of centromeres from mitosis to interphase in the absence of mammalian separase. J Cell Biol 172, 835-846.

Lafont, A.L., Song, J., and Rankin, S. (2010). Sororin cooperates with the acetyltransferase Eco2 to ensure DNA replication-dependent sister chromatid cohesion. Proc Natl Acad Sci U S A 107, 20364-20369.

Lander, E.S., Linton, L.M., Birren, B., Nusbaum, C., Zody, M.C., Baldwin, J., Devon, K., Dewar, K., Doyle, M., FitzHugh, W., et al. (2001). Initial sequencing and analysis of the human genome. Nature 409, 860-921.

Li, X., Scuderi, A., Letsou, A., and Virshup, D.M. (2002). B56-associated protein phosphatase 2A is required for survival and protects from apoptosis in Drosophila melanogaster. Mol Cell Biol 22, 3674-3684.

Lindqvist, A., Rodriguez-Bravo, V., and Medema, R.H. (2009). The decision to enter mitosis: feedback and redundancy in the mitotic entry network. J Cell Biol 185, 193-202.

Llano, E., Gomez, R., Gutierrez-Caballero, C., Herran, Y., Sanchez-Martin, M., Vazquez-Quinones, L., Hernandez, T., de Alava, E., Cuadrado, A., Barbero, J.L., et al. (2008). Shugoshin-2 is essential for the completion of meiosis but not for mitotic cell division in mice. Genes Dev 22, 2400-2413.

Losada, A., Hirano, M., and Hirano, T. (1998). Identification of Xenopus SMC protein complexes required for sister chromatid cohesion. Genes Dev 12, 1986-1997.

Losada, A., Hirano, M., and Hirano, T. (2002). Cohesin release is required for sister chromatid resolution, but not for condensin-mediated compaction, at the onset of mitosis. Genes Dev 16, 3004-3016.

Losada, A., Yokochi, T., Kobayashi, R., and Hirano, T. (2000). Identification and characterization of SA/Scc3p subunits in the Xenopus and human cohesin complexes. J Cell Biol 150, 405-416.

Luo, X., Tang, Z., Xia, G., Wassmann, K., Matsumoto, T., Rizo, J., and Yu, H. (2004). The Mad2 spindle checkpoint protein has two distinct natively folded states. Nat Struct Mol Biol 11, 338-345.

Lyons, N.A., and Morgan, D.O. (2011). Cdk1-dependent destruction of Eco1 prevents cohesion establishment after S phase. Mol Cell 42, 378-389.

MacKintosh, C., Beattie, K.A., Klumpp, S., Cohen, P., and Codd, G.A. (1990). Cyanobacterial microcystin-LR is a potent and specific inhibitor of protein phosphatases 1 and 2A from both mammals and higher plants. FEBS Lett 264, 187-192.

Manning, G., Whyte, D.B., Martinez, R., Hunter, T., and Sudarsanam, S. (2002). The protein kinase complement of the human genome. Science 298, 1912-1934.

Mapelli, M., Filipp, F.V., Rancati, G., Massimiliano, L., Nezi, L., Stier, G., Hagan, R.S., Confalonieri, S., Piatti, S., Sattler, M., et al. (2006). Determinants of conformational dimerization of Mad2 and its inhibition by p31comet. EMBO J 25, 1273-1284.

Marangos, P., and Carroll, J. (2008). Securin regulates entry into M-phase by modulating the stability of cyclin B. Nat Cell Biol 10, 445-451.

Masui, Y., and Markert, C.L. (1971). Cytoplasmic control of nuclear behavior during meiotic maturation of frog oocytes. J Exp Zool 177, 129-145.

Mei, J., Huang, X., and Zhang, P. (2001). Securin is not required for cellular viability, but is required for normal growth of mouse embryonic fibroblasts. Curr Biol 11, 1197-1201.

Melby, T.E., Ciampaglio, C.N., Briscoe, G., and Erickson, H.P. (1998). The symmetrical structure of structural maintenance of chromosomes (SMC) and MukB proteins: long, antiparallel coiled coils, folded at a flexible hinge. J Cell Biol 142, 1595-1604.

Michaelis, C., Ciosk, R., and Nasmyth, K. (1997). Cohesins: chromosomal proteins that prevent premature separation of sister chromatids. Cell 91, 35-45.

Mimura, S., Seki, T., Tanaka, S., and Diffley, J.F. (2004). Phosphorylation-dependent binding of mitotic cyclins to Cdc6 contributes to DNA replication control. Nature 431, 1118-1123.

Minshull, J., Golsteyn, R., Hill, C.S., and Hunt, T. (1990). The A- and B-type cyclin associated cdc2 kinases in Xenopus turn on and off at different times in the cell cycle. EMBO J 9, 2865-2875.

Moldovan, G.L., Pfander, B., and Jentsch, S. (2006). PCNA controls establishment of sister chromatid cohesion during S phase. Mol Cell 23, 723-732.

Morgan, D.O. (2007). In The Cell Cycle - Principles of Control (New Science Press Ltd).

Murray, A.W. (1991). Cell cycle extracts. Methods Cell Biol 36, 581-605.

Murray, A.W., and Kirschner, M.W. (1989). Dominoes and clocks: the union of two views of the cell cycle. Science 246, 614-621.

Murray, A.W., Solomon, M.J., and Kirschner, M.W. (1989). The role of cyclin synthesis and degradation in the control of maturation promoting factor activity. Nature 339, 280-286.

Nagao, K., Adachi, Y., and Yanagida, M. (2004). Separase-mediated cleavage of cohesin at interphase is required for DNA repair. Nature 430, 1044-1048.

Netzer, W.J., and Hartl, F.U. (1998). Protein folding in the cytosol: chaperonin-dependent and -independent mechanisms. Trends Biochem Sci 23, 68-73.

Olsen, J.V., de Godoy, L.M., Li, G., Macek, B., Mortensen, P., Pesch, R., Makarov, A., Lange, O., Horning, S., and Mann, M. (2005). Parts per million mass accuracy on an Orbitrap mass spectrometer via lock mass injection into a C-trap. Mol Cell Proteomics 4, 2010-2021.

Ong, S.E., and Mann, M. (2007). Stable isotope labeling by amino acids in cell culture for quantitative proteomics. Methods Mol Biol 359, 37-52.

Ookata, K., Hisanaga, S., Okano, T., Tachibana, K., and Kishimoto, T. (1992). Relocation and distinct subcellular localization of p34cdc2-cyclin B complex at meiosis reinitiation in starfish oocytes. EMBO J 11, 1763-1772.

Pagano, M., Pepperkok, R., Verde, F., Ansorge, W., and Draetta, G. (1992). Cyclin A is required at two points in the human cell cycle. EMBO J 11, 961-971.

Papi, M., Berdougo, E., Randall, C.L., Ganguly, S., and Jallepalli, P.V. (2005). Multiple roles for separase auto-cleavage during the G2/M transition. Nat Cell Biol 7, 1029-1035.

Pei, L. (1999). Pituitary tumor-transforming gene protein associates with ribosomal protein S10 and a novel human homologue of DnaJ in testicular cells. J Biol Chem 274, 3151-3158.

Pei, L., and Melmed, S. (1997). Isolation and characterization of a pituitary tumor-transforming gene (PTTG). Mol Endocrinol 11, 433-441.

Peters, J.M. (2006). The anaphase promoting complex/cyclosome: a machine designed to destroy. Nat Rev Mol Cell Biol 7, 644-656.

Peters, J.M., Tedeschi, A., and Schmitz, J. (2008). The cohesin complex and its roles in chromosome biology. Genes Dev 22, 3089-3114.

Petronczki, M., Siomos, M.F., and Nasmyth, K. (2003). Un menage a quatre: the molecular biology of chromosome segregation in meiosis. Cell 112, 423-440.

Pfleghaar, K., Heubes, S., Cox, J., Stemmann, O., and Speicher, M.R. (2005). Securin is not required for chromosomal stability in human cells. PLoS Biol 3, e416.

Pickart, C.M., and Cohen, R.E. (2004). Proteasomes and their kin: proteases in the machine age. Nat Rev Mol Cell Biol 5, 177-187.

Pickart, C.M., and Eddins, M.J. (2004). Ubiquitin: structures, functions, mechanisms. Biochim Biophys Acta 1695, 55-72.

Pines, J. (2011). Cubism and the cell cycle: the many faces of the APC/C. Nat Rev Mol Cell Biol 12, 427-438.

Pines, J., and Hunter, T. (1991). Human cyclins A and B1 are differentially located in the cell and undergo cell cycle-dependent nuclear transport. J Cell Biol 115, 1-17.

Pöhlmann, C. (2009). Elektrochemische Detektion von RNA mittels Nukleinsäurehybridisierung. Dissertation University of Bayreuth.

Ramos-Morales, F., Dominguez, A., Romero, F., Luna, R., Multon, M.C., Pintor-Toro, J.A., and Tortolero, M. (2000). Cell cycle regulated expression and phosphorylation of hpttg proto-oncogene product. Oncogene 19, 403-409.

Rao, H., Uhlmann, F., Nasmyth, K., and Varshavsky, A. (2001). Degradation of a cohesin subunit by the N-end rule pathway is essential for chromosome stability. Nature 410, 955-959.

Rauh, N.R., Schmidt, A., Bormann, J., Nigg, E.A., and Mayer, T.U. (2005). Calcium triggers exit from meiosis II by targeting the APC/C inhibitor XErp1 for degradation. Nature 437, 1048-1052.

Reis, A., Chang, H.Y., Levasseur, M., and Jones, K.T. (2006). APCcdh1 activity in mouse oocytes prevents entry into the first meiotic division. Nat Cell Biol 8, 539-540.

Reis, A., Madgwick, S., Chang, H.Y., Nabti, I., Levasseur, M., and Jones, K.T. (2007). Prometaphase APCcdh1 activity prevents non-disjunction in mammalian oocytes. Nat Cell Biol 9, 1192-1198.

Richardson, H.E., Stueland, C.S., Thomas, J., Russell, P., and Reed, S.I. (1990). Human cDNAs encoding homologs of the small p34Cdc28/Cdc2-associated protein of Saccharomyces cerevisiae and Schizosaccharomyces pombe. Genes Dev 4, 1332-1344.

Riedel, C.G., Katis, V.L., Katou, Y., Mori, S., Itoh, T., Helmhart, W., Galova, M., Petronczki, M., Gregan, J., Cetin, B., et al. (2006). Protein phosphatase 2A protects centromeric sister chromatid cohesion during meiosis I. Nature 441, 53-61.

Rodriguez-Gonzalez, A., Lin, T., Ikeda, A.K., Simms-Waldrip, T., Fu, C., and Sakamoto, K.M. (2008). Role of the aggresome pathway in cancer: targeting histone deacetylase 6-dependent protein degradation. Cancer Res 68, 2557-2560.

Romero, F., Multon, M.C., Ramos-Morales, F., Dominguez, A., Bernal, J.A., Pintor-Toro, J.A., and Tortolero, M. (2001). Human securin, hPTTG, is associated with Ku heterodimer, the regulatory subunit of the DNA-dependent protein kinase. Nucleic Acids Res 29, 1300-1307.

Sablina, A.A., and Hahn, W.C. (2007). The role of PP2A A subunits in tumor suppression. Cell Adh Migr 1, 140-141.

Saha, A., and Deshaies, R.J. (2008). Multimodal activation of the ubiquitin ligase SCF by Nedd8 conjugation. Mol Cell 32, 21-31.

Sakahira, H., and Nagata, S. (2002). Co-translational folding of caspase-activated DNase with Hsp70, Hsp40, and inhibitor of caspase-activated DNase. J Biol Chem 277, 3364-3370.

Sambrook, J., Fritsch, E. F., und Maniatis, T. (1989). Molecular cloning. Cold Spring Harbor Laboratory Press.

Sambrook, J., and Russell, D.W. (2001). Molecular cloning : a laboratory manual, 3rd edn (Cold Spring Harbor, N.Y., Cold Spring Harbor Laboratory Press).

Sanchez-Puig, N., Veprintsev, D.B., and Fersht, A.R. (2005). Human full-length Securin is a natively unfolded protein. Protein Sci 14, 1410-1418.

Schmidt, A., Duncan, P.I., Rauh, N.R., Sauer, G., Fry, A.M., Nigg, E.A., and Mayer, T.U. (2005). Xenopus polo-like kinase Plx1 regulates XErp1, a novel inhibitor of APC/C activity. Genes Dev 19, 502-513.

Schmitz, J., Watrin, E., Lenart, P., Mechtler, K., and Peters, J.M. (2007). Sororin is required for stable binding of cohesin to chromatin and for sister chromatid cohesion in interphase. Curr Biol 17, 630-636.

Schöckel, L., Möckel, M., Mayer, B., Boos, D., and Stemmann, O. (2011). Cleavage of cohesin rings coordinates the separation of centrioles and chromatids. Nat Cell Biol. Manuscript in press.

Schott, E.J., and Hoyt, M.A. (1998). Dominant alleles of Saccharomyces cerevisiae CDC20 reveal its role in promoting anaphase. Genetics 148, 599-610.

Shevchenko, A., Tomas, H., Havlis, J., Olsen, J.V., and Mann, M. (2006). In-gel digestion for mass spectrometric characterization of proteins and proteomes. Nat Protoc 1, 2856-2860.

Shi, Y. (2009). Serine/threonine phosphatases: mechanism through structure. Cell 139, 468-484.

Shintomi, K., and Hirano, T. (2009). Releasing cohesin from chromosome arms in early mitosis: opposing actions of Wapl-Pds5 and Sgo1. Genes Dev 23, 2224-2236.

Silverstein, A.M., Barrow, C.A., Davis, A.J., and Mumby, M.C. (2002). Actions of PP2A on the MAP kinase pathway and apoptosis are mediated by distinct regulatory subunits. Proc Natl Acad Sci U S A 99, 4221-4226.

Skibbens, R.V., Corson, L.B., Koshland, D., and Hieter, P. (1999). Ctf7p is essential for sister chromatid cohesion and links mitotic chromosome structure to the DNA replication machinery. Genes Dev 13, 307-319.

Solomon, M.J., and Burton, J.L. (2008). Securin' M-phase entry. Nat Cell Biol 10, 381-383.

Stemmann, O., Zou, H., Gerber, S.A., Gygi, S.P., and Kirschner, M.W. (2001). Dual inhibition of sister chromatid separation at metaphase. Cell 107, 715-726.

Strack, S., Cribbs, J.T., and Gomez, L. (2004). Critical role for protein phosphatase 2A heterotrimers in mammalian cell survival. J Biol Chem 279, 47732-47739.

Strack, S., Ruediger, R., Walter, G., Dagda, R.K., Barwacz, C.A., and Cribbs, J.T. (2002). Protein phosphatase 2A holoenzyme assembly: identification of contacts between B-family regulatory and scaffolding A subunits. J Biol Chem 277, 20750-20755.

Stratmann, R., and Lehner, C.F. (1996). Separation of sister chromatids in mitosis requires the Drosophila pimples product, a protein degraded after the metaphase/anaphase transition. Cell 84, 25-35.

Sudakin, V., Chan, G.K., and Yen, T.J. (2001). Checkpoint inhibition of the APC/C in HeLa cells is mediated by a complex of BUBR1, BUB3, CDC20, and MAD2. J Cell Biol 154, 925-936.

Sullivan, M., Lehane, C., and Uhlmann, F. (2001). Orchestrating anaphase and mitotic exit: separase cleavage and localization of Slk19. Nat Cell Biol 3, 771-777.

Sullivan, M., Hornig, N.C., Porstmann, T., and Uhlmann, F. (2004). Studies on substrate recognition by the budding yeast separase. J Biol Chem *279*, 1191-1196.

Sumara, I., Vorlaufer, E., Gieffers, C., Peters, B.H., and Peters, J.M. (2000). Characterization of vertebrate cohesin complexes and their regulation in prophase. J Cell Biol 151, 749-762.

Sweeney, C., Murphy, M., Kubelka, M., Ravnik, S.E., Hawkins, C.F., Wolgemuth, D.J., and Carrington, M. (1996). A distinct cyclin A is expressed in germ cells in the mouse. Development 122, 53-64.

Takahashi, T.S., Yiu, P., Chou, M.F., Gygi, S., and Walter, J.C. (2004). Recruitment of Xenopus Scc2 and cohesin to chromatin requires the pre-replication complex. Nat Cell Biol 6, 991-996.

Tang, Z., Shu, H., Qi, W., Mahmood, N.A., Mumby, M.C., and Yu, H. (2006). PP2A is required for centromeric localization of Sgo1 and proper chromosome segregation. Dev Cell 10, 575-585.

Tompa, P., and Csermely, P. (2004). The role of structural disorder in the function of RNA and protein chaperones. FASEB J 18, 1169-1175.

Tong, Y., and Eigler, T. (2009). Transcriptional targets for pituitary tumor-transforming gene-1. J Mol Endocrinol 43, 179-185.

Toth, A., Ciosk, R., Uhlmann, F., Galova, M., Schleiffer, A., and Nasmyth, K. (1999). Yeast cohesin complex requires a conserved protein, Eco1p(Ctf7), to establish cohesion between sister chromatids during DNA replication. Genes Dev 13, 320-333.

Touati S.A., Lister L.M., Böttger F., Stemmann O., Herbert M., and K., W. Separase Inhibition by Stable Cyclin B1, and not Cyclin A2. Manuscript under revision.

Toyoshima-Morimoto, F., Taniguchi, E., Shinya, N., Iwamatsu, A., and Nishida, E. (2001). Polo-like kinase 1 phosphorylates cyclin B1 and targets it to the nucleus during prophase. Nature 410, 215-220.

Tsou, M.F., and Stearns, T. (2006). Mechanism limiting centrosome duplication to once per cell cycle. Nature 442, 947-951.

Tung, J.J., Hansen, D.V., Ban, K.H., Loktev, A.V., Summers, M.K., Adler, J.R., 3rd, and Jackson, P.K. (2005). A role for the anaphase-promoting complex inhibitor Emi2/XErp1, a homolog of early mitotic inhibitor 1, in cytostatic factor arrest of Xenopus eggs. Proc Natl Acad Sci U S A 102, 4318-4323.

Uhlmann, F., Lottspeich, F., and Nasmyth, K. (1999). Sister-chromatid separation at anaphase onset is promoted by cleavage of the cohesin subunit Scc1. Nature 400, 37-42.

Uhlmann, F., Wernic, D., Poupart, M.A., Koonin, E.V., and Nasmyth, K. (2000). Cleavage of cohesin by the CD clan protease separin triggers anaphase in yeast. Cell 103, 375-386.

Vandre, D.D., and Wills, V.L. (1992). Inhibition of mitosis by okadaic acid: possible involvement of a protein phosphatase 2A in the transition from metaphase to anaphase. J Cell Sci 101 (Pt 1), 79-91.

Venter, J.C., Adams, M.D., Myers, E.W., Li, P.W., Mural, R.J., Sutton, G.G., Smith, H.O., Yandell, M., Evans, C.A., Holt, R.A., et al. (2001). The sequence of the human genome. Science 291, 1304-1351.

Viadiu, H., Stemmann, O., Kirschner, M.W., and Walz, T. (2005). Domain structure of separase and its binding to securin as determined by EM. Nat Struct Mol Biol 12, 552-553.

Vigneron, S., Brioudes, E., Burgess, A., Labbe, J.C., Lorca, T., and Castro, A. (2009). Greatwall maintains mitosis through regulation of PP2A. EMBO J 28, 2786-2793.

Vodermaier, H. C., Gieffers, C., Maurer-Stroh, S., Eisenhaber, F. & Peters, J. M. (2003). TPR subunits of the anaphase-promoting complex mediate binding to the activator protein CDH1. Curr Biol 13, 1459–1468.

Waizenegger, I., Gimenez-Abian, J.F., Wernic, D., and Peters, J.M. (2002). Regulation of human separase by securin binding and autocleavage. Curr Biol 12, 1368-1378.

Waizenegger, I.C., Hauf, S., Meinke, A., and Peters, J.M. (2000). Two distinct pathways remove mammalian cohesin from chromosome arms in prophase and from centromeres in anaphase. Cell 103, 399-410.

Wang, Y., Stanzel, M., Gumbrecht, W., Humenik, M., and Sprinzl, M. (2007). Esterase 2-oligodeoxynucleotide conjugates as sensitive reporter for electrochemical detection of nucleic acid hybridization. Biosens Bioelectron 22, 1798-1806.

Wang, Z., Moro, E., Kovacs, K., Yu, R., and Melmed, S. (2003). Pituitary tumor transforming gene-null male mice exhibit impaired pancreatic beta cell proliferation and diabetes. Proc Natl Acad Sci U S A 100, 3428-3432.

Watanabe, Y., Yokobayashi, S., Yamamoto, M., and Nurse, P. (2001). Pre-meiotic S phase is linked to reductional chromosome segregation and recombination. Nature 409, 359-363.

Watrin, E., Schleiffer, A., Tanaka, K., Eisenhaber, F., Nasmyth, K., and Peters, J.M. (2006). Human Scc4 is required for cohesin binding to chromatin, sister-chromatid cohesion, and mitotic progression. Curr Biol 16, 863-874.

Wheatley, S.P., Hinchcliffe, E.H., Glotzer, M., Hyman, A.A., Sluder, G., and Wang, Y. (1997). CDK1 inactivation regulates anaphase spindle dynamics and cytokinesis in vivo. J Cell Biol 138, 385-393.

Wirth, K.G., Wutz, G., Kudo, N.R., Desdouets, C., Zetterberg, A., Taghybeeglu, S., Seznec, J., Ducos, G.M., Ricci, R., Firnberg, N., et al. (2006). Separase: a universal trigger for sister chromatid disjunction but not chromosome cycle progression. J Cell Biol 172, 847-860.

Wolthuis, R., Clay-Farrace, L., van Zon, W., Yekezare, M., Koop, L., Ogink, J., Medema, R., and Pines, J. (2008). Cdc20 and Cks direct the spindle checkpoint-independent destruction of cyclin A. Mol Cell 30, 290-302.

Wu, J.Q., Hansen, D.V., Guo, Y., Wang, M.Z., Tang, W., Freel, C.D., Tung, J.J., Jackson, P.K., and Kornbluth, S. (2007). Control of Emi2 activity and stability through Mos-mediated recruitment of PP2A. Proc Natl Acad Sci U S A 104, 16564-16569.

Xia, G., Luo, X., Habu, T., Rizo, J., Matsumoto, T., and Yu, H. (2004). Conformation-specific binding of p31(comet) antagonizes the function of Mad2 in the spindle checkpoint. EMBO J 23, 3133-3143.

Xu, J., Wang, M., Gao, X., Hu, B., Du, Y., Zhou, J., Tian, X., and Huang, X. (2011). Separase phosphosite mutation leads to genome instability and primordial germ cell depletion during oogenesis. PLoS ONE 6, e18763.

Xu, Y., Xing, Y., Chen, Y., Chao, Y., Lin, Z., Fan, E., Yu, J.W., Strack, S., Jeffrey, P.D., and Shi, Y. (2006). Structure of the protein phosphatase 2A holoenzyme. Cell 127, 1239-1251.

Yamamoto, A., Guacci, V., and Koshland, D. (1996). Pds1p, an inhibitor of anaphase in budding yeast, plays a critical role in the APC and checkpoint pathway(s). J Cell Biol 133, 99-110.

Yang, J., and Phiel, C. (2010). Functions of B56-containing PP2As in major developmental and cancer signaling pathways. Life Sci 87, 659-666.

Yuan, J., Eckerdt, F., Bereiter-Hahn, J., Kurunci-Csacsko, E., Kaufmann, M., and Strebhardt, K. (2002). Cooperative phosphorylation including the activity of polo-like kinase 1 regulates the subcellular localization of cyclin B1. Oncogene 21, 8282-8292.

Zou, H., McGarry, T.J., Bernal, T., and Kirschner, M.W. (1999). Identification of a vertebrate sister-chromatid separation inhibitor involved in transformation and tumorigenesis. Science 285, 418-422.

Zou, H., Stemman, O., Anderson, J.S., Mann, M., and Kirschner, M.W. (2002). Anaphase specific auto-cleavage of separase. FEBS Lett 528, 246-250.

8. PUBLIKATIONSLISTE

Im Rahmen dieser Arbeit sind folgende Veröffentlichungen entstanden:

Holland, A.J., Böttger, F., Stemmann, O., and Taylor, S.S. (2007). Protein phosphatase 2A and separase form a complex regulated by separase autocleavage. J Biol Chem *282*, 24623-24632.

Touati S.A., Lister L.M., Böttger F., Stemmann O., Herbert M., and Wassmann K. Separase inhibition by stable cyclin B1, and not cyclin A2. Manuscript under revision.

9. DANKSAGUNG

An erster Stelle möchte ich mich bei Prof. Dr. Olaf Stemmann für die Aufnahme in seine Arbeitsgruppe, sowie für seine ständige Hilfs- und Diskussionsbereitschaft bedanken. Sein großer wissenschaftlicher Enthusiasmus hat mich stets sehr motiviert, und ich bin dankbar für die lehrreiche Zeit in seiner Arbeitsgruppe.

Mein Dank gilt außerdem allen Mitgliedern der Prüfungskommission der Universität Bayreuth, für Ihr Interesse und Ihre Zeit.

Cuiping Pan aus dem Labor von Matthias Mann (MPI Martinsried) danke ich für ihre großzügige Hilfe bei den massenspektrometrischen Analysen.

Allen Angehörigen des Lehrstuhls für Genetik der Uni Bayreuth, insbesondere meinen Mit-DoktorandInnen, danke ich für die gute Zusammenarbeit und den angenehmen Laboralltag in den letzten 2½ Jahren. Für die gute Stimmung und Organisation im legendären 'Messie-Labor' danke ich ganz besonders Andreas Brown, Michael Orth und Laura Schöckel. Many thanks außerdem an Laura für das große ASCB Abenteuer. Ein Extra-Dank geht an Bernd Mayer, der mir mit seinem Know-how und seiner Hilfsbereitschaft unzählige gute Ratschläge hat zukommen lassen. Susanne Hellmuth sei für die ausgezeichnete Zusammenarbeit am Separase-Securin Projekt ganz herzlich gedankt. Bernd, Susi und Laura danke ich außerdem für das Korrekturlesen dieser Arbeit. Für etliche Klonierungen sowie exzellente technische Assistenz danke ich Alexander Strasser (MPI Martinsried), Monika Ohlraun, Jutta Hübner und Marion Gradl. Markus Hermann danke ich für seine große Hilfsbereitschaft in allen technischen Anliegen. Zudem möchte ich Petra Helies und Brigitte Jaunich für die wesentliche Erleichterung und Erheiterung des Laboralltags danken.

Ein großes 'RG' geht an meine alten MPI KollegInnen, für den anhaltenden Support und für die große Zeit. Finch Finkbeiner und Co. danke ich ganz besonders für die vielen unvergesslichen Momente auch Abseits der Bench in den letzten 4½ Jahren.

Last but not least danke ich meinen Geschwistern, for being awesome, sowie meinen Eltern dafür, dass sie immer für mich da sind.

Hiermit versichere ich, die vorliegende Arbeit selbständig angefertigt und keine anderen als die angegebenen Quellen und Hilfsmittel verwendet zu haben. Ferner erkläre ich, dass ich nicht anderweitig mit oder ohne Erfolg versucht habe, diese Dissertation einzureichen. Ich habe keine gleichartige Doktorprüfung an einer anderen Hochschule endgültig nicht bestanden.

Bayreuth, den 13.07.2011

Franziska Böttger